BNL-73152-2004
MIT-NFC-065

OPTIMIZATION OF HETEROGENEOUS UTILIZATION OF THORIUM IN PWRs TO ENHANCE PROLIFERATION RESISTANCE AND REDUCE WASTE

Michael Todosow
Energy Sciences and Technology Department
Brookhaven National Laboratory

Mujid Kazimi
Department of Nuclear Engineering
Massachusetts Institute of Technology

Submitted: May 2004
Published: August 2004

Brookhaven National Laboratory
Upton, New York 11973-5000

BNL-73152-2004
MIT-NFC-065

OPTIMIZATION OF HETEROGENEOUS UTILIZATION OF THORIUM IN PWRs TO ENHANCE PROLIFERATION RESISTANCE AND REDUCE WASTE

Michael Todosow
Energy Sciences and Technology Department
Brookhaven National Laboratory

Mujid Kazimi
Department of Nuclear Engineering
Massachusetts Institute of Technology

Submitted: May 2004
Published: August 2004

Energy Sciences and Technology Department
Nuclear Science and Technology Division

Brookhaven National Laboratory
P.O. Box 5000
Upton, NY 11973-5000
www.bnl.gov

Managed by
Brookhaven Science Associates, LLC
for the United States Department of Energy under
Contract No. DE-AC02-98CH10886

DISCLAIMER

This report was prepared as an account of work sponsored by an agency of the United States Government. Neither the United States Government nor any agency thereof, nor any of their employees, nor any of their contractors, subcontractors or their employees, make any warranty, express or implied, or assumes any legal liability or responsibility for the accuracy, completeness, or any third party's use or the results of such use of any information, apparatus, product, or process disclosed, or represents that its use would not infringe privately owned rights. Reference herein to any specific commercial product, process, or service by trade name, trademark, manufacturer, or otherwise, does not necessarily constitute or imply its endorsement, recommendation, or favoring by the United States Government or any agency thereof or its contractors or subcontractors. The views and opinions of author's expresses herein do not necessarily state to reflect those of the United States Government or any agency thereof.

Printed on recycled paper

Collaborating Organizations:

Brookhaven National Laboratory
Massachusetts Institute of Technology
Ben-Gurion University of the Negev
Russian Research Center-Kurchatov Institute
Kyung Hee University
Korea Atomic Energy Research Institute
Korea Advanced Institute of Science and Technology

Contributors

BNL: L. Cheng, B. Bromley, J. Jo, M. Todosow, C. Gerardi (BNL-University of Maryland), W. Wieselquist (BNL-North Carolina State), A. Aronson, A. Mallen, A. Hanson

BGU: A. Galperin, G. Raitses, M. Segev

MIT: M. Kazimi, M. Driscoll, E.E. Pilat, P. Saha, D. Wang, D. Feng, Y. Long, E. Shwageraus, J. Lee, and W. J. Lee (MIT-KAERI)

TABLE OF CONTENTS

EXECUTIVE SUMMARY vii

A. INTRODUCTION.....1

B. TECHNICAL DETAILS.....3

B1. Technical Approach and Outline 3

B2. The Whole-Assembly Seed Blanket Concept 4

B2.1 Assembly and Core Neutronics Design.....4

B2.1.1 Assembly Neutronics Analyses (Task-1).....4

B2.1.2 Core Neutronics Design (Task-7) 11

B2.2 Assembly Thermal Analysis (Task-2) 19

B2.2.1 Reference Calculation.....19

B2.2.2 Sensitivity of MDNBR to Various Parameters.....23

B2.3 Assembly and Fuel Mechanical Design.....27

B2.3.1 Assembly Mechanical Design (Task-3) 27

B2.3.2 Fuel and Cladding Performance (Task-4) 27

B2.4 Fuel Cycle Cost (Task-5) 33

B2.5 Waste (Spent Fuel) Characteristics and Non-Proliferation Performance (Task-6).....41

B2.5.1 Spent Fuel Characteristics 41

B2.5.2 Proliferation Resistance.....44

B2.6 Safety Analyses (Task-8) 48

B2.6.1 Input Deck/Model 48

B2.6.2 Large Break Loss of Coolant Accident (LBLOCA).....51

B2.6.3 Complete Loss of Primary Flow (LOPF).....54

B2.6.4 Loss of Off-site Power (LOSP).....57

B3. The Seed-Blanket Unit (SBU-RTF) Concept.....60

B3.1 Assembly and Core Neutronics Design.....60

B3.1.1 Seed-Blanket Unit (SBU) Neutronics Analysis (Task-1) 60

B3.1.2 Core Neutronics Design (Task-7) 66

B3.2 Seed Blanket Unit (SBU) Thermal Analysis (Task-2) 71

B3.2.1 SBU Assembly Model 71

B3.2.2 1/8-Core Analysis 73

B3.3 Assembly and Fuel Mechanical design (Task-3).....88

B3.4 Fuel Cycle Cost (Task-5) 90

B3.5 Waste Characteristics and Non-Proliferation Performance (Task-6).....92

B3.6 Safety Analysis (Task-8).....94

B3.6.1 Approach for Safety Analyses.....94
B3.6.2 Reactivity Coefficients.....97
B3.6.3 SBU Accident Analysis.....98
C. SUMMARY AND CONCLUSIONS.....115
D. INTERNATIONAL COLLABORATION.....119
E. REFERENCES.....121

EXECUTIVE SUMMARY

Research Objectives

This work examines heterogeneous core design options for the implementation of the Th-^{233}U fuel cycle in pressurized water reactors (PWRs) without reprocessing or recycling. It identifies the core design and fuel management strategies which will maximize the benefits from inclusion of thorium in the fuel. The assessment concentrates on key measures of performance in several important areas, including proliferation characteristics of the spent fuel, reliability, safety, cost, environmental impact, and licensing issues. The focus is on once-through fuel cycles that do not involve reprocessing of the spent fuel. A 193-assembly Westinghouse reactor utilizing 17x17 fuel is taken as the model core.

One design, the Whole Assembly Seed and Blanket (WASB) concept, provides seed units and blanket units which separately occupy one full-size PWR assembly each, and the assemblies are arranged in the core in a modified checkerboard array (Figure-1).

The second design, the Seed-Blanket Unit (SBU), also known as the Radkowsky Thorium Fuel (RTF) concept, aggregates the thorium blanket and the uranium seed into subassembly units such that a complete seed-blanket unit is a one-for-one replacement for a conventional PWR fuel assembly (Figure-1).

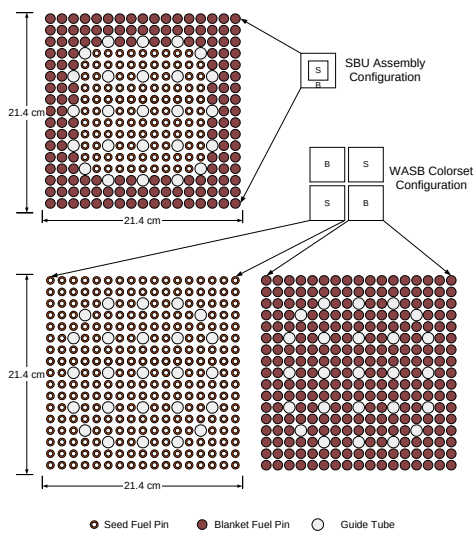

Figure-1 SBU and WASB Fuel Assembly Design

The studies for both approaches have (1) identified the core design and fuel management strategies that maximize the benefits from inclusion of thorium in the fuel and (2) extended the analyses to validate the results over a range of possible operating conditions.

Research Achievements

Two separate designs, SBU and WASB, have been developed which significantly improve the intrinsic proliferation resistance and waste characteristics of PWR fuel while achieving 18 month cycles. The total production of plutonium is reduced by a factor of about three and the volume of spent fuel by a factor of about two and a half relative to a present-day commercial PWR. Furthermore, the plutonium that is produced is of inferior quality for potential utilization in weapons: it has a higher heat generation from increased Pu-238 and a stronger spontaneous neutron source from an increased percentage of Pu-238, Pu-240, and Pu-242. Both designs have been checked from the neutronic and thermal hydraulic points of view, and a limited set of safety and fuel performance examinations were performed. Despite their somewhat different implementations, the two designs provide similar performance characteristics. It was concluded that there are waste volume advantages and plutonium reduction advantages, while maintaining the essential neutronic and thermal safety performance of current PWRs. There is no economic advantage to this fuel cycle under the present economic conditions as the fuel cycle cost of either the SBU or WASB approach is comparable to that of present PWRs. However, any increases in the prices for storing and handling spent fuel and/or reduced prices for uranium enrichment may change this conclusion. This fuel also requires special design and manufacturing capabilities to produce high burnup annular fuel pellets to be used in the seeds. Significantly, both approaches utilize assembly designs based on a Westinghouse 17x17 assembly where the sole modification is in the details of the fuel rods and the grids. Therefore, in principle, they are both retrofittable into existing PWRs with little or no modification

Specific achievements in the course of this NERI project are summarized below and are applicable to both SBU and WASB unless stated otherwise. The SBU development, which is an improved version of Radkowsky's RTF, has been done primarily by BNL with support from Ben Gurion University. It is closely related to an ongoing project under the DOE Initiatives for Proliferation Prevention program and private funding which is focused on RD&D activities in Russia and the West. The initial reference point for the SBU optimization studies is based on the results for the PWR from that study. The WASB development has been done primarily at MIT.

1) Mechanical designs were developed for both seed and blanket fuel assemblies within the constraints of the Westinghouse 17x17 design (assembly envelope, rod pitch, guide tube locations). Both SBU and WASB designs utilize solid thorium/uranium oxide pellets for the blanket, and annular uranium oxide pellets for the seed. In both cases the flow resistance of their grids has been increased to enhance coolant flow into the higher power seed region. For the WASB design the outer diameter of the blanket fuel rods has also been increased to increase the flow in the seed assemblies. The SBU design permits refueling by inserting and removing individual seed rods with a machine similar to one used to replace failed fuel rods. The WASB design allows whole seed assemblies to be removed individually. In either approach the upper and lower end-fittings can be identical to those currently employed. The final SBU design results in108 of the 264 fuel rods in each assembly being seed rods, amounting to 41 % of all the fuel rods in the core. By comparison, with the WASB design,

84 of the 193 fuel assemblies are seed assemblies so that 43.5% of the fuel rods in the core are seed rods, quite similar to the SBU design.

2} During the mechanical design of the assemblies, the neutronic designs were optimized to maximize breeding and fission of 233U in the blanket and to minimize production of Pu in the seed (where almost all the Pu is created). The adequacy of the deterministic lattice physics codes (BOXER and DRAGON for SBU and CASMO for WASB) in the highly heterogeneous situations characterizing seed-blanket cores, was verified by comparison with continuous energy Monte Carlo codes (MCNP and RECOL for SBU and MCNP for WASB).

3) Viable 18 month cycle core designs and fuel management plans were developed. Both SBU and WASB utilize 3 batch fuel management for the seed - i.e., 1/3 of the seed fuel is replaced every 18 months. Single batch fuel management is used for the blankets, with SBU blanket fuel remaining in-core for 6 cycles and WASB blankets for 9 cycles.

4) Acceptability of the neutronic aspects of the core designs was checked at nominal operating conditions via calculation of power distributions, radial and axial peaking factors, reactivity coefficients and control rod worths. The cycle energy and reactivity coefficients of both SBU and WASB designs are similar to those of conventional PWRs. Radial peaking factors in the seed fuel are significantly above those of conventional PWRs, but this has been compensated for in the designs by the higher flow provided in the seed regions. See items 1, 5 and 6 in this list for further discussion. Control rod worths are smaller than those of conventional cores and may require either reconfiguration of the control banks or redesign of the control rodlets themselves with a more highly absorbing material such as enriched B4C.

5) Acceptability of the thermal hydraulic aspects of the core designs to accommodate AOO (Anticipated Operational Occurrence) conditions was estimated by verifying adequate margin to centerline melt and to DNB using static calculations at 112 to 118% of nominal thermal power, the range of typical thermal power attained in this class of transients. These calculations were performed using conservative temperature and pressure input assumptions in one-eighth core models, with individual sub-channels represented in the hot assembly and lumped models for the remainder of the assemblies. These calculations used the W-3 correlation with COBRA-EN for SBU and VIPRE for WASB.

6) A sampling of preliminary safety analyses showed that both the SBU and WASB designs gave acceptable results for large-break loss of coolant accidents (LOCA), loss of primary flow (LOPF), and loss of off-site power (LOOP) transients. Following the LOCA, the maximum clad temperature in the seed exceeds the maximum temperature of a homogeneous UO_2 core, but remains well below the limit of 1200 C. All calculations included representations of average seed and blanket and hot seed areas in the core. Calculations were performed with RELAP5-3D for SBU and with MARS, a Korean adaptation of RELAP5, for WASB.

7) Spent fuel characteristics evaluated for both designs with the ORIGEN code show marginally less activity from the seed-blanket spent fuel in the near and medium term and somewhat more in the long term. However the increase occurs on the order of 100,000 years

in the future, when the total activity and heat generation have decayed to quite low levels. It is due to decay of daughter products of thorium.

Formally, the Russian Research Center – Kurchatov Institute, and several organizations participated in the collaboration. However, since the work in Korea and Russia was performed for significantly different reactor configurations (CE-System-80 and VVER-1000, respectively), and under different assumptions for the fuel cycle, their results are not included in this report.

A. INTRODUCTION

Issues affecting the implementation, public perception and acceptance of nuclear power include: proliferation, radioactive waste, safety, and economics. The thorium cycle directly addresses the proliferation and waste issues, but optimization studies of core design and fuel management are needed to ensure that it fits within acceptable safety and economic margins.

Typical pressurized water reactors, although loaded with uranium fuel, produce 225 to 275 kg of plutonium per gigawatt-year of operation. Although the spent fuel is highly radioactive, it nevertheless offers a potential proliferation pathway because the plutonium is relatively easy to separate, amounts to many critical masses, and does not present any significant intrinsic barrier to weapon assembly.

Uranium 233, on the other hand, produced by the irradiation of thorium, although it too can be used in weapons, may be "denatured" by the addition of natural, depleted or low enriched uranium. Furthermore, it appears that the chemical behavior of thoria or thoria-urania fuel makes it a more stable medium for the geological disposal of the spent fuel. It is therefore particularly well suited for a once-through fuel cycle.

The use of thorium as a fertile material in nuclear fuel has been of interest since the dawn of nuclear power technology due to its abundance and to potential neutronic advantages. Early projects include homogeneous mixtures of thorium and uranium oxides in the BORAX-IV, Indian Point I, and Elk River reactors, as well as heterogeneous mixtures in the Shippingport seed-blanket reactor. However these projects were developed under considerably different circumstances than those which prevail at present. The earlier applications preceded the current proscription, for non-proliferation purposes, of the use of uranium enriched to more than 20 w/o in ^{235}U, and has in practice generally prohibited the use of uranium highly enriched in ^{235}U. They were designed when the expected burnup of light water fuel was on the order of 25 MWD/kgU – about half the present day value - and when it was expected that the spent fuel would be recycled to recover its fissile content.

Several implementation scenarios have been examined for the Th-^{233}U cycle for use in both existing and next generation nuclear systems. The simplest approach conceptually is a "homogeneous" configuration, where the UO_2 fuel rods are replaced one-for-one by ThO_2-UO_2 rods (MacDonald, 1999). Alternatively, "heterogeneous" configurations can be developed where the uranium and thorium components are spatially separate; by convention, these are generally referred to as "seed" and "blanket", respectively. This separation can be either "macro" or "micro" (Todosow, et al, 2003) in nature. In the former, the uranium and thorium bearing portions of the fuel are in geometrically separate/distinct fuel rods, while in the latter, they are both included within a single fuel rod, or even within a single pellet, though still physically separate. Preliminary comparisons of some of the characteristics of homogeneous and heterogeneous schemes have shown that the heterogeneous approaches allow more flexibility, and permit a greater degree of optimization to reap the maximum nonproliferation and fuel utilization potential of the thorium cycle. In particular, the "macro" approaches allow different in-core residence times for the thorium-bearing fuel, to maximize uranium utilization and power generation from the bred ^{233}U. The more

complicated fuel management due to the presence of two types of fuel assemblies is expected to be more than compensated for by the higher fuel utilization that can be achieved in "macro" heterogeneous concepts

Two "macro" heterogeneous concepts are currently being examined, with the focus on fuel that can be used in a "typical", 193 assembly PWR of Westinghouse design. This work is therefore complementary to a study of homogeneous approaches currently underway by a team headed by the Idaho National Engineering and Environmental Laboratory (INEEL) (MacDonald, 1999), and to the study of micro-heterogeneous approaches at MIT (Shwagerans, et al, 2002).

The objective of this work has been to examine heterogeneous core design options for the implementation of the Th-^{233}U fuel cycle in pressurized water reactors (PWRs) and to identify the core design and fuel management strategies which will maximize the benefits from inclusion of thorium in the fuel. The assessment concentrates on key measures of performance in several important areas including proliferation characteristics of the spent fuel, reliability, safety, cost, environmental impact, and licensing issues.

The focus is on once-through fuel cycles that do not involve reprocessing of the spent fuel,or require uranium enrichments above 20 w/o, and are retrofittable into existing pressurized water power reactors with no, or minimal modifications. Design optimizations involve heterogeneous core options which aggregate the thorium in subassembly units or typical PWR assembly units.

Two heterogeneous thorium implementation options are explored in the course of this NERI investigation: 1) the Seed-Blanket Unit (SBU)/Radkowsky Thorium Fuel (RTF) concept, which employs a seed-blanket unit that is a one-for-one replacement for a conventional PWR fuel assembly; and 2) the whole assembly seed and blanket (WASB) where the seed and blanket units each occupy one full-size PWR assembly and the assemblies are arranged in the core in a modified checkerboard array. The first concept (SBU) has been examined primarily by Brookhaven National Laboratory (BNL) with support from Ben Gurion University, and the second one (WASB) has been investigated primarily by Massachusetts Institute of Technology (MIT).

B. TECHNICAL DETAILS

B1. Technical Approach and Outline

The technical work focused on fuel that can be used in a typical 193-assembly Westinghouse PWR, and was divided into several logical steps:

- Task-1: Assembly Neutronic Calculations
- Task-2: Assembly Thermal-Hydraulic and Thermal Calculations
- Task-3: Assembly Mechanical Design Issues
- Task-4: Examination of Fuel/Cladding Options
- Task-5: Fuel Cycle Cost
- Task-6: Waste Characteristics
- Task-7: Core and Fuel Cycle Assessment
- Task-8: Safety Analyses

While the SBU and WASB designs share several common attributes, they are significantly different in many respects. The work on each concept is therefore presented independently, rather than intermingling the activities on a task-by-task basis: Section-B2 describes the work on the WASB approach, and the work on the SBU is described in Section-B3.

In addition, the project collaborators in Korea have developed a WASB design for a reactor based on the Combustion engineering System-80 design utilizing metallic fuel for the seed, while an SBU variant for implementation in a VVER-1000, also utilizing metallic fuel for the seed, has been developed in Russia. There has also been significant work performed in Russia related to the fabrication, measurement of properties, and irradiation behavior of mixed thorium-uranium oxide fuel. This work is described elsewhere.

B2. The Whole-Assembly Seed Blanket Concept

B2.1 Assembly and Core Neutronics Design

B2.1.1 Assembly Neutronics Analyses (Task-1)

Fuel Design

In the WASB design, the seed fuel enrichment is just below 20%, a percentage generally accepted as being non-proliferative. The relatively high enrichment is necessary to compensate for the smaller volume of the uranium present in the core and for the high thorium capture rate. The purpose of the seed is to supply neutrons to the blanket in the most efficient way by thermalizing the neutron spectrum (high water content) so as to minimize plutonium formation. The top view of the seed fuel pin is presented in Figure B2.1.1. Annular fuel pellets are employed in the seed rods of WASB, which helps maximize the H/U ratio in the seed. In addition, this also offers space to accommodate the needed burnable poison. Mechanical and thermal benefits also stem from the use of annular fuel pellets instead of solid pellets as explained in Section B2.3.

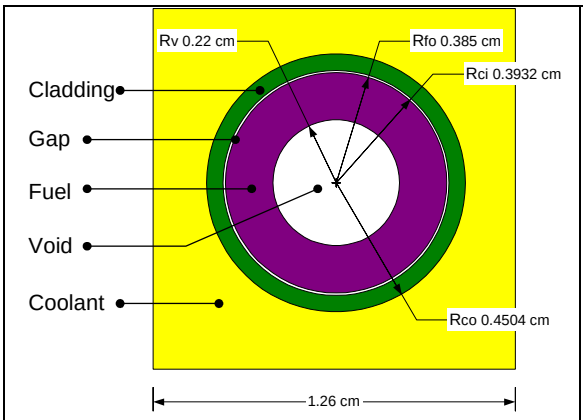

Figure B2.1.1 Seed Fuel Pin Unit Cell

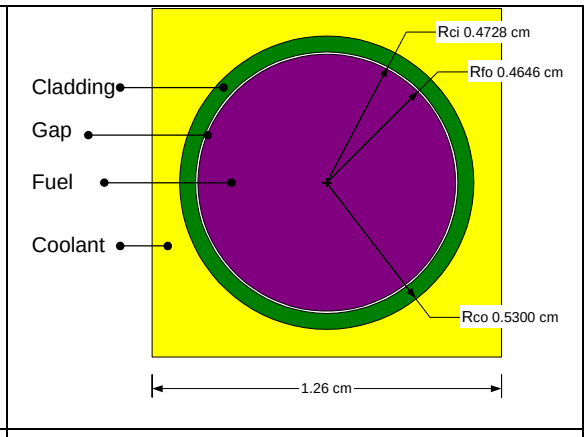

Figure B2.1.2 Blanket Fuel Pin Unit Cell

The blanket fuel assemblies in the core are dispersed among the seed assemblies. The blanket fuel composition is a mixture of ThO2 and UO2, where UO2 is only about 10% of the fuel volume. A blanket pin cell is shown in Figure B2.1.2. Under irradiation, thorium undergoes a rapid increase in U-233 concentration. The main challenge of efficient utilization of thorium in LWRs in a once-through fuel cycle is reduced to the problem of achieving very large accumulated burnup in the thorium. An addition of natural or slightly enriched uranium provides an appreciable fission rate during this period and allows reasonable power sharing between the seed and blanket, which, in turn, limits the seed power density to an acceptable level.

Table B2.1.1 summarizes parametric studies on blanket fuel compositions. It can be seen that the U-233 weight percentage in total uranium at high burnup decreases as the UO2

content of the blanket increases, but that the enrichment of U-235 in the blanket UO2 has no significant effect on the U-233 content. Thus it is an effective strategy to adjust the UO2 volume ratio to ThO2 in the fuel so that the U-233 weight percentage in the discharged fuel is below the 12% proliferation limit. Finally 13% UO2 - 87%ThO2 has been used for the blanket fuel composition, where the enrichment of U-235 is 10%.

Table B2.1.1 U-233 Weight Percentage in Total Uranium at 80 MWd/kgHM

v/o[a] / **Enrich.[b]**	**5%**	**10%**	**13%**	**15%**
5%	25.5%	14.7%	11.5%	10.0%
10%	26.4%	15.3%	12.0%	10.5%
15%	27.3%	15.9%	12.5%	10.9%

a: UO2 volume ratio in UO2-ThO2 fuel
b: U-235 enrichment in U

Fissile buildup in the blanket fuel as a function of burnup is shown in Figure B2.1.3 in units of weight percent of the initial heavy metal. The U-233 content levels off at an approximately constant level of 1.6%. The fissile plutonium content is much lower.

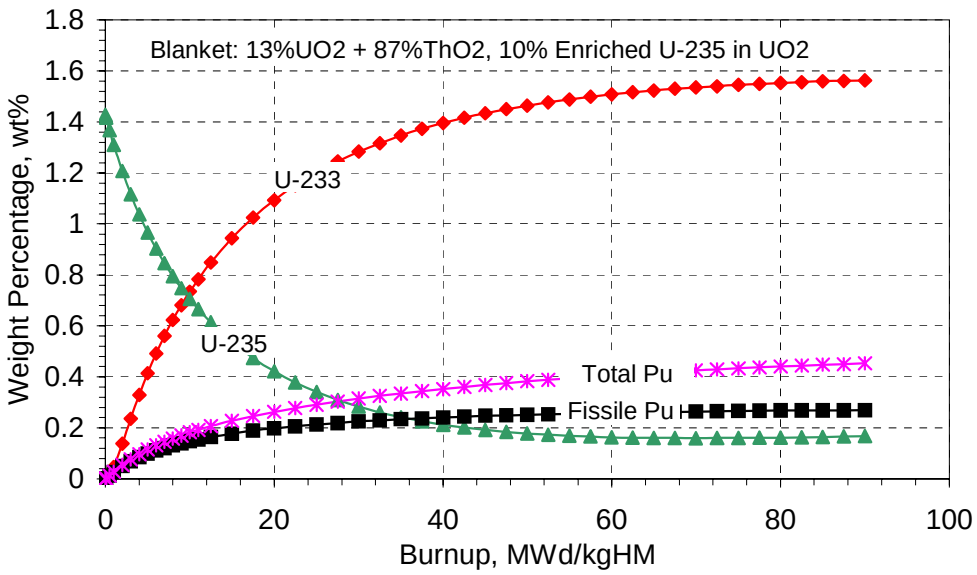

Figure B2.1.3 Changes in Blanket Fuel Composition with Burnup
(wt% is relative to initial heavy metal)

Effects of Water to Fuel Ratio on Seed and Blanket

Moderation in the seed and blanket of the WASB can be adjusted to achieve the optimum neutronic and thermal-hydraulic performance. Generally speaking, a high moderator to fuel volume ratio is desirable in the seed to reduce plutonium generation, and a low moderator to fuel volume ratio in the blanket to give a higher conversion ratio. Varying the fuel rod diameter is used here to investigate moderation effects on seed and blanket fuel design by means of a colorset model (i.e., a four-assembly, checkerboard, repeating array).

First, the moderator to fuel ratio of the seed fuel is varied to investigate its effects on the colorset neutronic behavior without varying the blanket fuel. The total heavy metal content of the seed fuel is conserved while varying the seed fuel rod inner void diameter and fuel outer diameter. Lower values of Vwater/Vfuel lead to poorer neutronic performance as shown in Figure B2.1.4. It is shown in Figure B2.1.5 that the conversion ratio decreases as the V_{water}/V_{fuel} value increases in the seed, however the effects on the conversion ratio of the blanket are negligible when only varying the moderator to fuel ratio of the seed. In addition, fissile and total plutonium contents in the seed fuel are also shown in Figures B2.1.6 and B2.1.7. It is obvious that a wetter seed lattice design is preferred in terms of neutronic performance and plutonium content. It should be noted that fuel rod design is not only determined by neutronic considerations, but also limited by thermal-hydraulic and mechanical requirements.

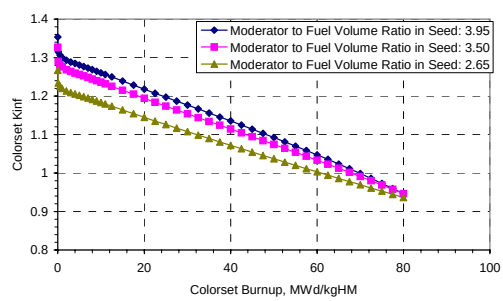

Figure B2.1.4 Impacts of Varying V_{water}/V_{fuel} on Kinf of a Colorset

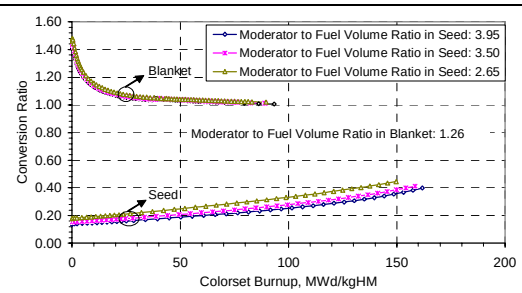

Figure B2.1.5 Impact of Varying V_{water}/V_{fuel} on CR in Seed

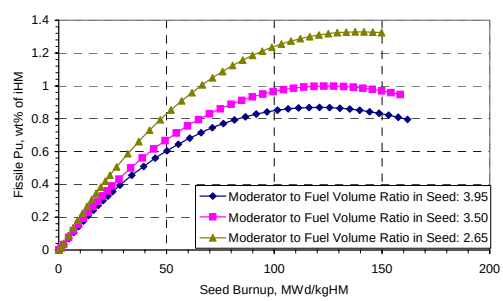

Figure B2.1.6 Impact of Varying V_{water}/V_{fuel} on Fissile Pu Content in Seed

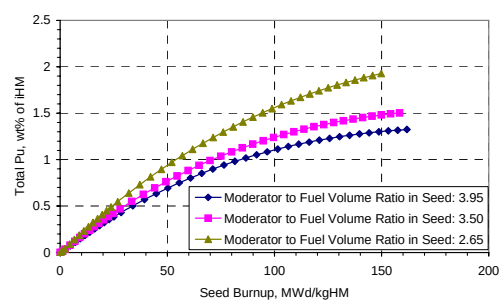

Figure B2.1.7 Impacts of Varying V_{water}/V_{fuel} on Total Pu Content in Seed

Calculations were also performed to analyze the impacts of varying the moderator to fuel ratio of the blanket fuel. Varying Vwater/Vfuel values is realized by changing the blanket fuel diameter. Hence heavy metal loading in the blanket is not preserved when varying the moderator to fuel ratio in the blanket.

The Nu-Fission/Absorption values of the seed and blanket fuel in a colorset are presented in Figure B2.1.8, and comparisons with single assembly results are also shown in the figure. Actually the Nu-Fission/Absorption values from single assembly calculations are just the multiplication factors, Kinf. It can be seen that the Nu-Fission/Absorption values from single assembly calculations are very close to those from colorset calculations. Hence reactivity is approximately a state function of burnup for a PWR assembly - in other words, a unique single-valued function of the specified burnup, and not of the depletion history or the manner in which the burnup was accumulated (Driscoll, et al, 1990).

In order to take into account the influence of neighboring assemblies a colorset was also employed to investigate the moderation effects of the blanket fuel. All results are shown in Figures B2.1.9, B2.1.10 and B2.1.11.

Figure B2.1.9 shows the impacts on Nu-Fission/Absorption values when varying the moderator to fuel volume ratio of the blanket assemblies in a colorset. It is concluded that a tight lattice is preferred due to higher reactivity and flatter reactivity swing during depletion. However, Figure B2.1.10 shows that there are only minor effects on the conversion ratio at the early stage of depletion when varying the moderator to fuel volume ratio of the blanket fuel. It is interesting that all three curves of the blanket fuel almost converge to the same conversion ratio after 30 MWd/kgHM, and that ratio remains constant until 90 MWd/kgHM. Note that the conversion ratio of the blanket is always above one, which means that the blanket fuel undergoes net breeding. U-233 builds up with depletion as shown in Figure B2.1.11, and once again a tight or dry lattice design is desirable due to its high U-233 content in the fuel.

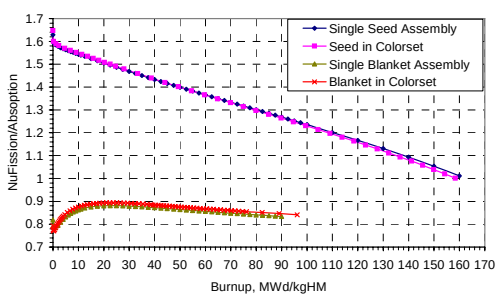

Figure B2.1.8Nu-Fission/Absorption Ratio in Seed and Blanket

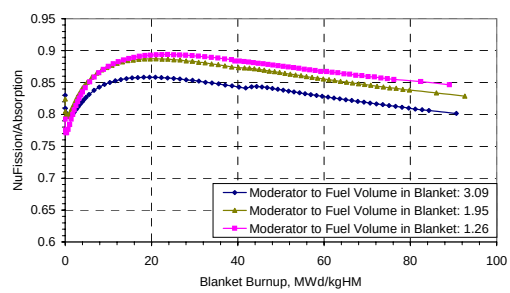

Figure B2.1.9 Impact of Varying V_{water}/V_{fuel} on Nu-Fission/Absorption in Blanket

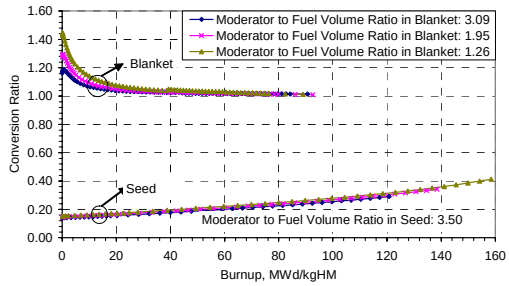

Figure B2.1.10 Impact of Varying V_{water}/V_{fuel} on Conversion Ratio in Seed and Blanket

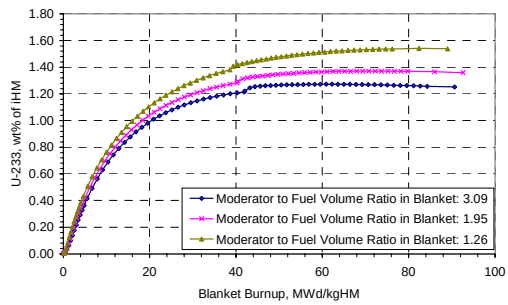

Figure B2.1.11 Impact of Varying Vwater/Vfuel on U-233 Content in the Blanket

Based on the preceding detailed analyses of the seed and blanket fuel assemblies, an "optimum" reference design of the WASB fuel, in terms of neutronic performance, has been proposed (and subjected subsequently to whole core analyses) as shown in Table B2.1.2.

Table B2.1.2 Seed and Blanket Assembly Optimized Parameters

PARAMETERS	VALUES	
	Seed	**Blanket**
Fuel Material Composition	UO_2 20 w/o U-235 in U	87 v/o ThO_2 + 13 v/o UO_2 10 w/o U-235 in U
Fuel Density, g/cm^3	10.302	9.403
Fuel Assembly Pitch, cm	21.5	
Fuel Pellet Radius, cm	Void: 0.22, Fuel: 0.385	0.4646
Gas Gap, cm	0.0082	
Cladding Thickness, cm	0.0572	
Pin Pitch, cm	1.26	
Moderator to Fuel Volume Ratio (conventional PWR = 1.95)	3.50	1.26

Burnable Poison Design

Burnable poisons are used to hold down beginning of cycle core reactivity and to shape the power distribution in the core so that physics design limits are met and hot spots are avoided. Gadolinia, erbia or zirconium diboride, all located in the central have been evaluated. Location in the void eliminates any detrimental effect on UO2 thermal conductivity: a significant benefit because of the high seed power density. This concept was originally proposed in a B&W patent (Pettus 1987 & 1989) but to our knowledge never applied in practice.

The oxide form Gd_2O_3 has been extensively used as burnable absorber in both PWRs and BWRs. B-10 does not generate residual-absorbing daughter products but does create helium after neutron absorption. As a result, internal pin pressure significantly increases through the cycle, raising concerns about fuel integrity. ABB-CE (now Westinghouse) has developed the application of erbium as a burnable poison for PWRs, in the form of Er2O3 admixed with enriched UO2 (Jonsson, et al, 1991).

In the WASB design, Er2O3 is used in the seed fuel rod design. Its selection is based on comparison calculations performed using CASMO-4 colorset calculation. Each poison is evenly loaded in the central void of each seed pin, as shown in Table B2.1.3. Figures B2.1.12 and B2.1.13 show their effects on the neutronic behavior of an individual seed assembly and a colorset.

Table B2.1.3 Burnable Poison Loading

	Fuel U	Er_2O_3 Nat. Er	Er_2O_3 Er-167	ZrB_2 B-10	Gd_2O_3 Nat. Gd
Mass per cm in a pin, g/cm	2.848	0.0332	0.0226	0.0011	0.0049
Bp w/o relative to Fuel		1.166%	0.794%	0.039%	0.172%

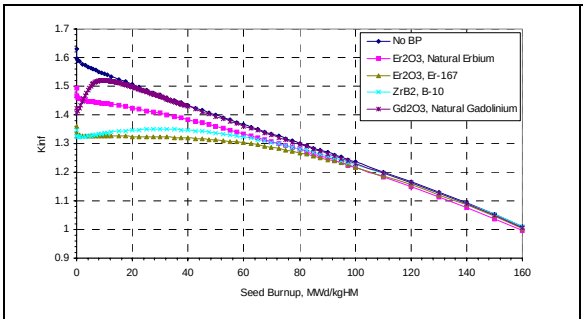

Figure B2.1.12 Seed Reactivity Response to Burnable Poisons

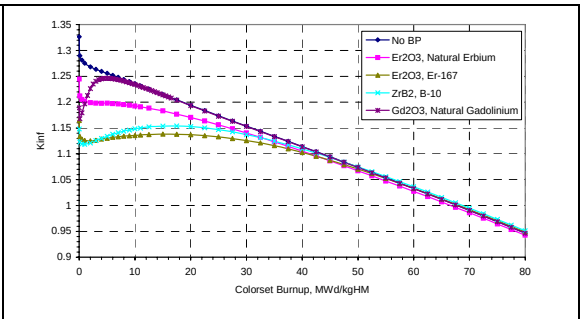

Figure B2.1.13 Colorset Reactivity Response to Burnable Poisons

The rapid burnout of gadolinium produces a sharp rise in assembly reactivity compared to the other poison schemes. From a reactivity viewpoint, the best poison is Er-167, which keeps the reactivity at a significantly lower level than the other poisons. When selectively loaded into the central void of the seed fuel pins, as shown in figure B2.1.14, it also reduces the power peaking in the seed fuel as shown in Figure B2.1.15.

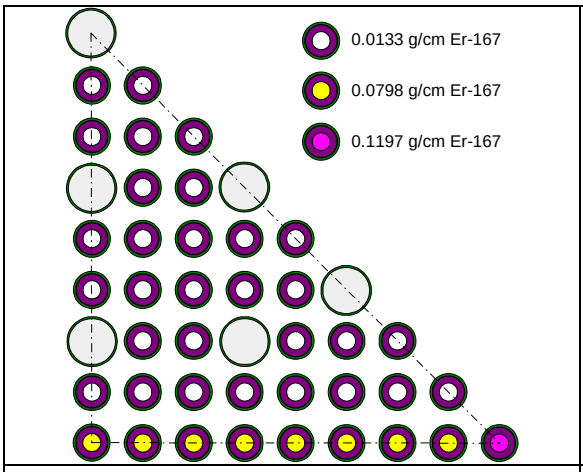

Figure B2.1.14 Burnable Poison Loading Pattern

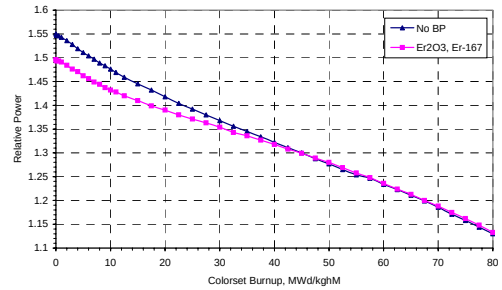

Figure B2.1.15 Relative Power of Seed over Cycle Exposure

Neutron Spectrum

The neutron spectrum of the WASB core was investigated using MCNP-4C based on a colorset model. Comparison of Figures B2.1.16 and B2.1.17 shows that the thermal flux in the seed increases with seed burnup due to the loss of fissile material. However, the thermal flux in the blanket experiences a much smaller drop because the loss of U-235 is approximately compensated by the buildup of U-233.

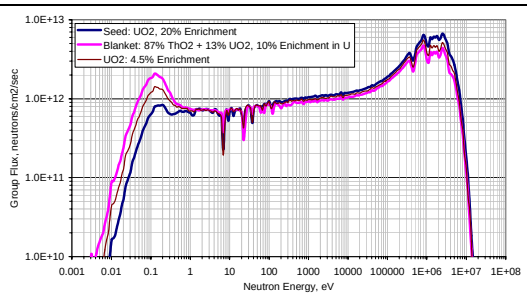

Figure B2.1.16 Neutron Spectra in WASB S&B Regions with Fresh Blanket

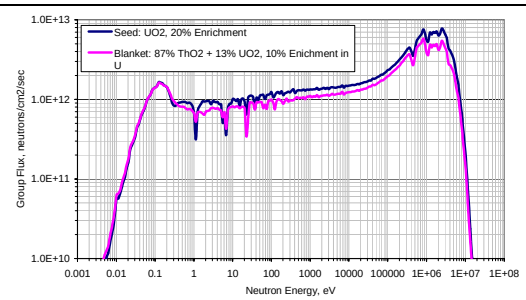

Figure B2.1.17 Neutron Spectra in WASB S&B Regions with Partially Burned Blanket

B2.1.2 Core Neutronics Design (Task-7)

The objective of the core design study is to identify the core and fuel management strategies which will maximize the benefits of the WASB fuel design. The focus is on once-through fuel cycles that do not involve reprocessing of the spent fuel. A 193 assembly Westinghouse PWR utilizing a 17×17 lattice is taken as the model core.

Core Modeling

The core was modeled in three dimensions with twenty-four axial nodes and four radial nodes per assembly. The core representation included radial and axial reflectors (top and bottom) that account for the coolant and structural materials. The core was analyzed at a condition of steady-state Hot Full Power (HFP) with all the control rods completely withdrawn, and was depleted to End Of Cycle (EOC).

Loading Pattern

The WASB core of choice consists of 84 seed assemblies and 109 blanket assemblies, whose design parameters are given in Table B2.1.4. The overall length of a fuel assembly is 406.3cm., and the active fuel length is 365.76cm. There are two separate fuel management streams: a three-batch stream for the seed (eighteen-month cycle length) and a single-batch stream for the blanket, which is to stay in the core for up to nine seed cycles. In order to reduce the neutron radiation damage to the pressure vessel and improve neutron economy, a low-leakage core strategy is applied to the WASB core. Figure B2.1.18 shows the pattern which reduces the flux by placing blanket assemblies at the periphery of the core. The seed assemblies and other blanket assemblies are scattered inside the core in a "checkerboard" scheme. The fresh seed assemblies are located in the core interior as far as possible to produce a fairly uniform power distribution in the interior of the core and to minimize core leakage.

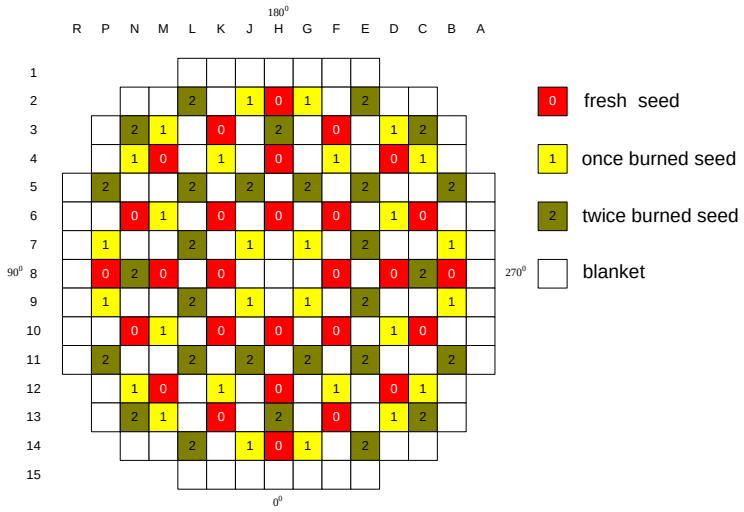

Figure B2.1.18 The WASB Core Layout and Refueling Scheme

Fuel Dimensions

Dimensions for the WASB fuel design are given in Table B2.1.4. Axial blankets of natural uranium are used for the high enrichment seed fuel, but not for the low enrichment blanket fuel. The blanket fuel has no burnable poison and no axial LERs. Figure B2.1.19 shows the axial zoning in the seed fuel.

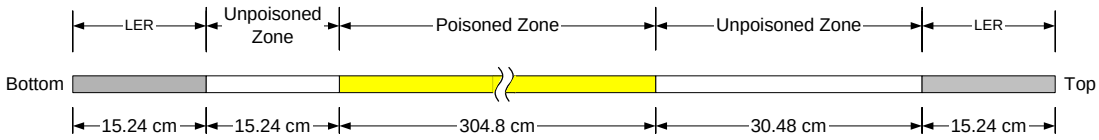

Figure B2.1.19 Axial Zoning in the Seed Fuel (not to scale)

Table B2.1.4 Mechanical Design Parameters of the Seed and Blanket Fuel

	Seed	Blanket
Fuel Assembly		
Overall Length, cm	406.3	406.3
Assembly Pitch, cm	21.5	21.5
Fuel Rod Pitch, cm	1.26	1.26
Number of Fuel Pins	264	264
Fuel Rod		
Active Fuel Length, cm	365.76	365.76
Clad OD, cm	0.9008	1.06
Clad ID, cm	0.7864	0.9456
Pellet Type	Annular	Solid
Pellet OD, cm	0.77	0.9292
Pellet ID, cm	0.44	NA
Initial Pellet Density, g/cm3	10.3024	9.4028
Burnable Poison		
Material	Er2O3, 100 w/o Er-167	N/A
Content*, mg/cm	Inner Pin: 9.12	N/A
Active Length, cm	304.8	
Axial Blanket		
Material	UO2	N/A
Enrichment, w/o U-235	0.711	N/A
Top Blanket Length, cm	15.24	N/A
Bottom Blanket Length, cm	15.24	N/A
Pellet Type	Annular	N/A

Heavy Metal Loading and Cycle Mass Flow

The core heavy metal content in the WASB core is summarized in Table B2.1.5. The WASB seed heavy metal loading is about 40% of the blanket. The total amount of heavy metal of the WASB core is about 9% less than the reference core, but the fissile content in the WASB fuel is 25% more than the reference core.

The WASB core is made up of three-batch seed and one-batch blanket assemblies. In Cycle 1 there are 28 fresh seed assemblies, 28 seed assemblies burned in 1 previous cycle, 28 seed assemblies burned in 2 previous cycles and 109 fresh blanket assemblies in the core; 1/3 of the seed assemblies are refueled at the end of each cycle whereas the blanket will sit in the core for up to 9 seed cycles. After 9 cycles the spent blanket is replaced with fresh blanket assemblies. At cycle 5 the inside and peripheral blanket assemblies are interchanged once in order to balance burnups of the assemblies. Figure B2.1.20 diagrams the cycle mass flow in the WASB core. The heavy metal mass flow of each cycle is much less than for a conventional UO2 core.

Table B2.1.5 Core Heavy Metal Loading, kg

	Seed		Blanket	S+B	Ref. UO2 core
	Seed Fuel	Axial Blanket			
U-235	4234	14	842	5090	4050
U-238	16936	1925	7576	26437	85950
Th-232			50579	50579	
Total	23109		58997	82106	90000

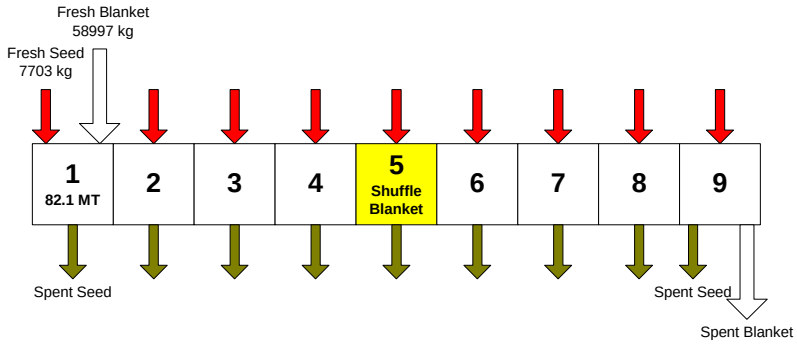

Figure B2.1.20 Cycle Mass Flow

Core Reactivity and Cycle Length

The excess reactivity in the WASB core is controlled by soluble boron and Er2O3 burnable poison. Figure B2.1.21shows the critical boron concentration as a function of core burnup. Fresh seed assemblies replace 28 thrice burned seeds at the start of each cycle. Thus the reactivity behavior difference among cycles comes from the blanket

reactivity change during its life. The outside and inside blanket assemblies are exchanged once at Cycle 5 to balance their burnups.

Figures B2.1.21 shows that the cycle lengths decrease gradually due to the reactivity loss of the blanket at the end of its life. The blanket reactivity increases initially with the buildup of U-233 and reaches a maximum after about three seed cycles, then decreases slowly because of the accumulation of fission products as shown in Figure B2.1.22. The blanket reactivity decline could be compensated by either a gradual increase in the fuel loading of the seed or earlier refueling of the blanket.

The cycle lengths of nine successive cycles are presented in Table B2.1.6. The average capacity factor (CF) of the WASB core between refuelings is about 91%: hence any cycle length in calendar months is about 10% longer than the EFPM values tabulated.

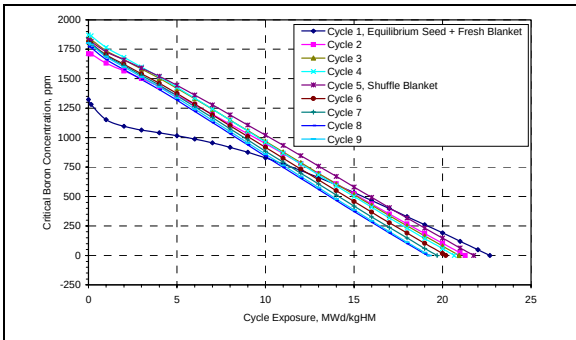

Figure B2.1.21 Critical Boron Concentration versus Cycle Burnup

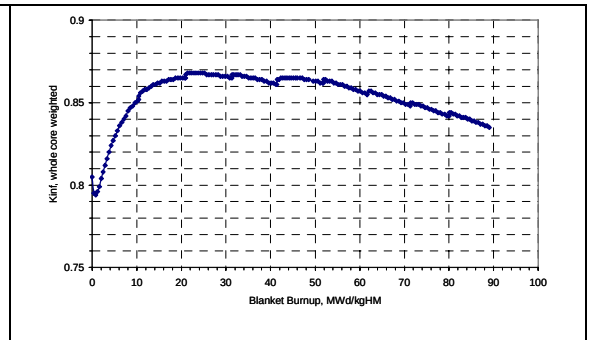

Figure B2.1.22 Blanket Kinf versus Burnup

Table B2.1.6 Cycle Length,

	Cycle 1	2	3	4	5	6	7	8	9	Avg.
Effective Full Power Months	17.9	16.8	16.6	16.4	17.2	16.0	15.6	15.2	15.2	16.3

Reactivity Parameters

Figure B2.1.23 shows the dependence of MTC on cycle exposure for both hot-zero-power (HZP) and hot-full-power (HFP). The WASB MTC is only a little more negative than that of a typical PWR. The Doppler-only power coefficients at BOC, MOC and EOC under critical conditions with equilibrium xenon are given in Figure B2.1.24. In practice, the fuel will change due to depletion, because of fuel swelling and cladding creep, which will affect the fuel temperature. SIMULATE does not consider this effect. Figure B2.1.25 presents the total power defect, including the effect of both moderator and fuel temperatures. The total power defect in the WASB core is higher than a typical PWR core.

The soluble boron worth is given in Figure B2.1.26. It is less than that of a conventional PWR due to the harder neutron spectrum in the WASB core. Thus for a lower excess reactivity at BOC, higher boron concentration is needed as shown in Figures B2.1.21.

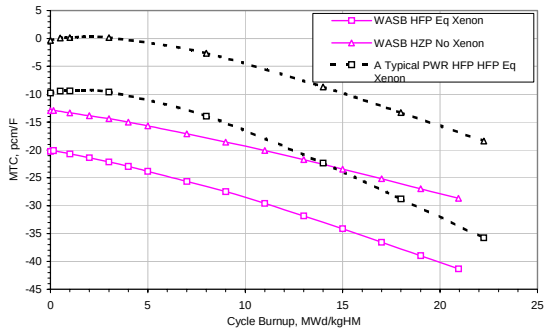

Figure B2.1.23 Moderator Temperature Coefficient

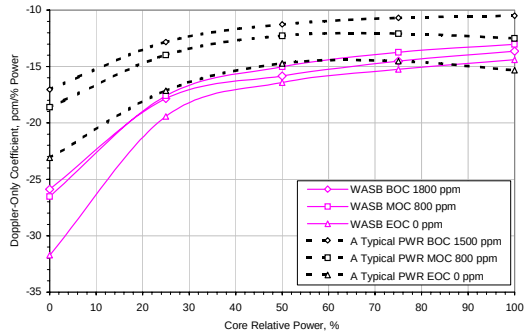

Figure B2.1.24 Doppler Only Power Coefficient

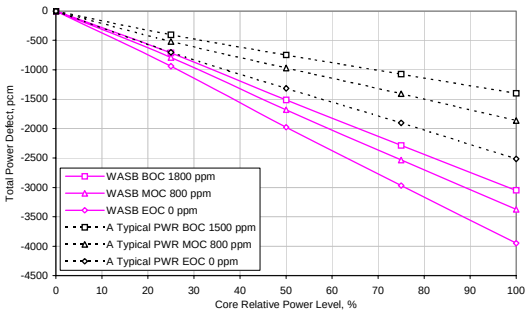

Figure B2.1.25 Total Power Defect

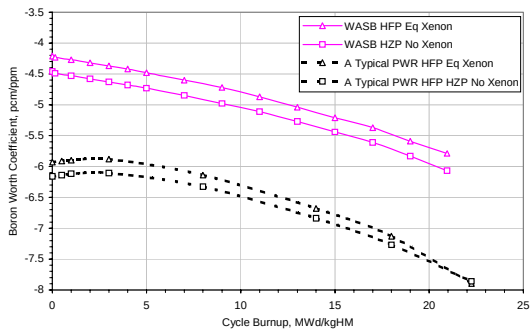

Figure B2.1.26 Soluble Boron Worth

Kinetic Parameters

Table B2.1.7 shows that the effective delayed neutron fractions in the WASB are slightly lower than those of a typical PWR, due to the lower β of U-233. However the values are comparable with the effective β values of MOX LWRs, which are around 0.004 (Kloosterman and Bende, 2000). The prompt neutron lifetime is also slightly lower in the WASB than in a typical PWR.

Table B2.1.7 Effective Delayed Neutron Fraction and Prompt Neutron Lifetime

	WASB		Typical PWR	
	BOC	EOC	BOC	EOC
β	0.0052285	0.0044754	0.006356	0.005218
l*, seconds	1.0513×10-5	1.4412×10-5	1.4351×10-5	1.8935×10-5

Power Distribution and Peaking Factors

Figure B2.1.27 shows the 1/4 core power distributions of the WASB at BOC, MOC and EOC. Maximum power always appears in the fresh seed assemblies at BOC. The relative power sharing between the seed and blanket is also shown in the figure. Changes in the power sharing are very small during core life, although a decrease in the seed power and accordingly an increase in the blanket power are observed. The average power share of the blanket in a cycle is about 35%, and that in the seed is around 65%.

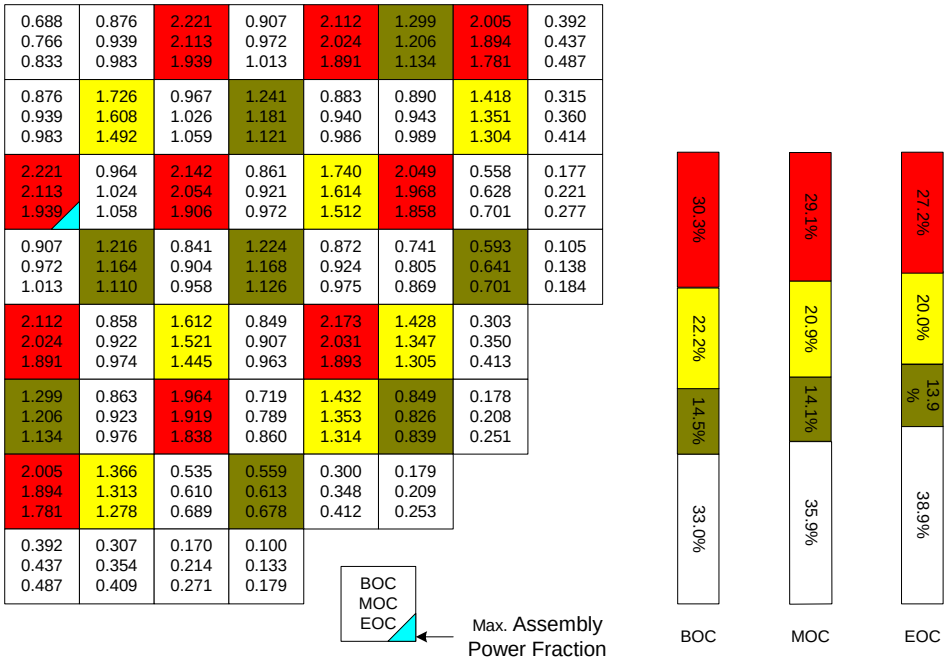

Figure B2.1.27 Relative Assembly Power and Power Sharing Between Seed and Blanket

The $F_{\Delta H}$ and F_Q values over the cycle are shown in Figure B2.1.28. The absolute maximum of each occurs in the fresh seed assemblies at BOC. These maxima (2.5 for FΔH and 3.15 for FQ) although beyond the typical values of 1.65 FΔH and 2.5 FQ for current PWRs, will be found acceptable during Anticipated Operational Occurences because the seed fuel design is quite different from conventional UO2 fuel. The seed fuel uses smaller, annular pellets, therefore the coolant flows at a higher velocity in the seed assemblies and the central fuel temperature remains low. The core average axial power shapes are shown in Figure B2.1.29 and and are quite similar to those in conventional PWRs.

Control Rod Worth

The standard Control rod configuration for the 17×17 lattice is a 24 finger silver-indium-cadmium (80 w/o Ag - 15 w/o In - 5 w/o Cd) Rod Control Cluster Assembly (RCCA). Both

this standard material and enriched B_4C absorber were analyzed for use in the RCCAs of the WASB core.

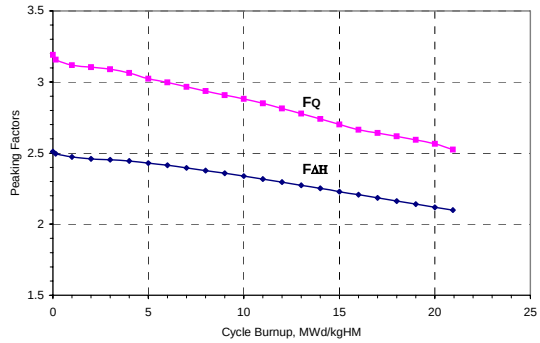

Figure B2.1.28 Changes of Peaking Factors Over Cycle Duration

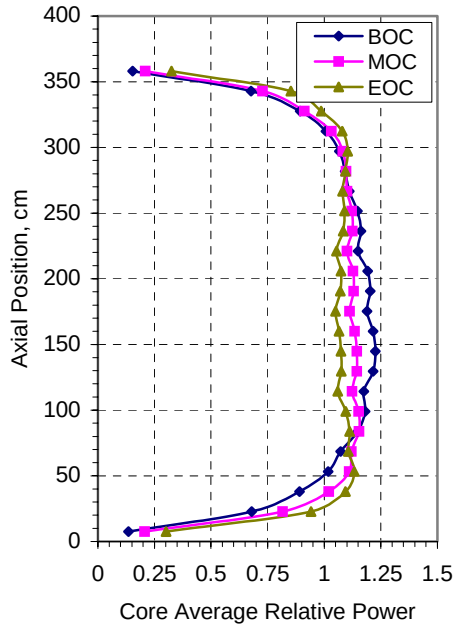

Figure B2.1.29 Axial Power Shapes

Whole core analyses show that in the WASB core, the control rods in the seed have higher worths than those in the blanket. Therefore a new control rod configuration pattern, has been devised so that all except one control rod will be inserted into seed assemblies versus 33 in the standard pattern. Control rod worth comparisons for the different cases are summarized in Table 2.1.8.

Generally speaking control rods with B4C have 20%-30% higher worth than control rods with Ag-In-Cd as shown in Table B2.1.8. The new control rod pattern also results in a significant improvement in control rod worth. Neither the use of enriched boron alone nor use of the altered control rod location pattern alone provides the WASB as much reactivity control as the standard PWR achieves. However, use of both enriched boron and the altered control rod pattern provides the WASB with somewhat more reactivity control than is present in the typical standard PWR. The new pattern requires a redesign of the vessel head of the reactor, which is an added cost in case of retrofitting in existing PWRs. The control rod worth could be further improved if higher enrichment B-10 is used for the poison material.

Table B2.1.8 Control Rod Bank Worth, pcm

	Typical PWR		Standard Pattern				New Pattern			
			AIC*		B4C**		AIC		B4C	
	BOC	EOC	BOC	EOC	BOC	EOC	BOC	EOC	BOC	EOC
Total	7199	N/A	4656	5185	6128	6671	6102	6508	7720	8007

* 80 w/o Ag + 15 w/o In + 5 w/o Cd
** 36.6 w/o B-10 + 63.4 w/o B-11

Boron Concentration

Minimum shutdown boron concentrations are shown in Table B2.1.9. It is obvious that the WASB core with the standard loading pattern of control rods requires more soluble boron for shutdown than the new WASB core design.

Table B2.1.9 Boron Concentration Requirements for Refueling and Startup

Conditions		Boron Concentration, ppm				
		Typical PWR	WASB Standard		WASB New Pattern	
		AIC*	AIC	B4C**	AIC	B4C
Refueling (Keff = 0.95), ARI, Cold		1968	3275	2925	2220	1310
Shutdown (Keff = 0.987), ARI,		1502	2563	2212	1588	783
Shutdown (Keff = 0.981), ARI,		1268	1857	1043	910	< 0
Shutdown (Keff = 0.987), ARO,		2190	3543			
Shutdown (Keff = 0.981), ARO,		2429	3505			
HZP, Keff = 1.0, ARO		2112	3047			
HFP Keff = 1.0 ARO	No Xe, Peak Sm 0 MWd/kgHM	1894	2350			
	Eq Xe and Sm 0.15 MWd/kgHM	1473	1821			

* 80 w/o Ag + 15 w/o In + 5 w/o Cd
** 36.6 w/o B-10 + 63.4 w/o B-11

B2.2 Assembly Thermal Analysis (Task-2)

The unique design of the WASB core has an impact on thermal-hydraulic performance. Whole core neutronic analyses, presented in Section B2.1.2, show that the seed fuel has much higher power than the blanket, especially for the fresh seed fuel. The maximum $F_{\Delta H}$ value of 2.5 in the core found at the BOC, is well beyond the values around 1.5 encountered in conventional PWRs. Hence detailed thermal-hydraulic analyses should be made to check if the WASB core has adequate thermal safety margin during normal or transient conditions. The most widely used criterion for fuel integrity is the departure from nucleate boiling ratio (DNBR) for PWRs. A typical PWR criterion is that the minimum DNBR (MDNBR) is equal to or greater than about 1.3 at an appropriate overpower condition (the limit is dependent on the CHF correlation used). In order to consider normal operating conditions and likely deviation, a conservative approach was used in the analysis carried out using VIPRE-01 (Cuta, et al, 1985). This reference calculation was performed at an overpower of 12% of rated power, at an inlet coolant temperature that is 2 ^{0}C above the expected value, and at a flow rate that is 5% lower than the nominal flow rate.

B2.2.1 Reference Calculation

Preliminary work on thermal-hydraulic design and analysis of the WASB core was focused on the assembly/colorset model (Busse and Kazimi, 2000). Later, a whole core model using VIPRE-01 was developed and the calculations and analyses presented in this section are based on that model.

For a whole core analysis, rod arrays are modeled as sub-channels and lumped sub-channels. In the area around the hottest pin, detailed sub-channel representation is necessary; three or more pitches away, rod arrays can be lumped gradually as lumped rods and sub-channels. Since seed fuel rods and blanket fuel rods have different diameters, it is not advisable to lump them. Therefore, in all calculations, each assembly is treated as one lumped channel.

Figure B2.2.1 shows the normalized power distribution for a typical equilibrium cycle of the WASB core, at BOC, MOC and EOC, in 1/4th of a whole core model. These power distributions are the results obtained by SIMULATE for the WASB core design with burnable poison. Because the power distribution is essentially symmetric in the 1/4th core, the VIPRE 1/8th core model uses the higher power peaking factors for each symmetric assembly, which should be conservative. Figure B2.2.2 shows the normalized pin power distribution in the hottest seed assembly. This is the result obtained from the CASMO colorset model. Note that the normalization includes guide tubes with zero power factors. The hottest pin is at the corner of the assembly and its peaking factor within the assembly is 1.153. Based on this power distribution, a rod and channel numbering scheme, known as the "corner" model, was used to investigate the MDNBR. However the calculation results from the corner model showed that the MDNBR does not occur at the corner of the hottest seed assembly because it is surrounded by much cooler sub-channels of the adjacent blanket assemblies (Todosow, et al, 2003).

0.688 0.766 0.833	0.876 0.939 0.983	2.221 2.113 1.939	0.907 0.972 1.013	2.112 2.024 1.891	1.299 1.206 1.134	2.005 1.894 1.781	0.392 0.437 0.487
0.876 0.939 0.983	1.726 1.608 1.492	0.967 1.026 1.059	1.241 1.181 1.121	0.883 0.940 0.986	0.890 0.943 0.989	1.418 1.351 1.304	0.315 0.360 0.414
2.221 2.113 1.939	0.964 1.024 1.058	2.142 2.054 1.906	0.861 0.921 0.972	1.740 1.614 1.512	2.049 1.968 1.858	0.558 0.628 0.701	0.177 0.221 0.277
0.907 0.972 1.013	1.216 1.164 1.110	0.841 0.904 0.958	1.224 1.168 1.126	0.872 0.924 0.975	0.741 0.805 0.869	0.593 0.641 0.701	0.105 0.138 0.184
2.112 2.024 1.891	0.858 0.922 0.974	1.612 1.521 1.445	0.849 0.907 0.963	2.173 2.031 1.893	1.428 1.347 1.305	0.303 0.350 0.413	
1.299 1.206 1.134	0.863 0.923 0.976	1.964 1.919 1.838	0.719 0.789 0.860	1.432 1.353 1.314	0.849 0.826 0.839	0.178 0.208 0.251	
2.005 1.894 1.781	1.366 1.313 1.278	0.535 0.610 0.689	0.559 0.613 0.678	0.300 0.348 0.412	0.179 0.209 0.253		
0.392 0.437 0.487	0.307 0.354 0.409	0.170 0.214 0.271	0.100 0.133 0.179				

BOC
MOC
EOC

Max. Assembly Power Fraction

Figure B2.2.1 Radial Power Distribution at BOC, MOC and EOC for a WASB Core (Cycle 3: Equilibrium Seed, and Blanket in the Third Seed Cycle)

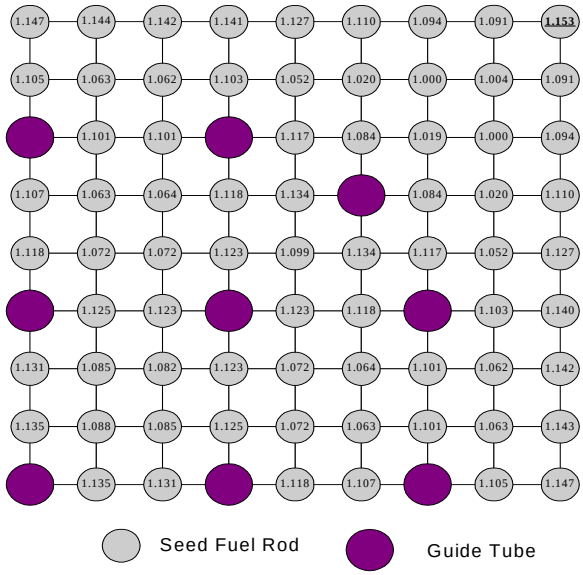

Figure B2.2.2 Normalized Pin Power Distribution in the 1/4th Hottest Seed Assembly for WASB

To investigate this effect, a "center" model was constructed. This includes the details of sub-channels in the area of Channel 10 as shown in Figure B2.2.3. Figure B2.2.3 shows that in this model, the two-sub-channels that receive the highest power from the adjacent four pins are numbered as Channels 1 and 2, and explicit sub-channels are modeled around these two. Figure 2.2.4 shows the channel numbering scheme in a 1/8th core.

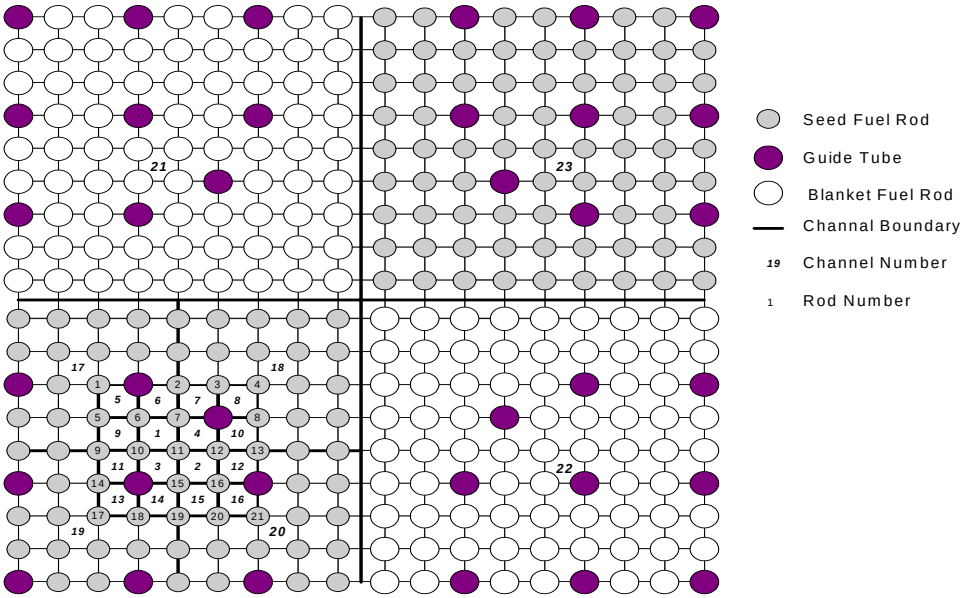

Figure B2.2.3 Rod and Channel Numbering in Hot Colorset

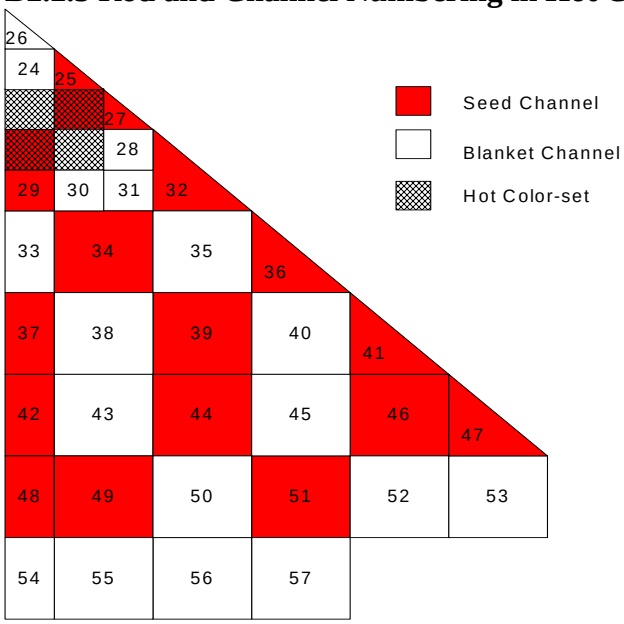

Figure B2.2.4 Channel Numbering in the 1/8th Core Model of VIPRE-01

Table B2.2.1 summarizes the key thermal and hydraulic parameters of the VIPRE-01 model. In order to address transient operation conditions, the core mass flow rate is reduced by 5 % from the normal 17.7 to 16.8 Mg/s, coolant inlet temperature is increased by 2 ^{0}C from the nominal 292.8 to 294.8 ^{0}C and core power is increased from the nominal 3411 MWt to the 112% overpower of 3820.3 MWt. A chopped cosine with peak-to-average ratio of 1.55 is used for the axial power profile. The different fuel and blanket geometries lead to several minor issues. Because the gap width between fuel rods in a seed assembly differs from that in a blanket assembly (their pin diameters are different), the gap width for a lumped channel

between a seed and a blanket assembly is modeled as the average of the two. Furthermore, turbulent mixing between the seed and blanket is not included, which is conservative from the MDNBR point of view. To drive more flow into the seed assemblies, a grid loss coefficient of 2.0 is used in the blanket compared to 0.6 in the seed in order to represent high resistance grids in the blanket compared to standard grids in the seed.

Table B2.2.1 VIPRE-01 Model Key Parameters

Reactor Power	112% overpower (3820 MWt)
Inlet Temperature (^{0}C)	294.8 (Increased by 2 ^{0}C)
Whole Core Coolant Flow Rate (Mg/s)	16.815 (decreased by 5%)
Local Loss Coefficient of Grids	0.6 (Seed), 2.0 (Blanket)
Axial Power Profile	Chopped cosine, peak-to-average ratio = 1.55
Axial Friction Coefficient (Turbulent)	$f_{ax} = 0.32 R_e^{-0.25}$
Turbulent Mixing Model	None
Cross Flow Resistance Coefficient	$K_G = 0.5$
CHF Correlation	W-3L, mixing factor 0.043, grid spacing factor 0.066

Table B2.2.2 shows that the MDNBR in the WASB core at BOC is 1.309, which means that the thermal-hydraulic design of the WASB core is acceptable from a DNBR point of view. The DNBR of 4.439 in Channel 22 shows that the blanket has a very large thermal-hydraulic safety margin (although it is assembly-averaged). Even at the end of cycle, when the blanket share goes from 33% to 39% of power, there remains good margin in that region (3.988 MDNBR). Figure B2.2.5 shows the BOC detailed DNBR distribution in seed and blanket sub-channels using the W3L correlation (Cuta, et al, 1985). It should be noted that the 1.3 MDNBR of the WASB core has been achieved by the use of high resistance grids (modeled by allocating a much higher grid form loss coefficient in the blanket), as a result, more flow is driven into the seed assemblies. The side effect of this method is that the pressure drop in the core becomes higher. For such a core, the pressure drop along the pins, which does not include inlet and outlet form loss, is 0.175 MPa compared to about 0.1 MPa in a standard PWR.

Table B2.2.2 Fuel and Cladding Maximum Temperatures and MDNBR Values

	Seed		Blanket	
	BOC	EOC	BOC	EOC
T_{max} in the Fuel, ^{0}C	1567	1407	966	1023
T_{max} in the Cladding, ^{0}C	436	427	376	378
MDNBR	1.309	1.628	4.439	3.988

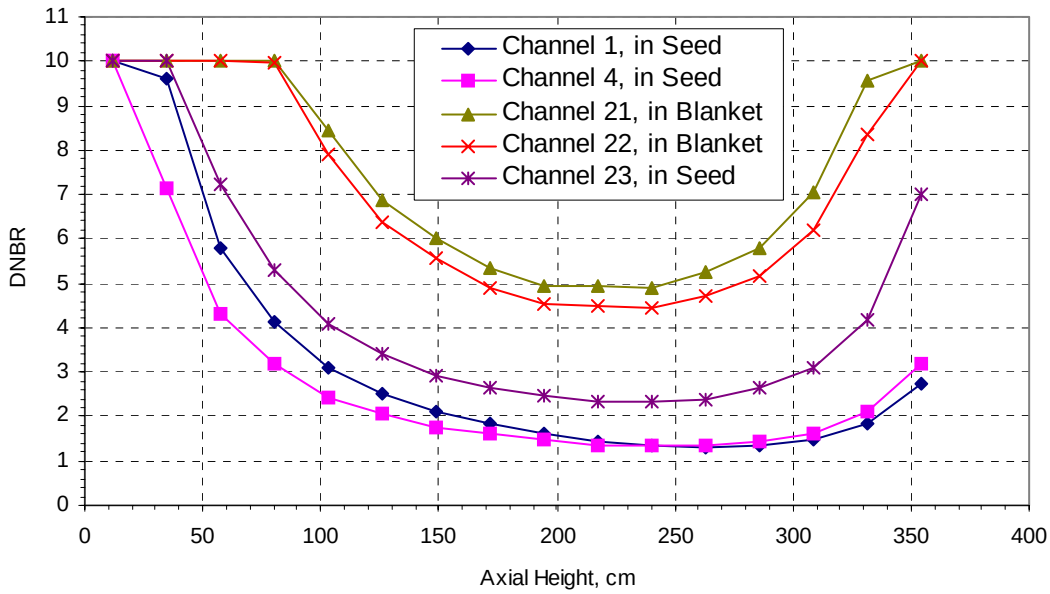

Figure B2.2.5 DNBR in Seed and Blanket Sub-Channels at BOC (DNBR > 10 are depicted as 10)

B2.2.2 Sensitivity of MDNBR to Various Parameters

The sensitivity of the MDNBR to various parameters such as inlet temperature, power, coolant flow rate and form loss coefficient, etc., has been investigated using the VIPRE model discussed earlier. The parameters in Table B2.2.1 are used as the reference parameters. The power distribution at BOC was used in the calculations. All other parameters are unchanged when varying one parameter.

Core Inlet Temperature

The effect of core inlet coolant temperature on MDNBR is shown in Table B2.2.3. It shows that the MDNBR is very sensitive to the inlet temperature. The MDNBR increases as the inlet temperature decreases. Note that the normal inlet temperature is 292.8 ^{0}C. If the WASB core is operated at a lower inlet temperature such as 290.8 ^{0}C, the MDNBR margin will be significantly improved.

Table B2.2.3 Effect of Core Inlet Temperature on MDNBR

ΔT_{in} (^0C)	MDNBR	Channel No.	Rod No.	Axial Position (cm)
-6	1.494	4	12	228.6 - 251.46
-4	1.443	4	12	228.6 - 251.46
-2	1.386	1	7	251.46 - 274.32
Reference, 294.8	1.309	1	7	251.46 - 274.32
+2	1.287	4	12	228.6 - 251.46
+4	1.169	1	7	251.46 - 274.32

Nominal Flow Rate

Table B2.2.4 shows the impact on the MDNBR of varying the core flow rate. Again, the MDNBR will increase as the flow rate increases. However, higher flow rate leads to a higher pressure drop in the core, hence higher pumping power.

Table B2.2.4 Effect of Core Flow Rate on MDNBR

% of nominal flow rate	MDNBR	Channel No.	Rod No.	Axial Position (cm)
90%	1.051	1	7	251.46 – 274.32
95%	1.178	1	7	251.46 – 274.32
Reference, 100%	1.309	1	7	251.46 – 274.32
105%	1.441	4	12	228.6 - 251.46
110%	1.552	4	12	228.6 - 251.46

Nominal Core Power

It is obvious that the MDNBR decreases as the core power increases as shown in Table B2.2.5. It should be noted that the reference case is 12% overpower compared to normal operating power. We can improve the MDNBR by reducing core nominal power; however it is not desirable to run the reactor at a lower power level because of economic considerations.

Table B2.2.5 Core Power Effect on MDNBR

% of Reference Power	MDNBR	Channel No.	Rod No.	Axial Position (cm)
85%	1.772	4	12	228.6 - 251.46
90%	1.622	4	12	228.6 - 251.46
95%	1.478	4	12	228.6 - 251.46
Reference, 100%*	1.309	1	7	251.46 – 274.32
105%	1.150	1	7	251.46 – 274.32

* Taken as 112% of rated power

Form Loss Coefficient

The seed has a much higher power than the blanket, especially for fresh seed assemblies at BOC. The results show that the most constrained rod (where the MDNBR is found) is always located in a seed assembly. The grid form loss coefficient in the blanket is increased in order to redirect more coolant flow into the seed, hence increase the MDNBR. Table B2.2.6 shows that an increase in the loss coefficient of the blanket can effectively improve the MDNBR; however it will also increase the pressure drop in the core.

Table B2.2.6 Effect of Loss Coefficient in Blanket on MDNBR

Loss Coefficient in Blanket*	MDNBR	Channel No.	Rod No.	Axial Position (cm)
0.6	0.985	1	7	251.46 – 274.32
1.0	1.107	1	7	251.46 – 274.32
1.5	1.217	1	7	251.46 – 274.32
Reference, 2.0	1.309	1	7	251.46 – 274.32
2.5	1.394	1	7	251.46 – 274.32

* 0.6 in Seed

Seed Fuel Pin Diameter

The diameters of seed rods and blanket rods, which are 0.9 cm and 1.06 cm respectively, have been optimized from a neutronic rather than a thermal-hydraulic point of view. Although an analysis of the sensitivity of DNBR to the rod diameters should ideally be done by iterating between thermal-hydraulics and neutronics, a preliminary investigation has been carried out by assuming that the power distribution is invariant when the rod diameters change. Since there are two kinds of fuel rods in the core, a sensitivity analysis of rod diameters can be done by changing either the seed rod diameter or blanket rod diameter. However, the DNBR restrictions always come from the seed rods, so changing the diameter of the seed rods will affect both the heat flux and the flow rate in these seed channels and thus directly affects the MDNBR. The results, shown in Figure B2.2.6, show that better thermal-hydraulic performance can be achieved by increasing the seed rod radius by about

10% from the present value of 0.45 cm to about 0.495 cm. Although the large seed rod diameter increases the pressure drop in the seed channels, thus driving coolant flow into the blanket, the accompanying decrease in the surface heat flux is the dominant effect and leads to a larger MDNBR until the rod radius exceeds 0.495 cm, at which point the effect of reduced coolant flow in the seed channel becomes dominant, thus the MDNBR decreases.

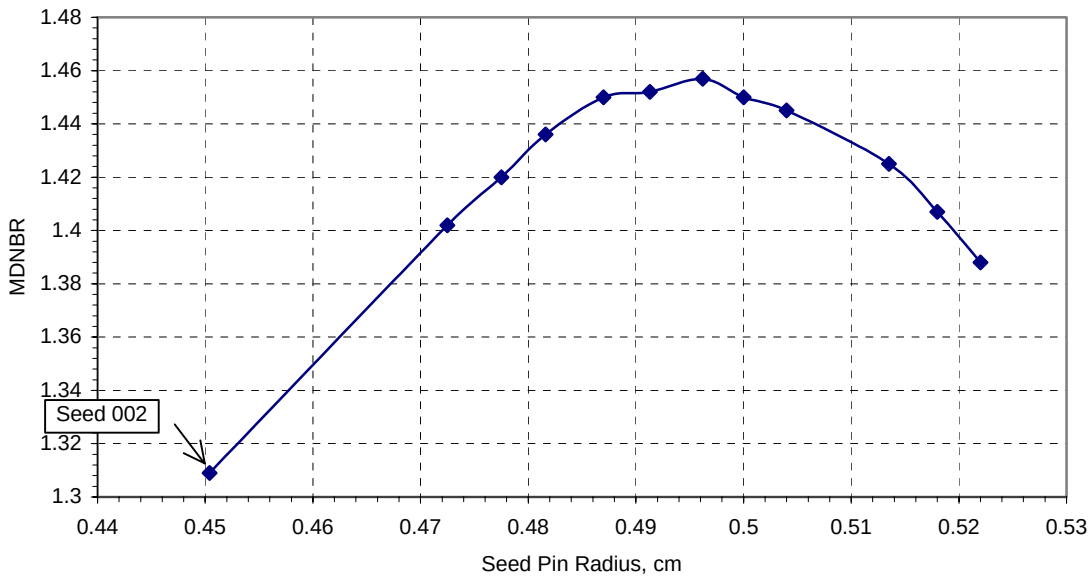

Figure B2.2.6 Sensitivity of DNBR to Seed Fuel Pin Radius

B2.3 Assembly and Fuel Mechanical Design

B2.3.1 Assembly Mechanical Design (Task-3)

As mentioned earlier, both the seed and blanket fuel assemblies of the WASB design consist of 17x17 arrays so that the WASB assemblies may be backfitted into existing PWRs. However, the seed and blanket fuel pin diameters are different from the typical PWR fuel pin diameters and the coolant velocities in the seed and blanket regions are significantly different because more core flow is diverted to the seed region in order to maintain adequate steady-state thermal margin as discussed in Section B2.2. This results in higher core pressure drop in the WASB design compared to a typical all uranium PWR design as shown in Tables B2.6.2 and B2.6.3 in Section B2.6 (Safety Analyses). So it is important to get estimates of "Hold-down" or "Lift-off" forces for both the seed and blanket assemblies.

A simple force balance as given below is the basis of lift-off force calculation:

$$F_{lift\text{-}off} = F_{friction} + F_{pressure} + F_{spacers} - W_{assembly} \qquad \text{(B2.3.1)}$$

The first term in the R.H.S represents the upward skin friction or drag force on the surface of the fuel pins, the second term represents the upward pressure force caused by the core pressure drop, the third term represents the additional upward pressure force due to the spacers and the last term represents the downward weight force of the assembly. Flow parameters as presented in Table B2.6.3 have been taken for the calculations. It has been assumed that the grid spacers block about one-third of the flow area in the seed assemblies, whereas the spacers in the blanket assemblies block about two-thirds of the available flow area in those assemblies. This is consistent with the requirement that substantial amount of flow be diverted from the blanket assemblies to the seed assemblies.

The results for 100% full power condition are shown in Table B2.3.1 below.

Table B2.3.1 Results of Lift-off Force Calculations for Seed and Blanket Assemblies

Assembly Type	$F_{friction}$ (Newton)	$F_{pressure}$ (Newton)	F_{spacer} (Newton)	$W_{assembly}$ (Newton)	$F_{lift\text{-}off}$ (Newton)
Seed	1420	4192	1211	4468	2355
Blanket	1064	5815	1703	7989	593

It can be seen that the "heavier" blanket assemblies will require less "Hold-down" force which is to be expected.

B2.3.2 Fuel and Cladding Performance (Task-4)

Design of reliable WASB fuel and cladding presents a challenge for both the seed and blanket assemblies. The seed, operating at a much higher linear power than the conventional PWR fuel, has to be designed to prevent excessive release of fission gas,

which would over-pressurize the fuel rods internally. It must also be designed to prevent excessive corrosion of the outside surface, i. e., cladding, of the fuel rods. The blanket, although operates at a much lower linear power than the typical PWR fuel, is expected to remain in-core for up to nine 18-month cycles, equivalent to about 13 calendar years. Therefore, it must also be designed to prevent excessive corrosion on the outside surface during its long residence time. Fission gas release may also be a problem because of the high burnup of the blanket, but is expected to be less of a problem than corrosion because of the low linear power and, therefore, low temperature of the fuel material.

The seed and blanket consist of two types of fuel, and both reach very high burnups. The UO_2 seed fuel would reach up to a batch average burnup of 145 MWd/kgHM and the ThO_2/UO_2 blanket fuel would reach up to 88 MWd/kgHM. The fuel behavior code, FRAPCON3-ThHB (Long, et al, 2002), a modified version of NRC's FRAPCON-3 code, which has the capability of modeling high burnup uranium fuel and thorium fuel, was used to analyze the performance of these fuels.

FRAPCON Model

The FRAPCON code is designed to perform the steady-state fuel rod calculations. The code uses a single channel coolant enthalpy rise model. Key parameters of the seed and blanket fuel used in the present study are shown in Table B2.3.2 below.

Since the core analyses showed that the power history of each batch of fuel was relatively uniform over each cycle, a constant power history approximation, as shown in Figure B2.3.1, was used in the fuel behavior analysis for each cycle. The seed fuel rod experiences a decreasing power during three cycle operation, whereas the power of the blanket rod is approximately constant over its whole lifetime. Three axial power shapes at BOL, MOL and EOL for the seed and blanket fuel, which were obtained from the SIMULATE code calculations for the whole core, have been used in the FRAPCON analysis.

Table B2.3.2 WASB Fuel Parameters for FRAPCON Model

Parameter	Seed	Blanket
w/o of UO_2 in Fuel	100%	13%
U-235 Enrichment in U	20%	10%
Fuel Rod Radius, cm	0.4504	0.53
Cladding Thickness, cm	0.0572	0.0572
Gap, cm	0.0082	0.0082
Void Radius, cm	0.22	0
Fuel Density	94%	94%
Plenum Length, cm	40	40
Initial Fill Gas Pressure, Pa	10^6	10^6
Pitch, cm	1.26	1.26
Inlet Coolant Temperature, K	565.95	565.95
Coolant Mass Flux, kg/m^2s	4450	3230

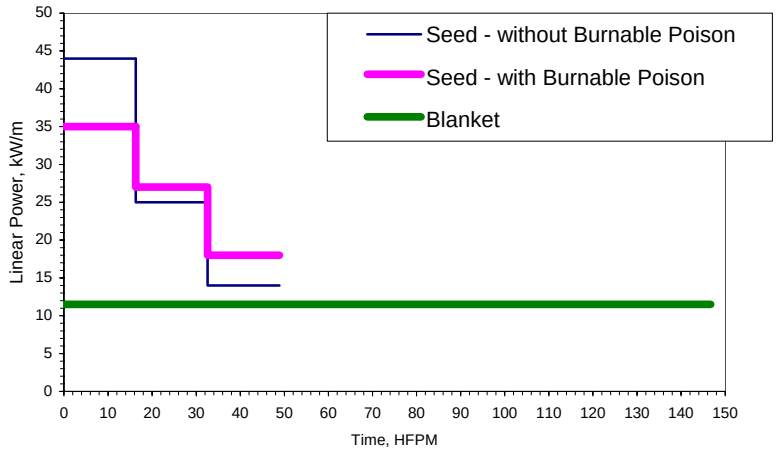

Figure B2.3.1 Assembly Average Power Histories Used in Fuel Behavior Analysis

Results and Discussion

Figures B2.3.2 and B2.3.3 show the calculated fission gas release and internal pressure, respectively, for the seed fuel with and without burnable poison. The burnable poison effectively restrains fission gas release at the early stage of fuel irradiation because of the lower power operation. However at high burnup, the difference is small. The reason is that as the average burnup approaches 145 MWd/kgHM, the fission gas release is mostly a function of burnup and a large portion of fission gas will be released regardless of the power history. Thus with the present neutronics, power history and fuel rod design, a large fraction of the fission gas would be released in the seed fuel, and the internal pressure would exceed the system pressure of 15.5 MPa.

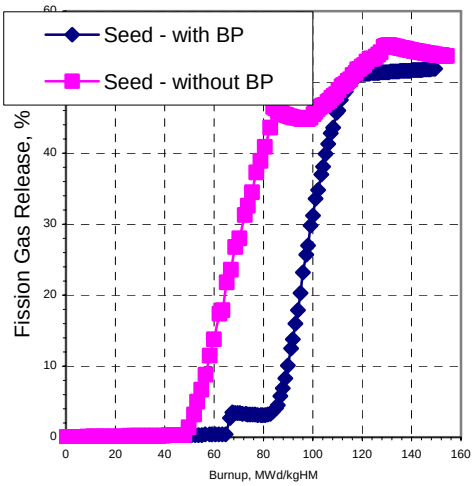

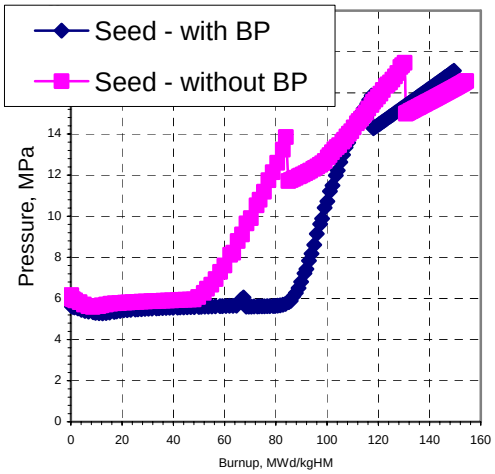

Figure B2.3.2 Fission Gas Release in Seed **Figure B2.3.3 Internal Pressure in Seed**

In order to reduce the internal pressure, the plenum volume was increased three times the current value. Figure B2.3.4 shows that increasing the plenum length from 0.4 m to 1.2 m can significantly reduce the internal pressure at EOL. However, adding 0.8 m to the fuel pin length (20% of current length) will increase the core pressure drop, which may not be easily

accommodated in current reactors. The impact of such a change needs to be investigated further.

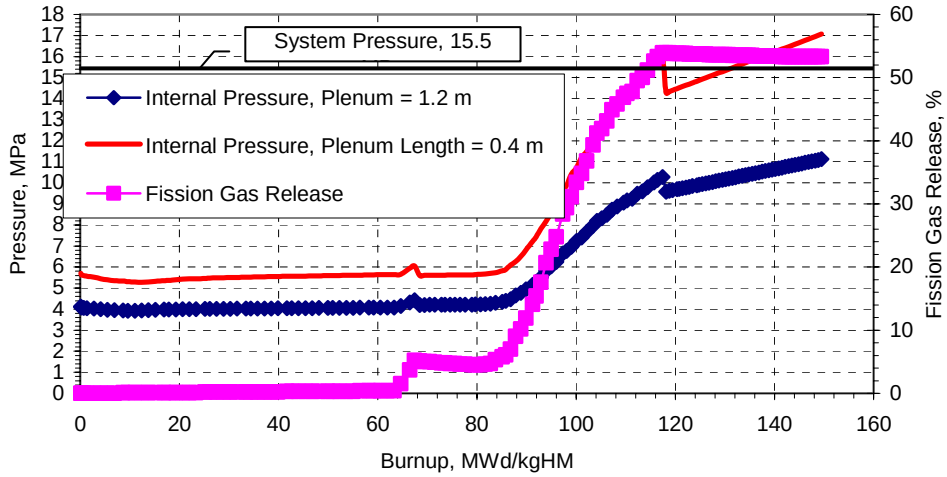

Figure B2.3.4 Effect of Plenum Length on Internal Pressure in Seed Fuel

Similarly, the blanket fuel has been analyzed using FRAPCON-ThHB. The results in Figure B2.3.5 show that the blanket fuel performance is much more favorable, as fission gas release and internal pressure start to rise significantly only near the end of life. If the residence time of the blanket in the core is reduced to only seven or eight cycles of operation due to neutronic reactivity limitations, the blanket behavior would be even better.

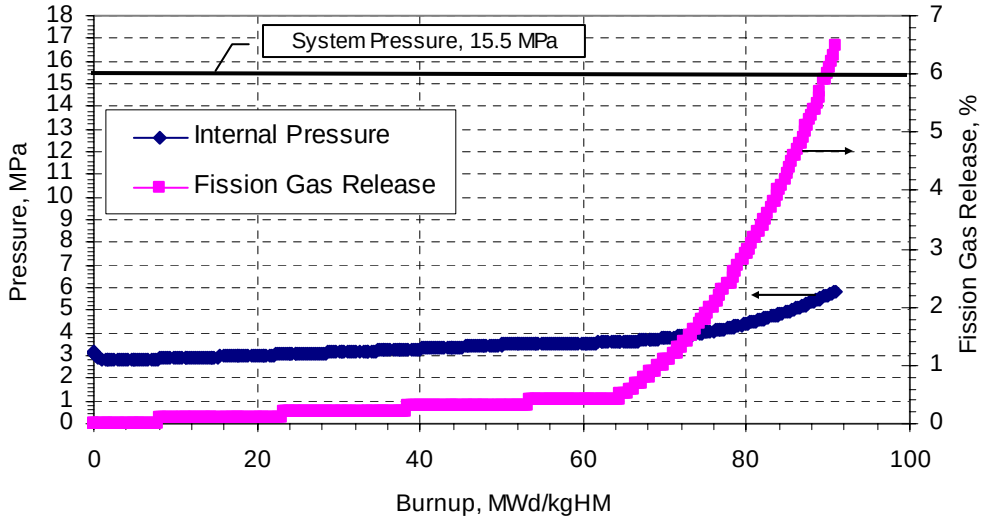

Figure B2.3.5 Fission Gas Release and Internal Pressure in Blanket Rod

Corrosion of seed and blanket cladding is an important issue since corrosion is a function of both the surface temperature and the time that the cladding is exposed to that temperature. The calculated (FRAPCON-ThHB) oxide thicknesses for both the seed and blanket fuel rods with Zircoloy-4 as the cladding material were well above the limit of 150 microns. The more advanced material M5, now coming into use in commercial PWRs, was then assumed

as the cladding material. M5 is less sensitive to temperature; exhibits less data scatter than Zr-4, and did not show any irradiation or high burnup transition up to 64 MWd/kgHM (Willse, 2000). Figures B2.3.6 and B2.3.7 show the expected oxide thickness on the outside surface of the seed and blanket fuel rods at EOL as a function of axial position. The oxide thickness for M5 is expected to be much lower than that for Zr-4. However, the model used for the M5 cladding in FRAPCON-ThHB is a simple one and it needs further verification (Long, et al, 2002).

The blanket is expected to experience more corrosion than the seed because of the three times longer exposure time. Since a typical corrosion film-thickness limit is on the order of 100 microns, Figures B2.3.6 and B2.3.7 indicate that an advanced cladding material like M5 can deliver good corrosion performance, with large margins for the WASB fuel.

The more demanding power history of the seed and the longer residence time of the blanket bring challenges to the thermal and mechanical performance of fuel rods. The calculated results show the internal pressure of the seed rod is more of a concern than that of the blanket because the large expected fission gas release in the seed fuel leads to an internal pressure greater than the system pressure at EOL. Further analysis shows that the internal pressure can be reduced if a longer plenum is used for the seed fuel rods. The calculated results also indicate that cladding material with improved corrosion resistance such as M5 is required to prevent excessive cladding corrosion.

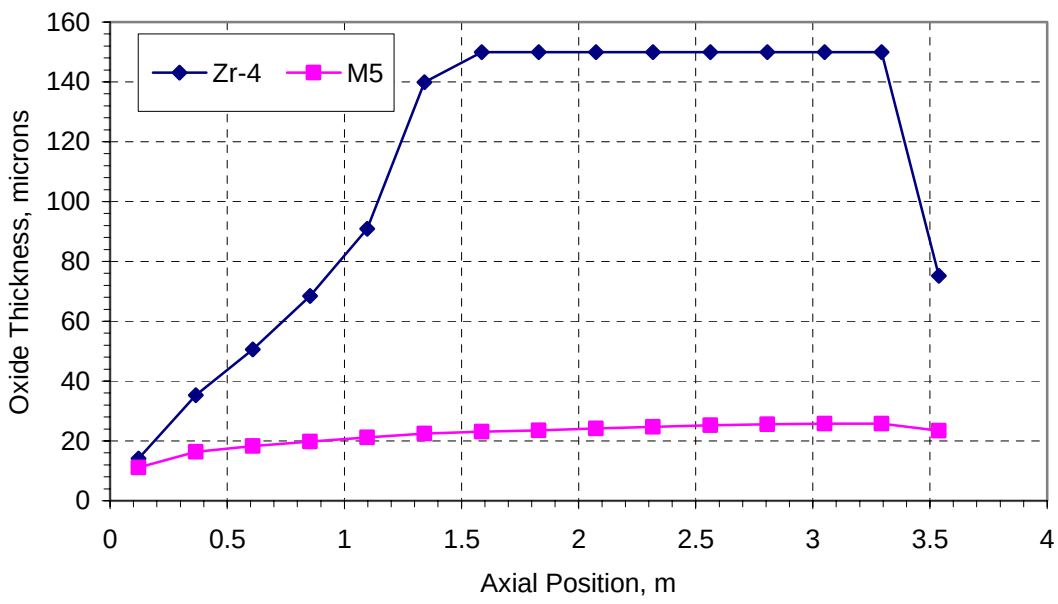

Figure B2.3.6 Corrosion of Poisoned Seed Rod at Discharge of 4.5 Years

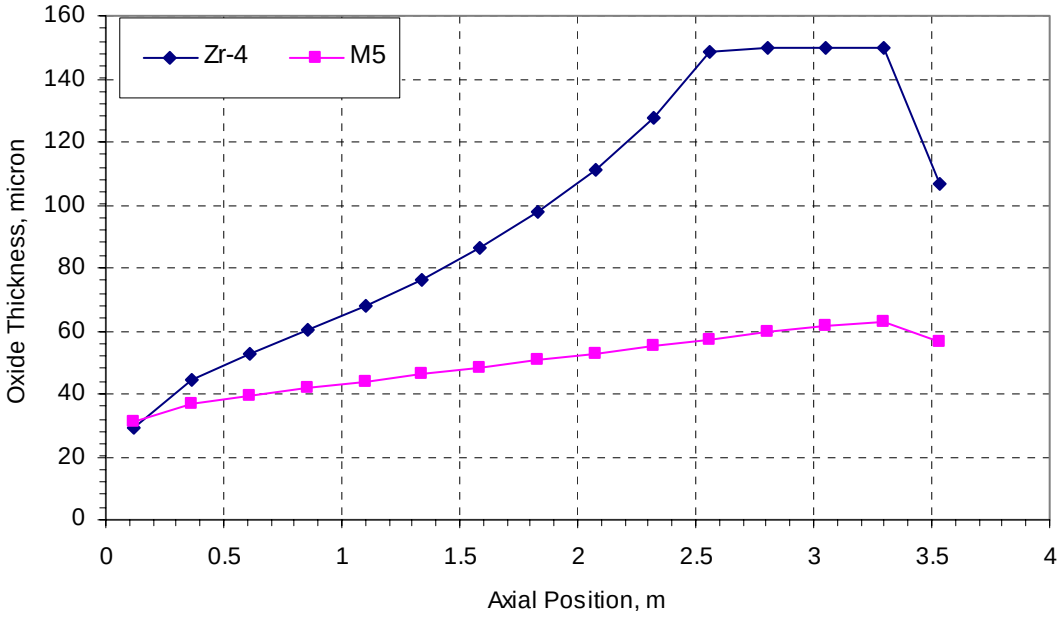

Figure B2.3.7 Corrosion of Blanket Rod at Discharge of 13.5 Years

B2.4 Fuel Cycle Cost (Task-5)

The fuel cycle of the WASB core includes two separate fuel material flows: seed and blanket. The fuel management schemes and burnups are different for each flow. Therefore there are two streams of cash flows for fuel cycle materials and services during the reactor lifetime. A fuel cycle cost calculation model for the WASB core has been developed based on the OECD' levelized lifetime cost methodology (OECD/NEA, 1994).

The levelized cost methodology discounts the time series of expenditures and incomes to their present values in a specified base year by applying a discount rate. Applied to fuel cycle costs, the levelized lifetime methodology provides costs per unit of electricity generated, which are the ratios of the total present value lifetime expenses to total present value expected output. When this method is applied, the economic merits of different fuel cycles are derived from the comparison of their respective average lifetime levelized costs. Technological and economic assumptions underlying the results are transparent and the method allows for sensitivity analysis.

The cash flow for fuel cycle materials and services commences before the fuel starts to generate electricity and continues well after the fuel is discharged. In order to calculate the overall fuel cycle cost, the magnitude of each component cost and the appropriate point in time that it occurs must be identified. The quantities of fuel required and the timing are obtained from the reactor neutronics calculations and assumptions about capacity factor and length of refueling outage. The quantities of materials and services are adjusted to allow for process losses in the various component stages of the nuclear fuel cycle and then multiplied by the unit costs to obtain the component costs.

The component costs for a fuel batch are the sum of a "front end" cost, and a "back end" cost. The front end cost consists of four components:

Cost of fabrication: calculated as either the fabrication cost per unit of heavy metal loaded times the mass of heavy metal loaded into the core (from the neutronics calculation).

Fabrication costs for assemblies of enriched urania fuel and thoria fuel are expected to differ. In this analysis, the fabrication price for urania assemblies is taken as $250 per kgU for a conventional PWR, that of the more highly enriched urania seed fuel with annular pellets as double this value - $500.kgU, and that of 300 $/kg is used for the blanket fuel fabrication unit cost assuming the ThO2/UO2 blanket fuel is more expensive to fabricate. The fabrication cost for each batch is assumed to be paid three months before insertion of the fuel batch into the reactor.

As is usual in the industry, fabrication costs include the cost of the chemical and physical transformations needed to get the fuel material into pellet form, and the cost of delivering finished fuel assemblies to the nuclear reactor.

Cost of enrichment: calculated as the product of the unit price for enrichment services (expressed as dollars per separative work unit or SWU), and the number of SWU required. The number of SWU is obtained as the product of the mass of enriched uranium loaded during fabrication and the SWU to product ratio. The SWU-to-product ratio is obtained from tables or formulas, and is a function of the fuel enrichment, the enrichment of the material fed into the process, and the enrichment of the waste material (tails), assumed here to be 0.25 w/o. Enrichment is the processing of increasing the uranium enrichment from its "feed" value, assumed here to be 0.711 w/o characteristic of natural uranium, to the enrichment needed in the fuel pellets. Enrichment costs apply only to urania. There is no enrichment cost for thoria. The enrichment unit price used in this study is $80/SWU. The enrichment cost for each batch is assumed to be paid six months before insertion of the batch into the reactor.

Cost of conversion: calculated as the product of the unit price for conversion services and the mass of heavy metal converted. The mass of heavy metal converted is the product of the feed-to-product ratio and the mass of uranium or thorium loaded. The feed-to-product ratio is related only to the enrichments used, and is the ratio of (product enrichment less tails enrichment) to (feed enrichment less tails enrichment). For thorium the feed-to-product ratio is unity.

Conversion prices for uranium and thorium are taken as 6$/kgHM in this study. This is approximately the commercial price for uranium conversion as of this report. The conversion cost for each batch is assumed to be paid three months before insertion of the fuel batch into the reactor.

Cost of uranium or thorium: calculated as the product of the unit price for uranium or thorium, and the mass of uranium or thorium required. As in the case of conversion, the mass of uranium is the product of the feed-to-product ratio and the mass of uranium loaded. For thorium, the mass required is the mass loaded, and the feed-to-product ratio is unity.

The price of natural uranium and natural thorium are taken as $50/kgHM in this study. This is approximately the commercial price for uranium as of this report. The uranium cost for each batch is assumed to be paid twelve months before insertion of the fuel batch into the reactor, and the thorium cost is assumed to be paid six months before insertion of the fuel batch into the reactor.

The back-end cost consists of two components:

Cost of spent fuel storage: calculated as the product of the cost of temporary storage in units of dollars per assembly and the number of assemblies stored. A cost of $50,000 per assembly is used here. The storage cost for each batch is assumed paid on discharge of the batch from the reactor.

Cost of spent fuel disposal: calculated as the product of the price of disposal per unit heavy mass of fuel and the mass of fuel disposed. A value of $500/kgHM is used in this study. The disposal cost for each batch is assumed paid on discharge of the batch from the reactor.

Discounting of Cash Flow and Electrical Generation

All the component costs during the life of the reactor (L) are discounted back to a selected base date t_0 and added together in order to arrive at a total fuel cost in present value terms. In addition, because the neutronic analysis utilized an equilibrium cycle (the initial cycle included not only a fresh seed batch, but also a once-burned and a twice-burned batch), the initial unamortized present value of these burned batches is added to the costs and the final unamortized present value of burned seed batches remaining in-core after 9 cycles is subtracted.

Because electricity is generated more or less continuously during the life of the reactor, the discrete annual discount rate r is then replaced by $r' = \ln(1+r)$, the equivalent continuous discount rate, and the discount factor is replaced by the exponential form:

$$\frac{1}{(1+r)^{t-t_0}} = e^{-r'(t-t_0)} \qquad \text{(B2.4.1)}$$

Economic Assumptions and Result Analysis

Based on the model developed above, a fuel cycle cost analysis spreadsheet has been developed for the seed and blanket. The component unit cost assumptions are summarized in Table B2.4.1. The lead time to irradiation for each component is shown in Table B2.4.2. It should be noted that the lag time to discharge for spent fuel storage is zero in the calculations. In addition, some important assumptions are:

1. Annual continuous discount rate is 8%;
2. Plant thermal efficiency is 33.7%;
3. The refueling period costs are neglected. Thus, the impact of different capacity factors among the various cycle lengths is not accounted for.

Table B2.4.1 Component Unit Costs

Thorium	50 $/kgTh
Natural Uranium	50 $/kgU
Conversion	6 $/kgHM
Enrichment	80 $/kgSWU
Fabrication (UO_2 – PWR)	250 $/kgU
Fabrication (Seed)	500 $/kgU
Fabrication (Blanket)	300 $/kgHM
Spent Fuel Storage	50000 $/Assembly
Spent Fuel Disposal	500 $/kgHM

Table B2.4.2 Lead and Lag Time to Irradiation, months

U_3O_8 (Natural Uranium)	12 (time to irradiation)
Thorium	6 (time to irradiation)
Conversion (UF_6)	6 (time to irradiation)
Enrichment	6 (time to irradiation)
Fabrication	3 (time to irradiation)
Spent Fuel Storage	0 (time after discharge)
Spent Fuel Disposal	90 (time after discharge)

In the fuel cycle cost calculations, the average discharge burnup of the seed fuel is 145 MWd/kgHM and the blanket fuel is at 88 MWd/kgHM. The reference PWR is an all-U PWR case, the enrichment of U-235 in uranium is 4.5 w/o and the discharge burnup is 50 MWd/kgHM.

Table B2.4.3 and Figure B2.4.1 show the fuel cycle cost comparison between the WASB and the reference PWR. It can be seen that, under the above assumptions, the total WASB fuel cycle cost is about 2% less than that of the all-U fuel cycle, but is about 9% more expensive than the all-U fuel cycle without including the disposal cost. The major contributions to the fuel cycle cost are from the enrichment cost and the uranium ore purchase cost for both cases. The enrichment cost of the WASB is 35% more expensive than that of the all-U case. The WASB is more economic in respect to fabrication cost than the reference case: about 77% of the reference all-U case due to less fuel refueling. The WASB has lower spent fuel storage cost than the all-U case due to reduced spent fuel assembly discharge. Note that the significant advantage of the WASB is the spent fuel disposal cost: it amounts to about one-third of the reference all-U case. However, unlike the per kg basis used in the Table 2.4.1 calculation the U.S. DOE charges the fixed value of 1 mill/kWe-hr for spent fuel disposal. The blanket fuel cycle cost is only about 15% of the seed. It should be noted that this analysis ignored differences in burnable poison and soluble boron needs, which affect the fuel cost, also ignored in this analysis are any differences in the outage time associated with refueling.

Table B2.4.3 Fuel Cycle Cost, mills/kWe-hr

Component	Reference PWR	WASB		
		Seed	Blanket	
			U	Th
Purchase	1.63	1.57	0.13	0.03
Conversion	0.19	0.19	0.01	0
Enrichment	1.53	1.93	0.14	0
Fabrication	0.75	0.34	0.24	
Front End Cost	4.10	4.03	0.55	
Spent Fuel Storage	0.28	0.15	0.02	
Total	**4.38**	**4.76**		
Spent Fuel Disposal	0.72	0.16	0.07	
Total, (+ disposal)	**5.10**	**4.99**		

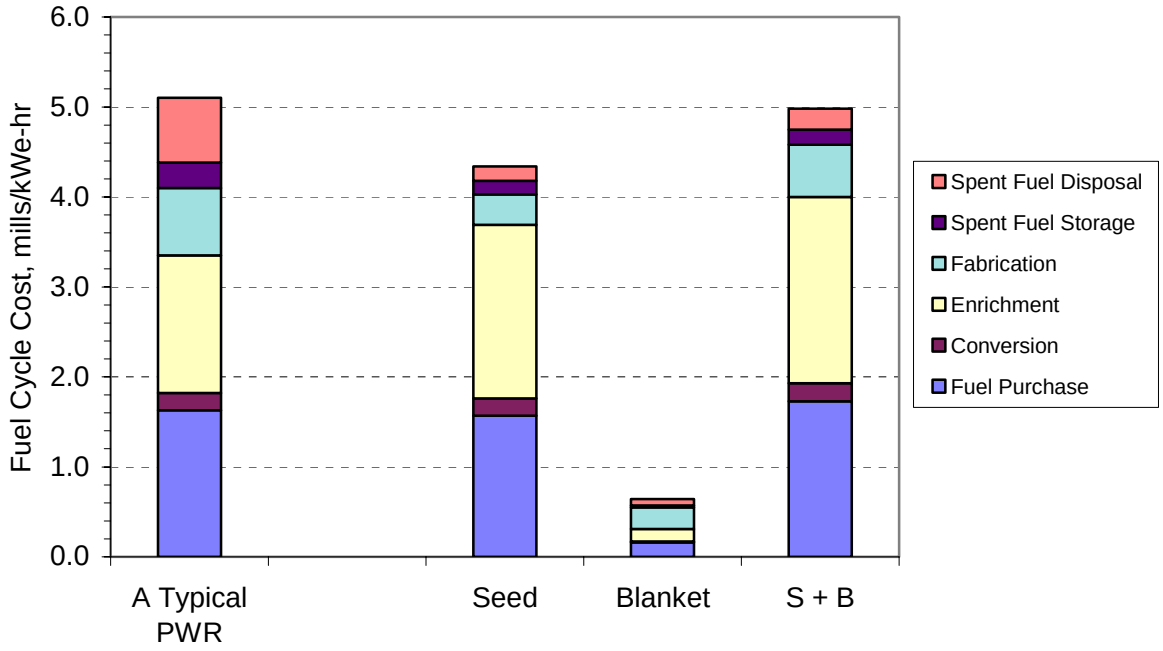

Figure B2.4.1 Comparison of Fuel Cycle Costs

Sensitivity Analysis

Figure B2.4.2 shows the fuel cycle cost of the WASB changes as a function of the uranium ore unit cost. It indicates that the fuel cycle cost is very sensitive to the natural uranium cost. For example, the fuel cycle cost will increase by 1 mill/kWe-hr if the uranium unit cost increases from 50 $/kgU to 80 $/kgU.

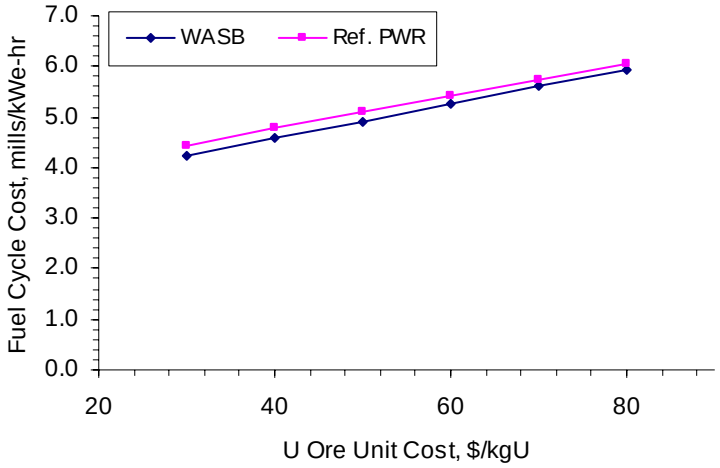

Figure B2.4.2 Fuel Cycle Cost vs. U Ore Unit Cost

Figure B2.4.3 shows the impact of varying the separative work unit (SWU) cost on the fuel cycle cost. The fuel cycle cost increases as the SWU cost increases. The slope of the WASB curve is greater than that of the reference case, which means the SWU unit cost has greater impact on the WASB fuel cycle cost because of the greater SWU requirements in the WASB fuel. It can be seen that at 97 $/kgSWU, the WASB fuel cycle cost is equal to the all-U fuel cycle. In the long term it can be predicted that isotopic separation costs should become cheaper. This will further reduce the fuel cycle cost of the WASB, which will make the WASB more competitive.

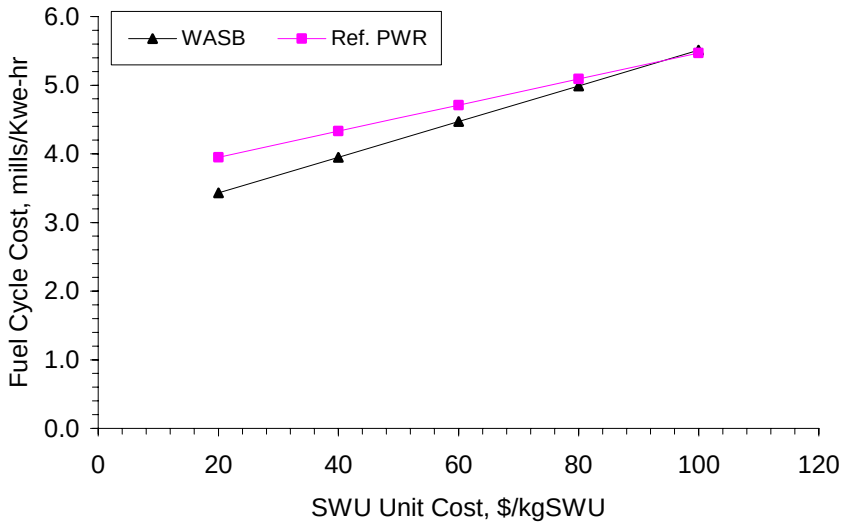

Figure B2.4.3 Fuel Cycle Cost vs. SWU Unit Cost

The fuel cycle cost is extremely insensitive to the seed fuel fabrication unit cost. Figure B2.4.4 shows that the waste disposal cost of the conventional all-U case is more sensitive to the disposal unit cost than the WASB fuel cycle because the WASB core has much less waste production. The WASB fuel cycle will be more competitive than the reference case if

the disposal unit cost increases. However, the disposal cost is not only dependent on the disposal unit cost, but also on the assumption of the lag time for disposal (measured from discharge). The disposal cost will decrease when the lag time increases.

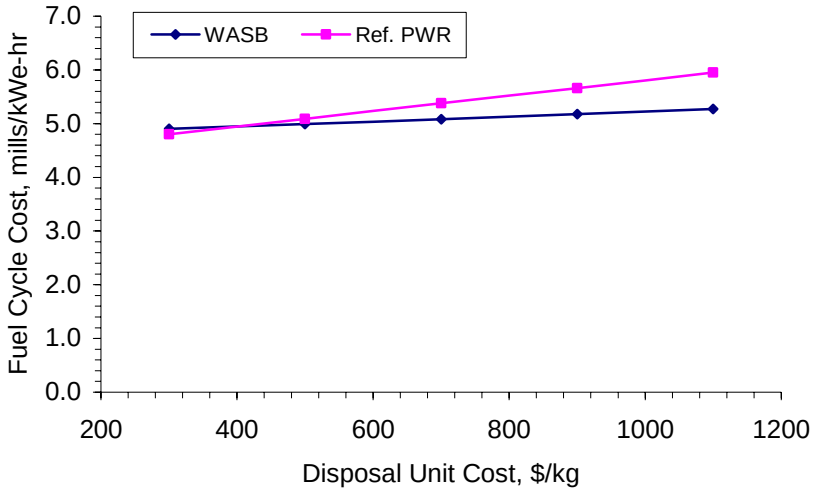

Figure B2.4.4 Fuel Cycle Cost vs. Spent Fuel Disposal Unit Cost

The discount rate effect on the fuel cycle cost is shown in Figure B2.4.5. The WASB cost increases more quickly than the reference all-U case. At the discount rate of about 9.5% per year the fuel cycle cost of the WASB is equal to that of the reference all-U case. Above this point, the WASB fuel cycle cost is more expensive than the all-U case. Note that the cost here is based on a per kilogram waster disposal fee, not the current 1 mill/kWe-hr fee.

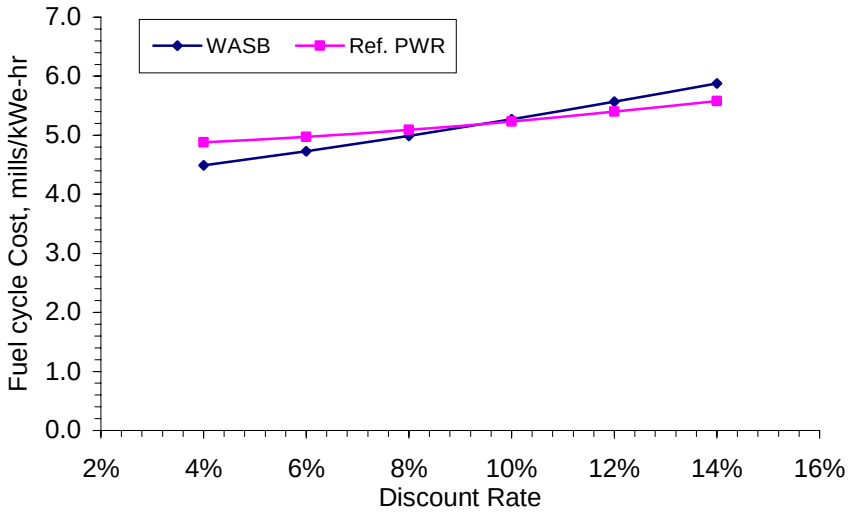

Figure B2.4.5 Fuel Cycle Cost vs. Discount Rate

There are uncertainties in the fuel cycle component unit costs, which will affect the calculated fuel cycle cost calculation results. The results show that the major costs in the fuel cycle cost are the fuel uranium purchase cost and the enrichment cost, which are more

than half of the total cost. It can be concluded that the WASB fuel cycle is nominally less expensive than conventional PWRs with respect to fabrication cost, spent fuel storage and disposal costs. However, the front end fuel cycle cost of the WASB is about 12% more expensive than conventional PWRs because of its greater SWU requirements. In the very long term isotopic separation costs should become cheaper and uranium more expensive, which will help eliminate this difference. In addition, the fuel cycle cost of the WASB design has two contributors: the seed and the blanket. The seed fuel is much more expensive than the blanket fuel: the blanket fuel cycle cost is only about 13% of the total cost.

B2.5 Waste (Spent Fuel) Characteristics and Non-Proliferation Performance (Task-6)

B2.5.1 Spent Fuel Characteristics

Spent Fuel Discharge Rate

One third of the seed assemblies are refueled every cycle, and all the blanket assemblies are refueled every nine cycles. The seed assembly discharge burnup is about 145 MWd/kgHM, and the blanket is at 88 MWd/kgHM. The WASB discharges nearly 40% fewer assemblies per GWe-yr than does a typical 18 month cycle PWR, and the discharged mass of heavy metal is about half that of a typical PWR, as shown in Table B2.5.1.

Table B2.5.1 Spent Fuel Discharge Rate

	WASB			Typical PWR
	Seed	Blanket	S + B	
Assemblies/GWe-yr	16.2	7.0	23.2	37.3
MTHM/GWe-yr	4.5	3.8	8.3	17.4

Radioactivity and Decay Heat

Radioactivity and decay heat from the seed and blanket spent fuel were studied using MCODE (Xu, 2002) depletion calculations and ORIGEN (Cochran and Tsoulfanidis, 1999) to determine isotopic buildup and decay after discharge.

Figures B2.5.1 to B2.5.3 show the radioactivity, and Figures B2.5.4 to B2.5.6 the heat load, of the WASB spent fuel. As a function of decay time, they behave in generally similar ways. Per unit heavy metal in the seed, as shown in Figures B2.5.1 and B2.5.4, both are about twice that of conventional UO2 fuel but the total heavy metal per seed assembly is only about half of that of conventional fuel, so the activity and heat load per assembly are both comparable to that of conventional fuel, as shown in Figures B2.5.2 and B2.5.5. Per unit energy generated, Figures B2.5.3 and B2.5.6 show that WASB produces both less radioactivity and less heat generation than conventional fuel in the short term (up to about five years after discharge), and a comparable amount in the near term (< 10,000 years). Between 10,000 and 1,000,000 years, there is a local peak in both due to the decay products of U-233 in the blanket, controlled by the nearly 160,000 year half life of the U-233. However, by this time activity and heat generation are at relatively low levels.

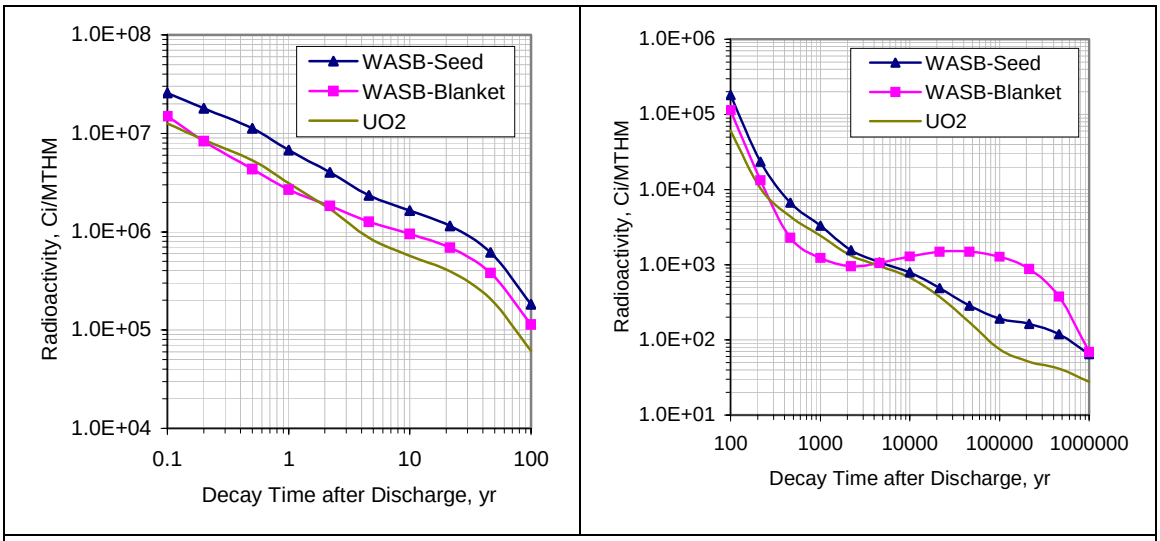

Figure B2.5.1 Radioactivity of the WASB Spent Fuel per Mass of Initial Heavy Metal

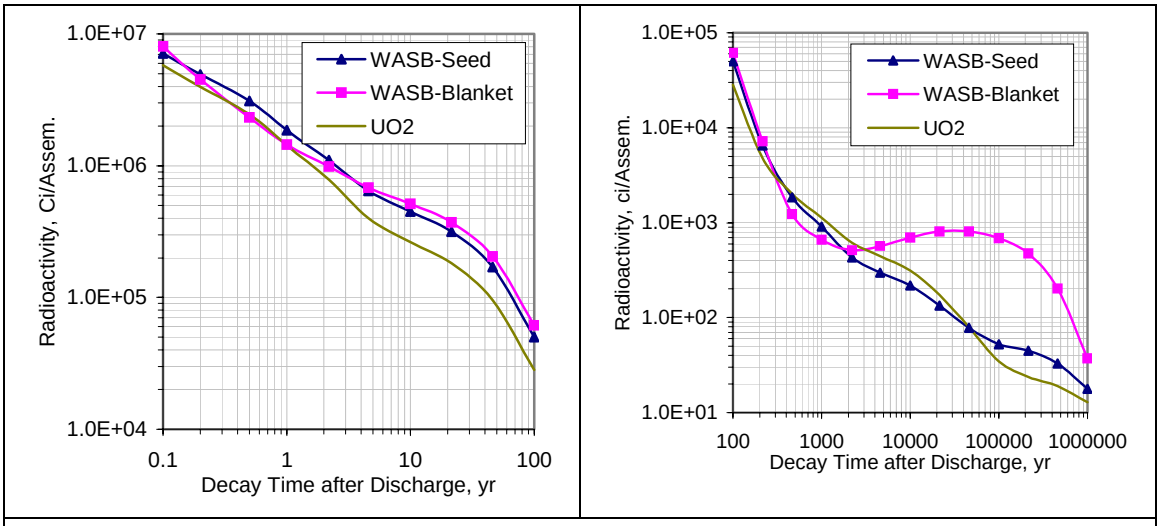

FigureB2.5.2 Radioactivity of the WASB Spent Fuel per Assembly

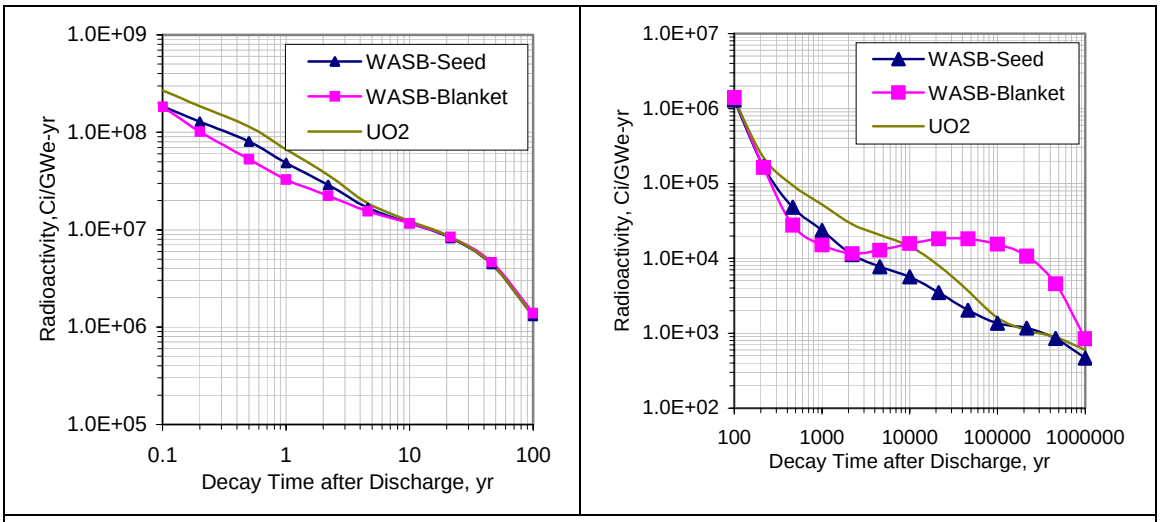

Figure B2.5.3 Radioactivity of the WASB Spent Fuel per Electrical Energy Generation

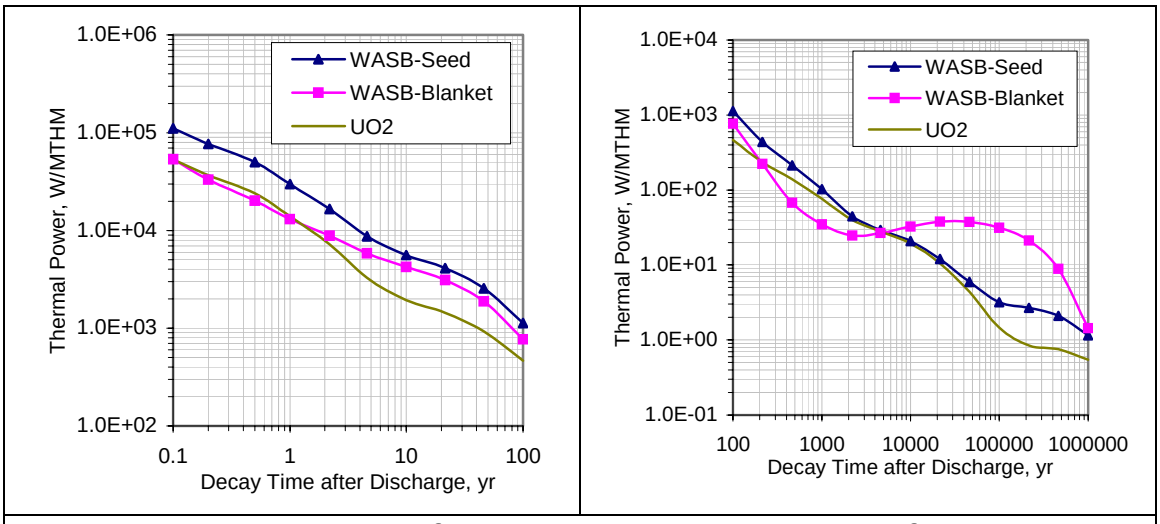

Figure B2.5.4 Decay Heat of the WASB Spent Fuel per Mass of Initial Heavy Metal

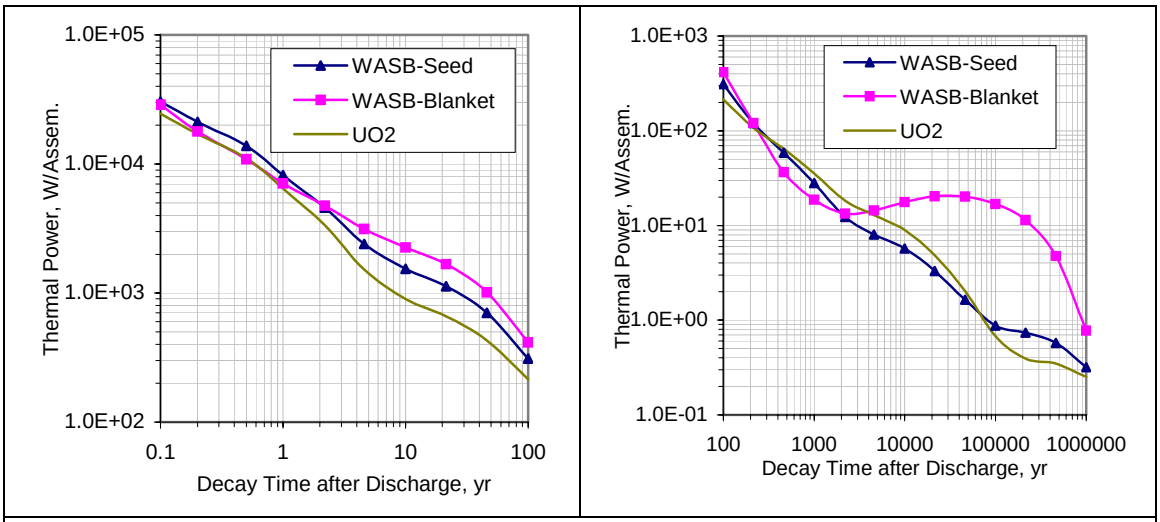

Figure B2.5.5 Decay Heat of the WASB Spent Fuel per Assembly

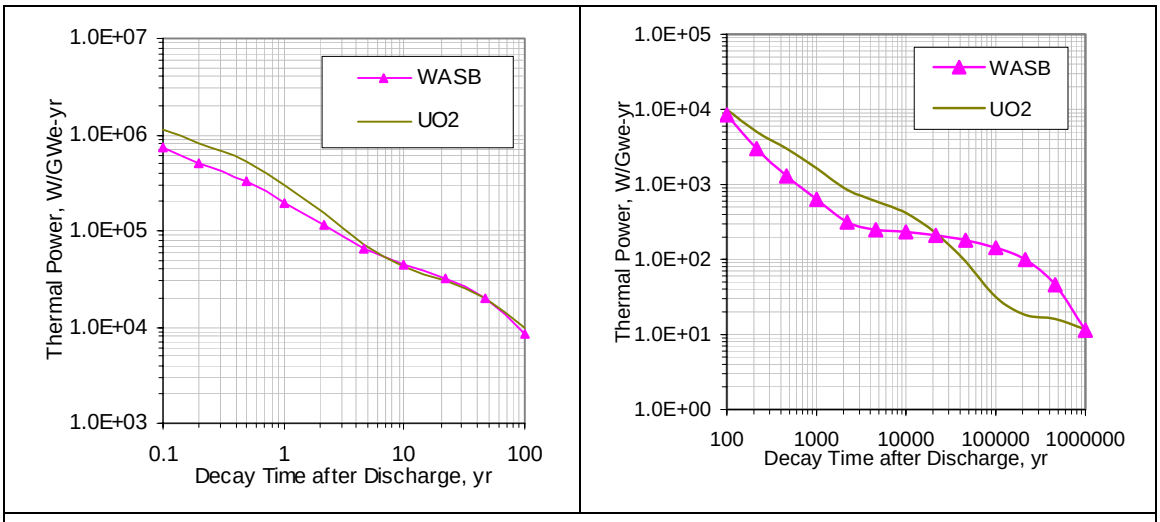

Figure B2.5.6 Decay Heat of the WASB Spent Fuel per Electrical Energy Generation

B2.5.2 Proliferation Resistance

Attributes important for determining the effectiveness of the isotopic barrier include critical mass, spontaneous neutron generation, heat-generation rate, radioactivity, and isotopic enrichment. It is generally agreed that in uranium, U-235 enrichments of less than 20 w/o and U-233 enrichments of less than 12 w/o are non-proliferative (Forsberg, et al, 1999).

Plutonium Production

WASB Pu production rates are compared with those of conventional PWRs in Table B2.5.2. WASB produces both fissile Pu (Pu-239 + Pu-241) and total Pu at annual rates that are about 40% that of conventional PWRs.

Table B2.5.2 Plutonium Production, kg/GWe-yr

	WASB			High Burnup UO_2 [a)]	Typical PWR[b)]
	Seed	Blanket	S + B		
Fissile Pu	48	11	59	110	157
Total Pu	74	18	92	171	233

a) 9.75 w/o enriched UO_2 fuel, and B_d = 100 MWd/kgHM
b) 4.5 w/o enriched UO_2 fuel, and B_d = 50 MWd/kgHM

WASB Pu isotopics are compared with those of conventional PWRs and other compositions in Table B2.5.3. WASB produces about the same fraction of fissile Pu as U235-fueled PWRs, and significantly more Pu238.

Table B2.5.3 Isotopic Composition of Various grades of Plutonium (w/o)

Grade	Pu-238	Fissile Pu
Super-grade	-	98
Weapons-grade	0.012%	94
MOX-grade	1.9%	58
A Typical PWR	2.6%	57
High Burnup UO_2	7.1%	64
WASB – Seed	8.7%	65
WASB – Blanket	9.7%	60

Critical Mass, Spontaneous Fission and Heat Generation

The critical mass of average heavy metal from WASB spent fuel is on the order of 20 kgHM, about the same as that of spent fuel from a typical PWR.

Table B2.5.4 shows that the total spontaneous fission source for a critical mass of the WASB seed plutonium is 25% higher than that of PWR grade plutonium, and that of the blanket plutonium is about twice that of the typical PWR.

Table B2.5.4 Spontaneous Fission Source for Different Plutonium Compositions, 1000 n/s

	Weapons - grade	Typical PWR	High Burnup all-UO_2	WASB – Seed	WASB - Blanket
Total per kg of Pu	61	430	540	550	680
Total per Critical Mass	710	9,400	12,000	12,000	18,000

Table B2.5.5 shows that total heat generation by the WASB plutonium is much higher than that produced by the PWR grade plutonium, even for high burnup PWRs. Thus it is reasonable to assume that a weapon device made from the WASB-Pu would be more unstable.

Table B2.5.5 Heat Generation Rates for Different Plutonium Compositions, Watts

Isotope	Weapons - grade	Typical PWR Fuel	High Burnup PWR Fuel	WASB – Seed	WASB - Blanket
Total per kg of Pu	2.4	18	43	69	57
Total per Critical Mass	28	400	960	1500	1500

Proliferation Analysis for U-233

Forsberg, et al, (1999) have developed a combined proliferation limit of 12% fissile uranium (U-233 plus 0.6 times U-235) for cases such as the blanket when both U-233 and U-235 are present. Figure B2.5.7 shows that the proliferation index, defined as:

$$U\ proliferation\ index = \frac{^{233}U + 0.6^{235}U}{U^{tot}} \times 100\%. \qquad \text{(B2.5.1)}$$

meets this limit.

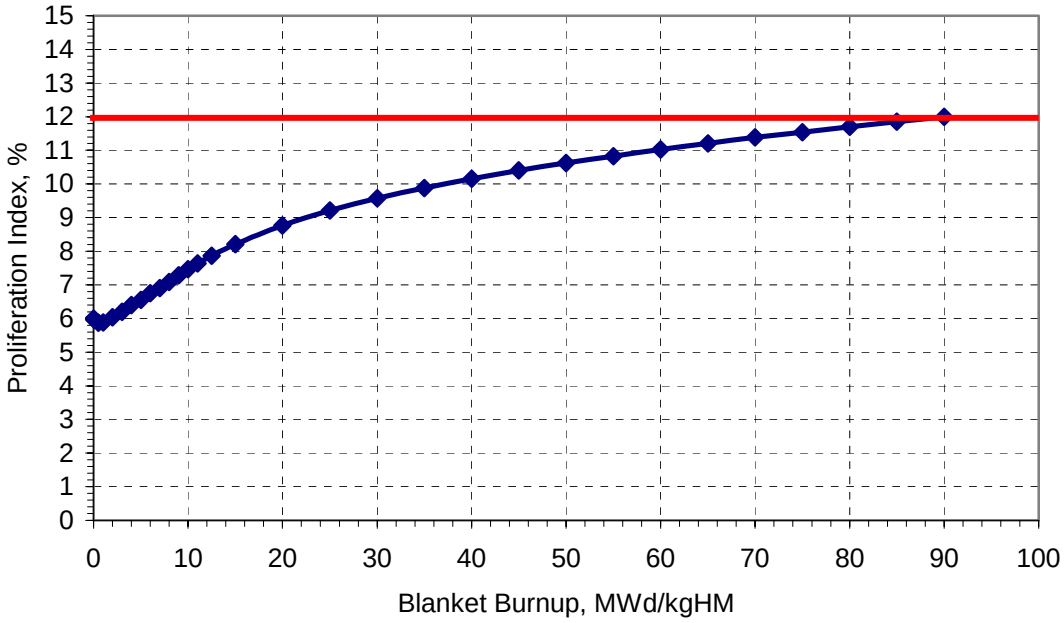

Figure B2.5.7 Blanket U Proliferation Index

B2.6 Safety Analyses (Task-8)

The main purpose of safety analyses is to ensure that a nuclear reactor can be operated safely under various normal and abnormal operating conditions including postulated accidents. Chapter 15 of Final Safety Analysis Report (FSAR) of an operating nuclear power plant documents the results of such analyses. Complete FSAR type of analyses for WASB design was beyond the scope of this project. However, the following accident/ transients were analyzed for both the WASB design and a typical all UO_2 PWR design for comparison purposes and to obtain a "feel" for the safety margin of the WASB design:

a) Large Break Loss of Coolant Accident (LBLOCA)

b) Complete Loss of Primary Flow (LOPF)

c) Loss of Off-site Power (LOSP).

Selection of these transients was influenced by the high thermal power in the seed fuel assemblies and to study its effects during transients where the coolant inventory and core flow rate are reduced very rapidly. A typical 4-Loop PWR plant was taken as the model plant and a particular version of RELAP5 computer code called MARS (Lee, et al, 2002), available at MIT, was used as the analysis tool.

B2.6.1 Input Deck/Model

The input deck was developed from USNRC's typical 4-Loop PWR input for Small-break LOCA analysis with modifications in reactor vessel nodalization, core and fuel modeling and transient systems modeling. The reactor vessel nodalization includes a 'Split Downcomer' with two flow channels, one representing the broken side and the other representing the intact side. A cross-flow junction loss coefficient of 50 is used between the two channels of the downcomer based on UPTF (Upper Plenum Test Facility) assessment results for ECC bypass and penetration. For the typical PWR design, two core flow channels with provision for cross-flow and one bypass channel are used to model the reactor core. The average core channel represents 192 average-power fuel assemblies, whereas the hot channel represents the hot or highest-power fuel assembly of the core. Figure B2.6.1 shows the System nodalization and Table B2.6.1 shows the important parameters used in the core and fuel modeling.

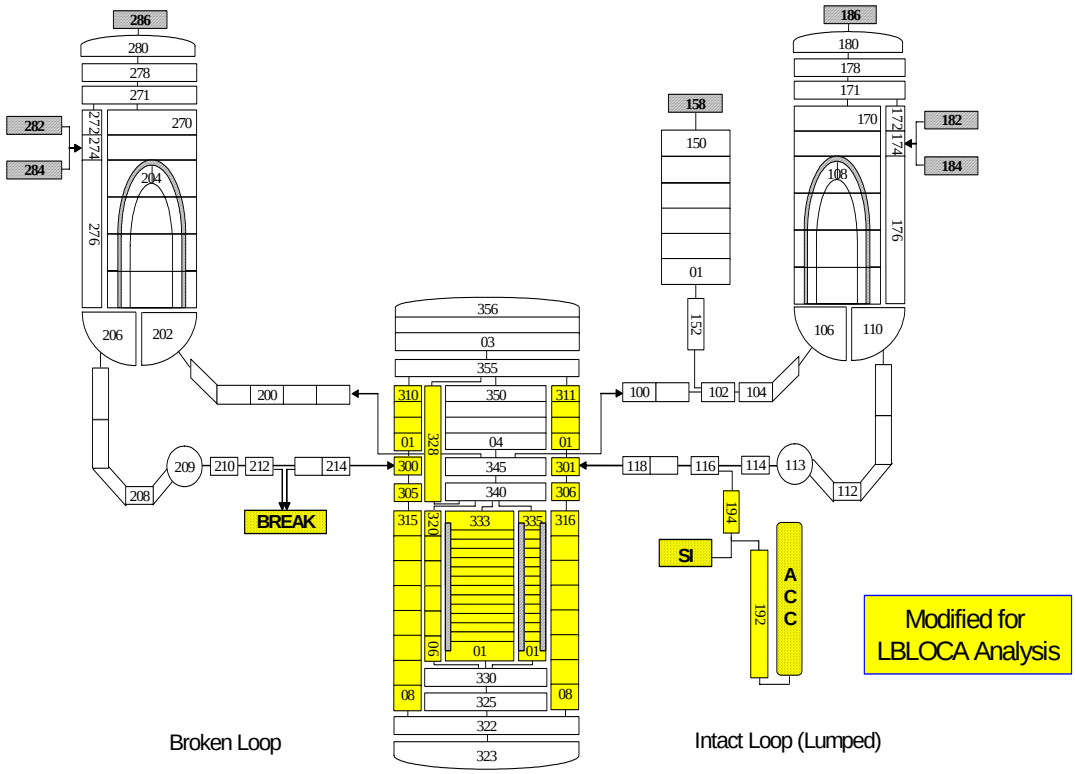

Figure B2.6.1 System Nodalization for Safety Analysis of a Typical 4-Loop PWR

Table B2.6.1 Important Parameters used for Core and Fuel Modeling

Parameters	Models
Initial Power	3479.22 MWth (102 %FP)
Transient Power	
- Decay Heat	ANS73 * 1.2
- Kinetics and Trip Reactivity	conservative
Core & Fuel Modeling	
- # of Axial Nodes	16
- Core Flow Channels	Average (192 FA) and Hot (1 FA)
- Total Peaking	2.5 (q'_{peak} = 14.23 kW/ft)
. Axial Power Distribution	1.5 chopped cosine
. Hot Assembly Peaking	1.573
. Hot Pin Radial Peaking	1.667 (embedded in hot channel)
- Direct Heating	2.6 %
- Gap Conductance	Constant

The steady-state as obtained from the code calculation is shown as the 'Simulated' values in Table B2.6.2 below.

Table B2.6.2 Comparison between Desired and Calculated Steady State Values for PWR Design

Parameters	Desired*	Simulated
Core Power (MWth)	3479.2	3479.2
Pressurizer Pressure (bar)	155.1	155.1
Cold Leg Temperature (K)	564.85	566.47
Hot Leg Temperature (K)	599.25	598.66
Total Loop Flow (kg/s)	18630.0	18707.8
Effective Core Flow (kg/s)	17700.0	17796.1
Bypass Flow Fraction (%)	5.0	4.9
Core Pressure Drop (bar)	-	1.32
Pressurizer Level (%)	50.0	49.0
SG Secondary Pressure (bar)	58.0	60.7

* Desired Conditions are based on typical 4-Loop PWR data

For the WASB design, three core channels as shown in Figure B2.6.2 are used. These are: (1) Average seed channel consisting of 83 Fuel Assemblies, (2) Hot seed channel with the hottest seed pin embedded in it, (3) Blanket channel consisting of all 109 blanket fuel assemblies. For the present calculations, the same core kinetics parameters as the typical PWR design have been used.

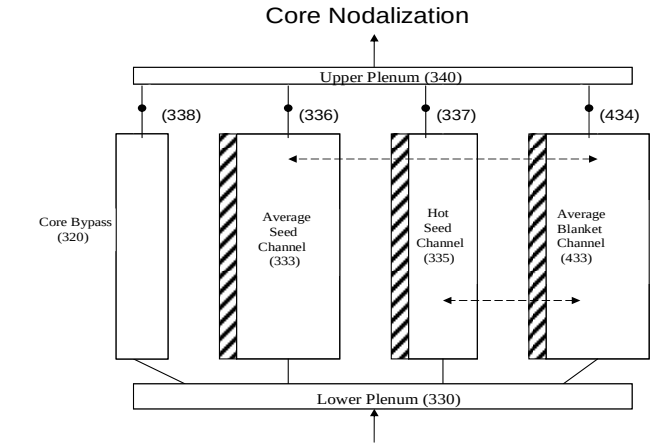

NOTE: Average Seed Channel (comp. no. 333) = 83 FA @ 27.06 MWt/FA
Hot Seed Channel (comp. no. 335) = 1 FA @ 39.25 MWt/FA
Average Blanket Channel (comp. no. 433) = 109 FA @ 10.26 MWt/FA

Figure B2.6.2 Core Nodalization for WASB Design

The steady-state results as obtained for the WASB core are shown as the "Simulated" values in Table B2.6.3 below.

Table B2.6.3 Comparison between Desired and Calculated Steady State Values for WASB Design

Steady-State Results for WASB Design

Parameters	Desired	Simulated
Core Power (MWth)	3479.2	3479.2
Pressurizer Pressure (bar)	155.1	155.1
Cold Leg Temperature (K)	564.85	566.39
Hot Leg Temperature (K)	599.25	598.96
Total Loop Flow (kg/s)	18630	18417.33
Effective Core Flow (kg/s)	17700	17481.81
Bypass Flow Fraction (%)	5	5.08
Core Pressure Drop (bar)	-	2.28
SG Secondary Pressure (bar)	58	60.7
Channel 333 Inlet Flow (kg/s)		10055
Channel 333 Outlet Flow (kg/s)		10133
Channel 335 Inlet Flow (kg/s)		113.91
Channel 335 Outlet Flow (kg/s)		133.37
Channel 433 Inlet Flow (kg/s)		7312.9
Channel 433 Outlet Flow (kg/s)		7215.5

Please note that the core flow rate for the WASB design is about 2% lower than that in the PWR design. The reason for this difference is the higher core and consequently the higher primary loop pressure drop for the WASB design compared to the typical PWR design. As expected, there is a significant cross flow from the blanket assemblies (Channel 433) to the seed assemblies (Channels 333 and 335).

B2.6.2 Large Break Loss of Coolant Accident (LBLOCA)

For LBLOCA simulation, a double-ended cold leg break as shown in Figure B2.6.1 is assumed. The Henry-Fauske critical flow model as implemented in the MARS/RELAP5 code is used to calculate the break flow rate. The containment back-pressure, initially at 1 bar, is modeled to vary as shown in Figure B2.6.3. This pressure conservatively represents 90% of the containment pressure used in FSAR of the reference PWR.

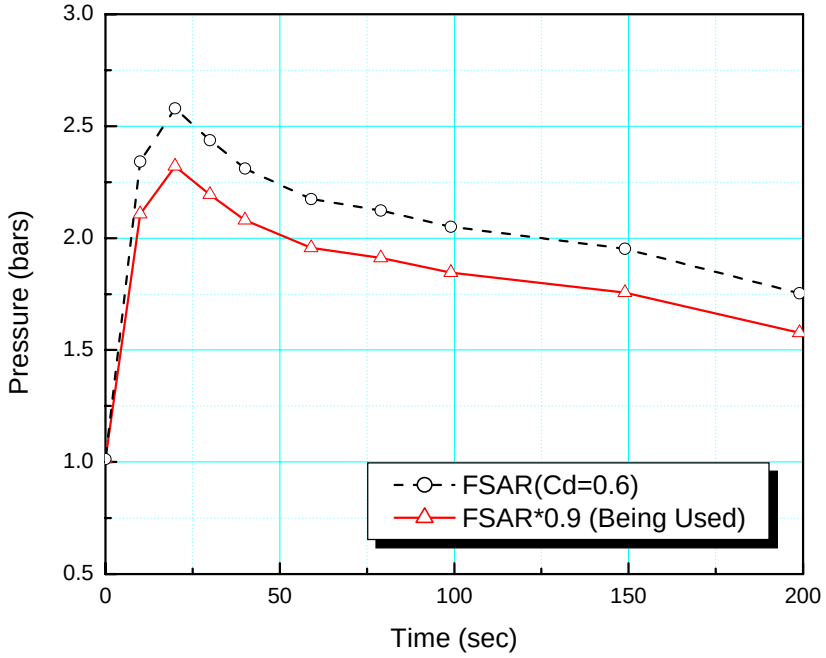

Figure B2.6.3 Containment Back Pressure used in the LBLOCA Calculations for both PWR and WASB Designs

Several important boundary conditions, listed below, are used for the LBLOCA calculations:

a) The core decay heat after scram is set at 120% of the ANS73 value,
b) Reactor coolant pumps are assumed to trip and coastdown at initiation of the break,
c) Conservative values are used for the safety injection flow rates,
d) The Accumulator is turned OFF at low accumulator liquid level to prevent non-condensable gas injection into the primary system,
e) The Reflood fine-mesh rezoning is turned ON at Pressure less than 10 bar.

The results of the LBLOCA calculation for the usual all UO_2 fuel assemblies, i. e., the typical PWR design, look reasonable. The calculated cladding temperatures at the hot rod (Node 8 to 13) in the hot channel are shown in Figure B2.6.4. As expected, a sharp 'blowdown' peak is seen, followed by a more gradual 'reflood' peak. This trend is in agreement with the previous best-estimate LBLOCA calculations for PWRs (Rohatgi, et al, 1987, Levy, 1999) and LOFT experiments (Levy, 1999, Bayless, 1982).

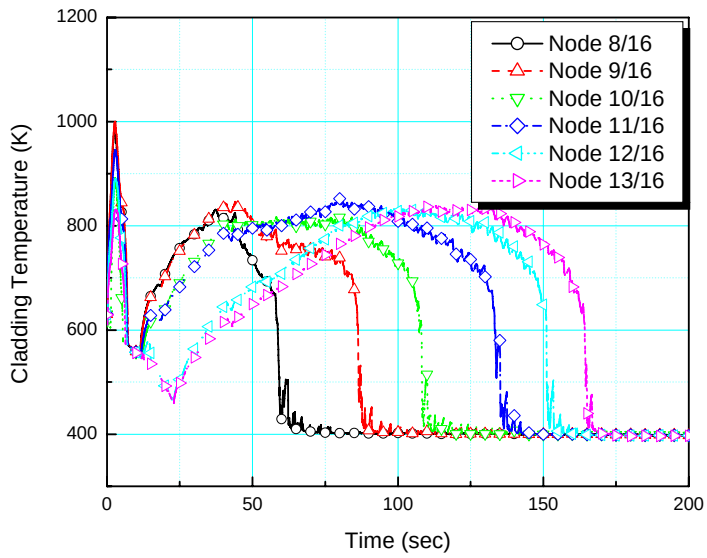

Figure B2.6.4 Hot Rod Cladding Temperatures during LBLOCA for PWR Design

The same LBLOCA was run for the WASB design with the same boundary conditions listed earlier. The hot rod (embedded in the hot seed assembly) cladding temperatures for the WASB design are shown in Figure B2.6.5 below. The general trend is similar to the PWR design shown in Figure B2.6.4 above. However, both the 'blowdown' and the 'reflood' peaks for the WASB design are of higher magnitude compared to those for the typical PWR design. This is not surprising since the power density in the seed fuel rod of the WASB design is much higher than that in the PWR design.

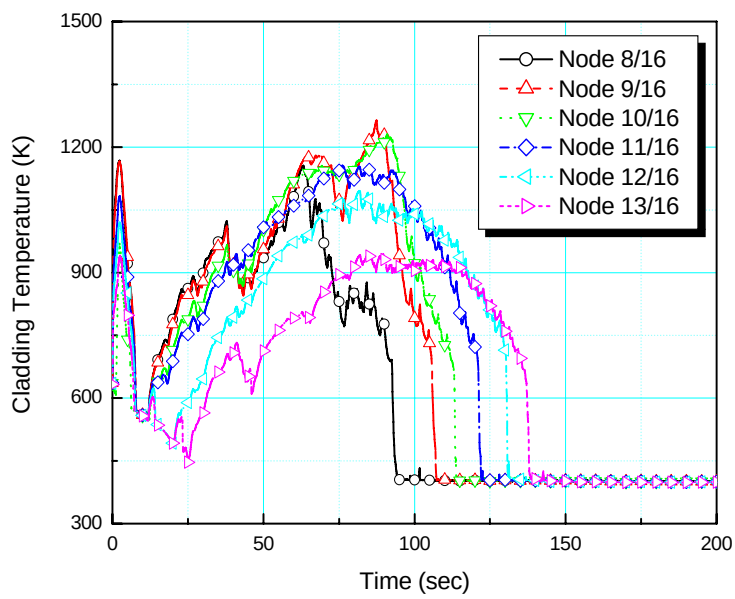

Figure B2.6.5 Hot Rod Cladding Temperatures during LBLOCA for WASB Design

A direct comparison of the hot spot cladding temperature between the typical PWR and the WASB designs for the LBLOCA is shown in Figure B2.6.6. Please note that even though the peak cladding temperature (PCT) for the WASB design is about 260°K higher than that for the typical PWR design, the PCT of 1265°K for the WASB design is still about 200°K lower than the present regulatory safety limit of 1204°C.

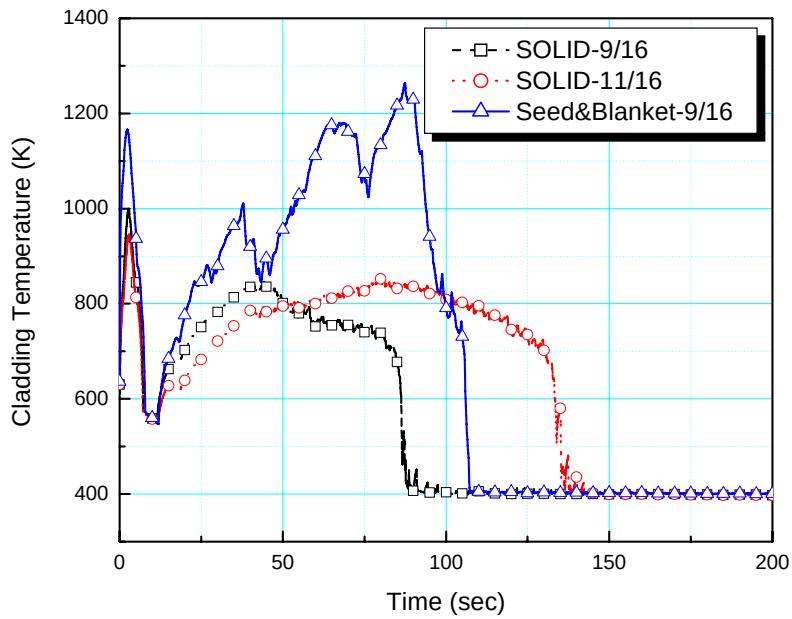

Figure B2.6.6 Comparison of LBLOCA PCTs between the PWR and WASB Designs

As a part of sensitivity analysis, the internal void of the seed rod was filled with ZrO_2 and the LBLOCA was rerun for the WASB design. However, higher initial stored energy led to a higher blowdown cladding temperature peak of about 1400°K at the hottest seed location. There was no significant quenching after the blowdown, in contrast with the seed rod with internal void. Finally, the 'reflood' peak for the PCT was around 1500°K for the 'filled' hottest seed rod. Therefore, the 'filled' seed rods seem to have no advantage from the safety margin viewpoint for a LBLOCA. All WASB safety calculations are, therefore, for the basic design with internal hole in the seed rods.

B2.6.3 Complete Loss of Primary Flow (LOPF)

It is assumed that all four Reactor Coolant Pumps (RCPs) are tripped at time zero. The reactor is tripped at low core flow (87% of nominal flow) signal with 1.0 second time delay. The turbine is tripped immediately which caused the turbine stop valve to close. The transient was run for a short period of ten seconds to investigate if the lower core flow triggers 'Departure from Nucleate Boiling (DNB)' while the core power was still high and a sharp increase in cladding temperature, particularly in the hot rod embedded in the hot seed assembly. Figures B2.6.7 through B2.6.9 compare the results of some important parameters for both the typical PWR and the WASB designs.

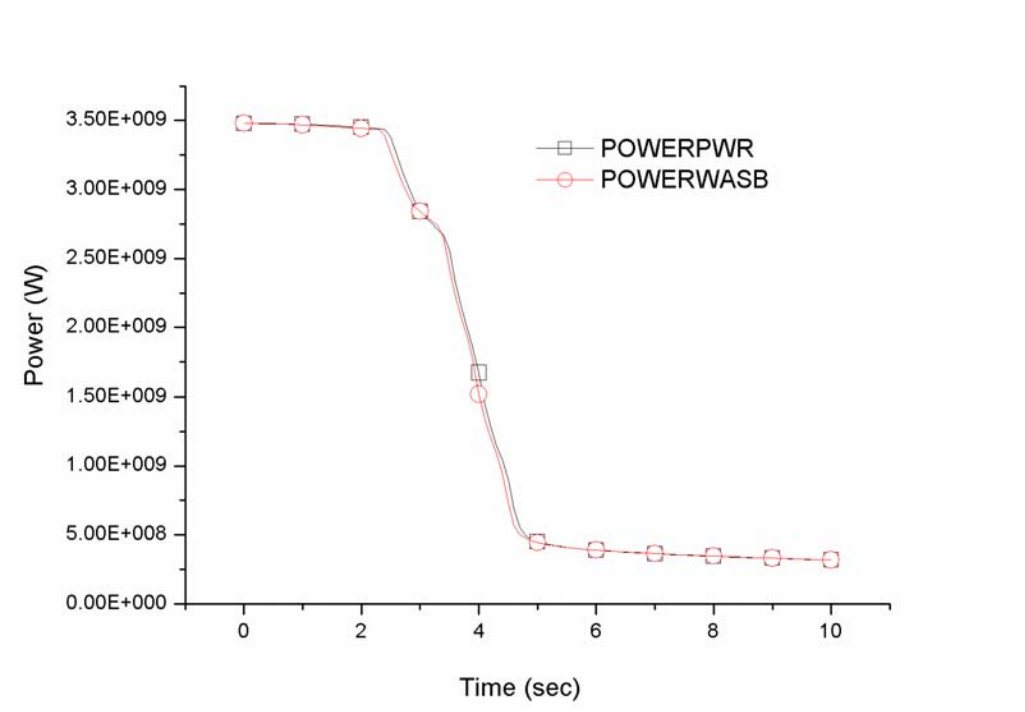

Figure B2.6.7 Reactor Power during LOPF Transient (PWR and WASB)

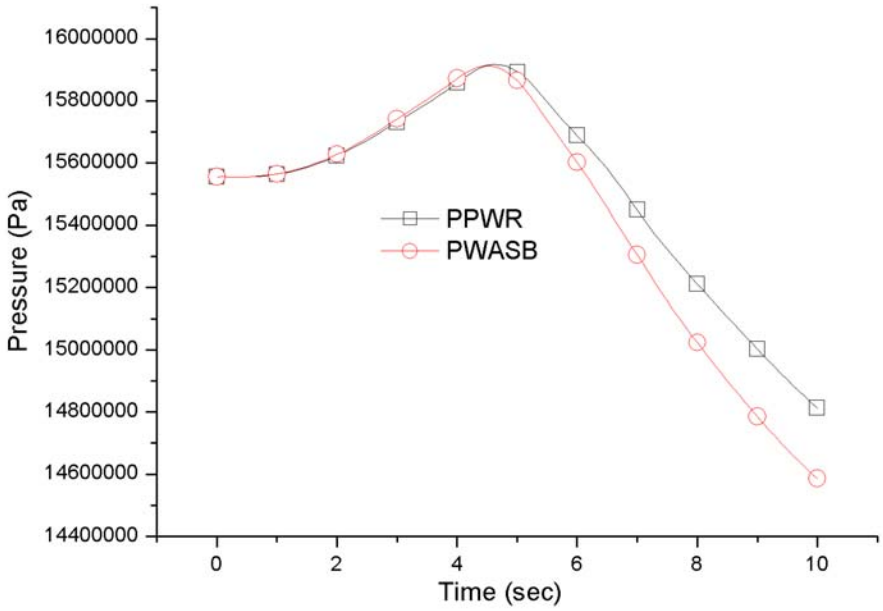

Figure B2.6.8 Primary (Pressurizer) Pressure during LOPF Transient (PWR and WASB)

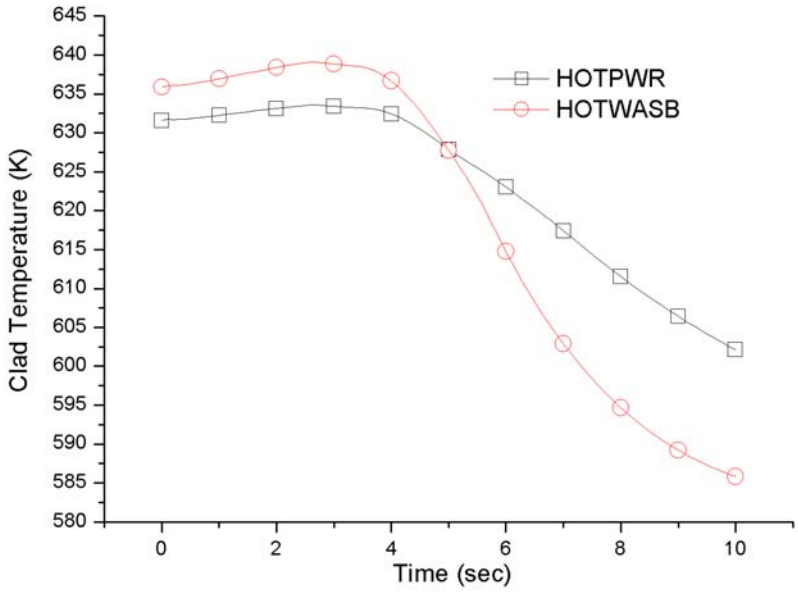

Figure B2.6.9 Hot Spot Cladding Temperature during LOPF Transient PWR and WASB)

It can be seen that the response of the WASB core is very similar to the typical PWR core for this complete loss of primary flow transient, and no sharp rise in cladding temperature, typical of a post-DNB situation, was observed. Figure B2.6.10 shows the hot spot cladding temperatures at various fuel assemblies in the WASB core, and no sharp temperature rise is observed in any location.

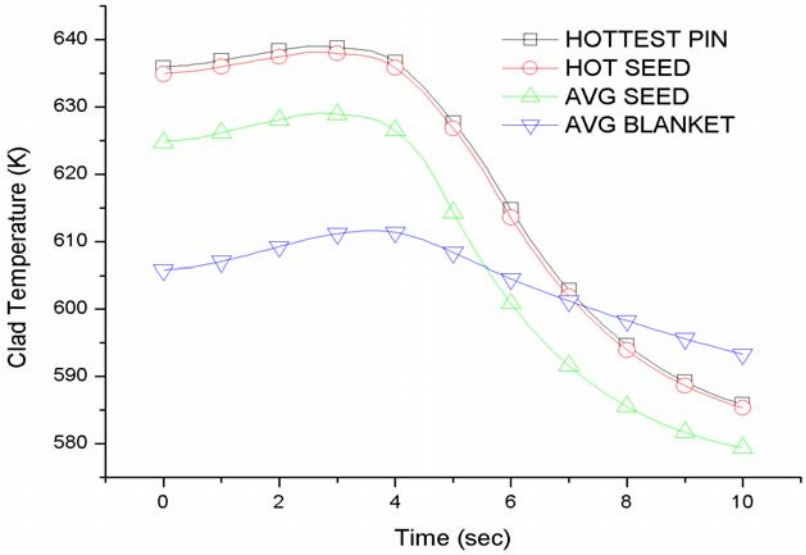

Figure B2.6.10 Hot Spot Cladding Temperatures at Various Fuel Assemblies of WASB Core during LOPF Transient

B2.6.4 Loss of Off-site Power (LOSP)

It is assumed that all non-emergency AC power is lost and consequently, all Reactor Coolant Pumps (RCPs) and Main Feedwater Pumps (MFPs) are tripped at time zero. The reactor is tripped at low core flow (87% of nominal flow) signal with 1.0 second time delay. The turbine is tripped immediately which caused the turbine stop valve to close. Steam generator secondary side pressure increased and the steam safety valves opened to relieve the pressure. After 75 seconds from the reactor trip, only one emergency feedwater pump could be started to inject emergency feedwater into four steam generators. The transient was run for 200 seconds for both the typical PWR and the WASB designs. Figures B2.6.11 to B2.6.14 compare the results of several important parameters for both the designs.

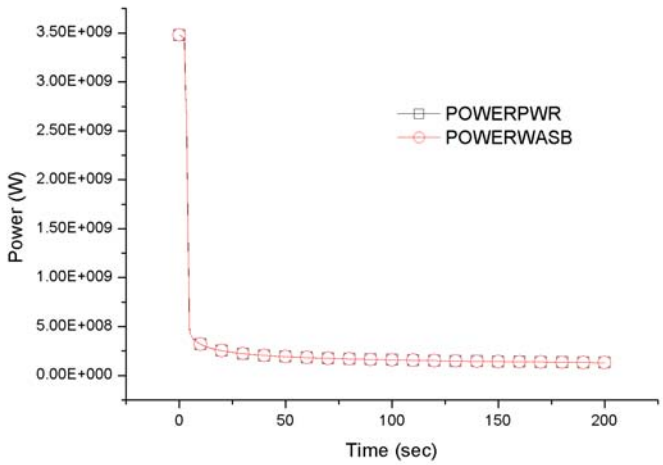

Figure B2.6.11 Reactor Power during LOSP Transient (PWR and WASB)

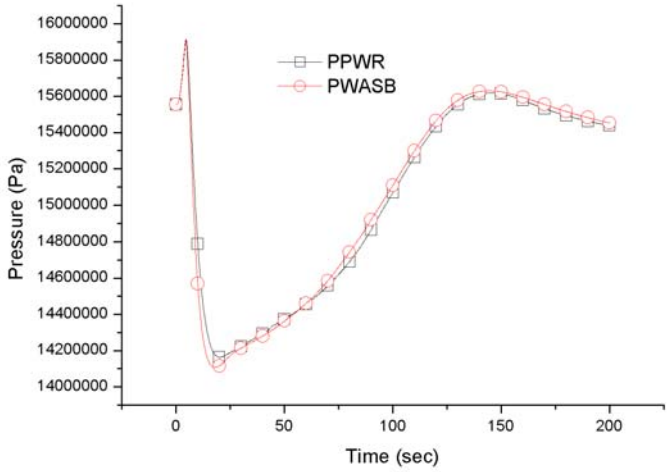

Figure B2.6.12 Primary (Pressurizer) Pressure during LOSP Transient (PWR and WASB)

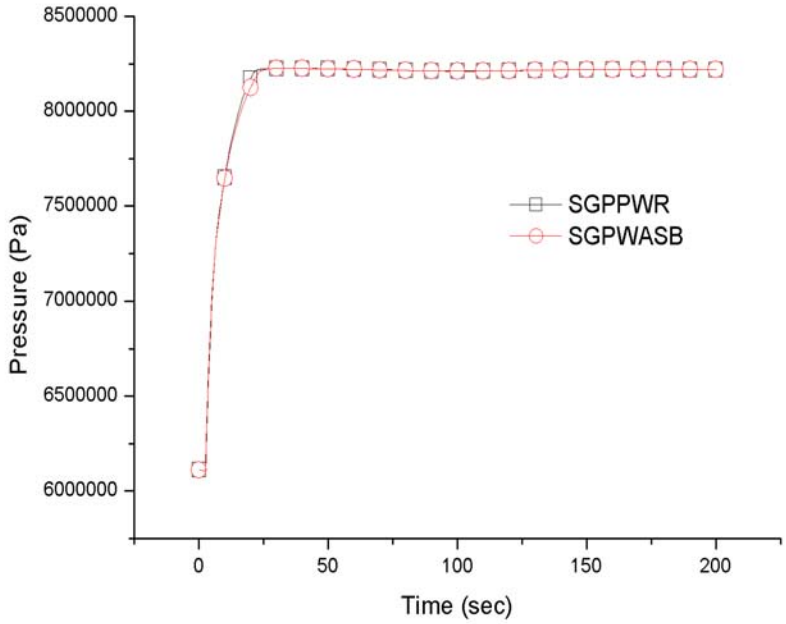

Figure B2.6.13 Steam Generator Secondary Pressure during LOSP Transient (PWR and WASB)

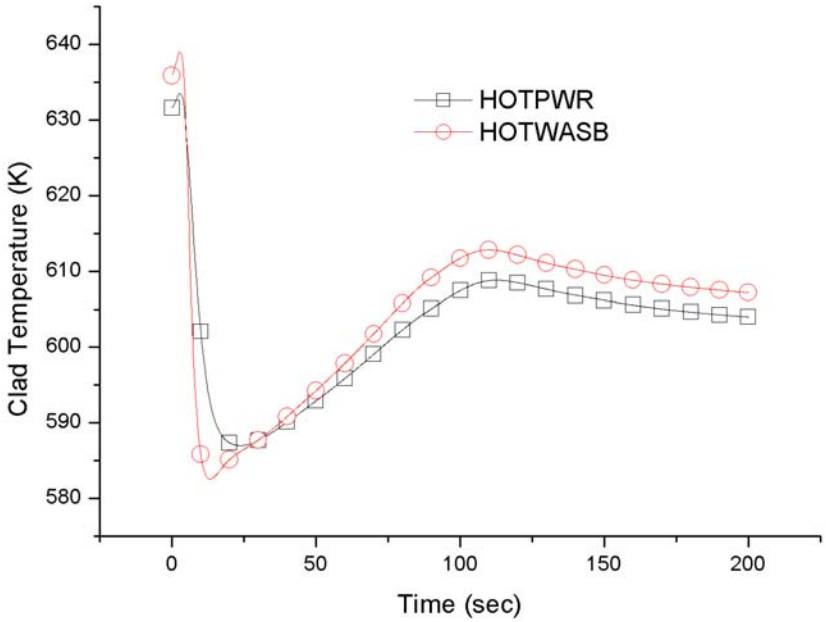

Figure B2.6.14 Hot Spot Cladding Temperature during LOSP Transient (PWR and WASB)

It can be seen from the above figures that the response of the WASB core is similar to that of the typical all UO_2 PWR core for this loss of off-site power transient. Also, there is no sudden increase in cladding temperature in any fuel assembly of the WASB design for this transient as shown in Figure B2.6.15 below.

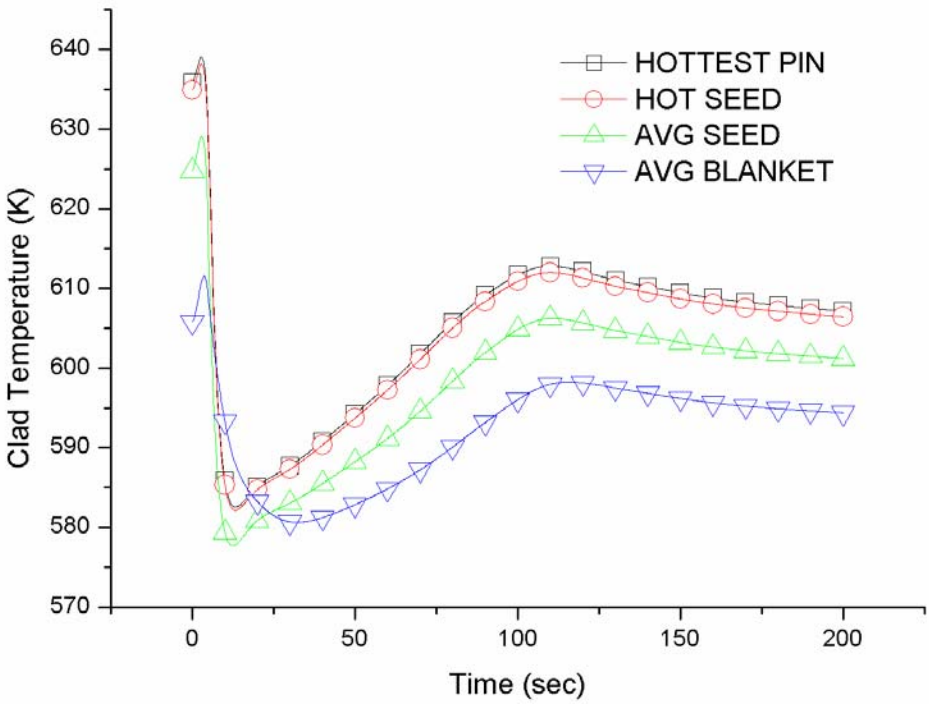

Figure B2.6.15 Hot Spot Cladding Temperatures at Various Fuel Assemblies of WASB Core for LOSP Transient

In summary, the response of the WASB core for the loss of primary flow (LOPF) and loss of off-site power (LOSP) transients is very similar to that of the typical all UO_2 PWR core and no post-DNB type situation was calculated. For large break LOCA, the Peak Cladding Temperature (PCT) for the WASB core was found to be significantly higher than that for the typical all UO_2 PWR core; however, the WASB design still shows a margin of about 200°C from the present regulatory safety limit of 1204°C.

B3. The Seed-Blanket Unit (SBU-RTF) Concept

B3.1 Assembly and Core Neutronics Design

B3.1.1 Seed-Blanket Unit (SBU) Neutronics Analysis (Task-1)

The objective of this task was to develop a baseline and "optimized" design for the Seed-Blanket Unit (SBU). In order to define and optimize a practical and feasible design for the SBU concept, an iterative procedure involving nuclear, thermal-hydraulic and mechanical design analyses is required. Initially, neutron transport and burnup calculations of the entire SBU assembly are performed to determine the impact of modifications of the material compositions, geometry, and mechanical design on the reactivity and power distributions in the SBU, as well as reactivity coefficients to estimate transient/accident behavior and control characteristics. Once acceptable performance is obtained, thermal-hydraulic analyses are performed to assess whether the design satisfies thermal-hydraulic constraints (e.g., MDNBR, overpower margin). This iterative procedure continues until a consistent design is obtained. The results are then used in three-dimensional, full-core simulations in a similar iterative fashion until a consistent design that satisfies performance and other objectives is obtained.

Neutronics Analyses

The evaluation of the neutronic performance of SBU options was performed by BNL and BGU. Much of the motivation behind the development of an improved SBU was a desire to reduce the rod peaking factors and thus improve T-H performance. The SBU rod-wise power peaking factors are combined with core-wide radial and axial peaking to obtain the three-dimensional peaking factor that is used in determining the core T-H and safety performance. Therefore, minimization of each of these components, all other characteristics being equal, allows greater flexibility in other aspects of the design, or increases operating and/or safety margins.

The optimized SBU design is the product of an extensive series of sensitivity studies involving consideration of: alternate fuel forms (uranium nitride, uranium carbide, and cermet); fuel pin geometry variations to change the moderator-to-fuel ratio (V_m/V_f) for neutronic performance and coolability; guide-tube material, etc.

The SBU has the same general dimensions as a standard 17x17 366-cm long Westinghouse PWR fuel assembly (Westinghouse, 1973) with 264 fuel rods, and 25 locations for guide tubes for water holes/ control rods/instrumentation, burnable poison rods, or control rods. In order to satisfy the retrofittability constraint, the guide-tube dimensions and locations are the same as in a standard assembly to allow use of the same control rods and fixed burnable poison rods (if desired). The seed sub-assembly (SSA) consists of the inner 11x11 rod array, and contains 108 UO_2 pins with ZrB_2/ZrO_2 poison plugs. The outer blanket sub-assembly (BSA) contains the remaining 156 fuel rods, each of which is a mix of enriched UO_2 and ThO_2. Two SBU designs were developed, referred to as "baseline" and "optimized". In both options, the blanket and seed pins have the same outer diameter (0.95 cm), but there are

differences in the size, and composition of burnable poison plugs and central voids, as shown in Figure B3.1.1 and Table B3.1.1.

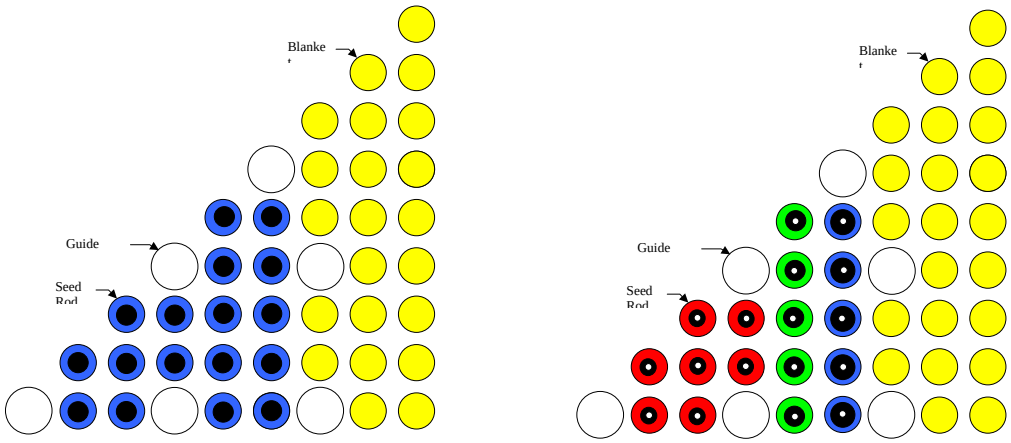

Figure B3.1.1 Layout of Fuel Pins in 1/8th Baseline (left) and Optimized (right) SBU Designs

In the baseline design, all seed pins have the same dimensions and isotopic compositions for the fuel (20 w/o UO_2) and central poison plug (2.5% ZrB_2 in ZrO_2). The baseline blanket fuel pins are 13% by volume of 12.2 w/o UO_2 in ThO_2. In contrast, the optimized SBU design employs three different types of seed pins and a modified blanket pin composition. The inner seed pins have a slightly higher fuel volume, ~20% larger than the baseline. The middle seed pins have the same fuel volume as the baseline, while the outer seed pins have a slightly lower fuel volume, ~15% smaller than the baseline. The spatial gradient of fuel volume helps to reduce the radial power peaking while maintaining the reactivity needed for a long burnup. It is noted that the power tends to peak in one of the corner seed pins adjacent to the blanket and the corner guide tube / water hole. In addition, all seed pins in the optimized fuel assembly (FA) have a 0.4-cm diameter central void that allows space for fission product gases. The volume fraction of ZrB_2 in the annular poison plugs varies as well, ranging from 4.52% in the outer seed pin to 8.31% in the inner seed pins. The volume fraction of ZrB_2 in the middle seed is higher than that in the baseline case (2.5%) in order to conserve the number of boron atoms with the presence of a void. The fuel in all optimized seed pins has the same enrichment as the baseline: 20 w/o. The optimized blanket pin is slightly different in design. The number density for U-235 is the same, but the volume fraction and enrichment have been adjusted to 15% and 10.57 w/o (10.69 a/o) respectively. The higher fraction of UO_2 and hence U-238 is meant to increase the proliferation resistance of the fissile uranium (U-235 and U-233) after long burnup levels consistent with the criteria proposed by ORNL (Forsburg, et al, 1999).

Table B3.1.1 Seed-Blanket Unit (SBU) General Design Parameters

SBU Design	Baseline		Optimized	
Parameter	Seed	Blanket	Seed	Blanket
Fuel Assembly Length (cm)	366		366	
Fuel Assembly Size (cm)	21.42		21.42	
Fuel Assembly Pitch (cm)	21.50		21.50	
Dimensions (cm)	13.86	21.42	13.86	21.42
Number of Fuel Pins	108	156	108	156
Fuel Cell Pitch (cm)	1.26	1.26	1.26	1.26
Fuel Rod Radius (cm)	0.475	0.475	0.475	0.475
Clad Thickness (cm)	0.057	0.057	0.057	0.057
Gap Thickness (cm)	0.0085	0.0085	0.0085	0.0085
Fuel Pellet Radius (cm)	0.4095	0.4095	0.4095	0.4095
Enrichment of UO_2 (w/o)	20	12.2	20	10.57
% Volume UO_2 in ThO_2	100	13	100	15
Poison Radius (cm)	0.275	0	Inner 0.2392 Middle 0.2750 Outer 0.2991	0
ZrB_2 Volume in Poison (%)	2.5	0	Inner 8.31 Middle 5.31 Outer 4.52	0
ZrO_2 Volume in Poison (%)	97.5	0	95.5 to 91.7	0
Central Void	No	no	yes	no
Central Void Radius (cm)	0	0	0.2	0
Fuel Temp. (C)	650	650	650	650
Clad Temp. (C)	327	327	327	327
Water Temp. (C)	306.4	306.4	306.4	306.4
Guide Tube Temp. (C)	306.4	306.4	306.4	306.4
Water Pressure (MPa)	15.5	15.5	15.5	15.5
Mod./Fuel Volume Ratio	~3	1.67	2.5 to 3.6	1.67

The BOXER lattice-physics code developed at the Paul Scherrer Institute in Switzerland (Paratte, et al, 1995, 1996) was used for performing neutron transport and burnup calculations for the baseline and optimized SBU designs. The BOXER code was designed primarily to analyze light water reactor (LWR) fuel assemblies, and has been extensively benchmarked/validated for these applications. In addition, there has been considerable benchmarking performed for homogeneous and heterogeneous thorium-bearing configurations against Monte Carlo and other lattice codes as a function of burnup.

Two sets of burnup calculations were performed with BOXER to simulate the expected fuel management scheme characteristics: a standard 3-batch scheme for the seed, with the blankets assumed to remain in the core for 6-9 seed cycles; each cycle would be 18-months long consistent with current U.S. commercial reactor practice. The first set, started with a

fresh seed and fresh blanket, and was burned to an SBU average burnup of 80 GWd/t, consistent with three, 18-month cycles at a 100% capacity factor. In the second set of calculations, a fresh seed sub-assembly was inserted into the blanket from the previous 80 GWd/t SBU burnup. The isotopic composition of the blanket at an average burnup of ~80 GWd/t for the SBU was used as the initial isotopic composition in the blanket sub-assembly for the second three cycles of burnup with the next fresh seed sub-assembly. This second set would emulate the second three cycles in a core calculation.

Results for these four sets of burnup calculations are shown in Figures B3.1.2 and B3.1.3. Figure B3.1.2 is a plot of the SBU infinite multiplication factor (K-Inf) versus the burnup level. The variation of K-Inf with burnup is almost identical for both the baseline and optimized SBU designs for both the first set and the second set.

Figure B3.1.3 shows the relationship between the average burnup levels in the seed and blanket sub-assemblies with the average burnup in the optimized SBU for the first and second SSA loadings. The baseline case gives similar results. The average burnup in the SSA is almost twice that of the SBU while average burnup in the BSA is approximately 60% of the SBU burnup. At 80 GWd/t, the burnup in the SSA is ~ 154 GWd/t (first seed) and 149 GWd/t (second seed), while the burnup in the BSA is ~ 48.6 GWd/t (first seed) and 49.5 GWd/t (second seed).

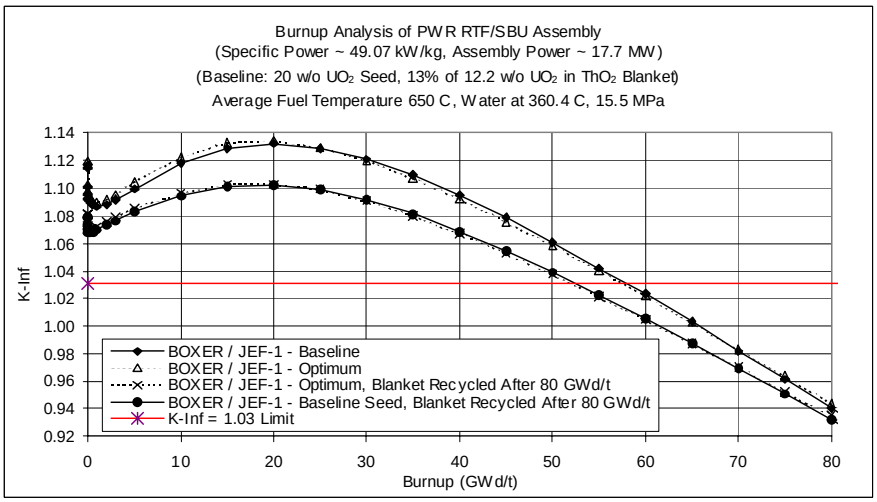

Figure B3.1.2 BOXER Calculations of SBU Fuel Assembly Reactivity Variation with Burnup

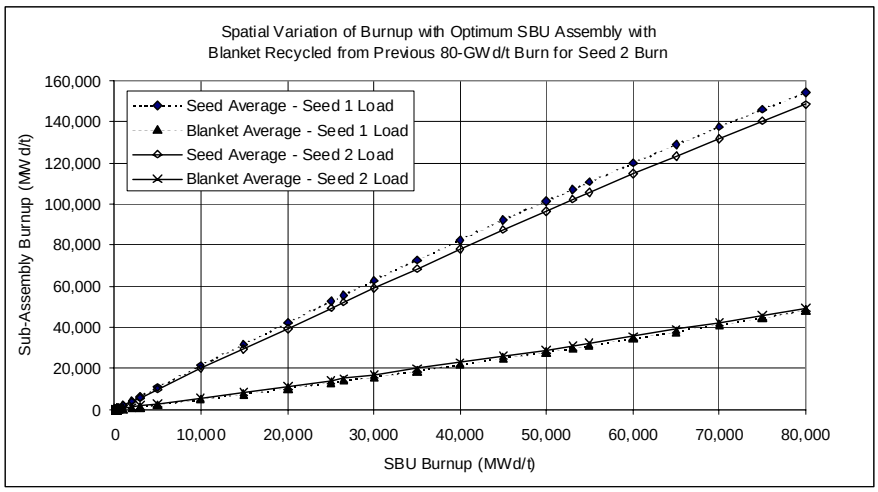

Figure B3.1.3 Variation of Sub-Assembly Burnup Level with SBU Burnup

Thermal-hydraulics Issues

The COBRA-EN (COBRA, 2001) sub-channel thermal-hydraulics code was used to compute the flow distribution, pressure drop, and departure from nucleate boiling ratios (DNBR) throughout the SBU assembly under various power conditions. The relative pin power distributions were extracted from the previous BOXER neutronic calculations for fresh seed sub-assemblies in fresh blanket sub-assemblies with zero burnup. The relative axial power distribution and the assembly peaking factor (F_{xy}) were taken from the full-core calculations using the SILWER code [Section B3.1.2]. Both axial power distributions and assembly power peaking factors can vary from cycle to cycle, but a typical one with a normalized axial peak of ~ 1.6 at 140 cm above the bottom of the 366-cm core, and a conservative assembly peaking factor of F_{xy}=1.5 were initially used in the COBRA calculations. The core-average linear rod power at full power was approximately 18.2 kW/m.

BOXER calculations demonstrated that the use of graded fuel and poison volume loading in the seed pins helps to reduce the pin peaking factor from 2.1 in the baseline case to less than 1.9 in the optimized case. As a result, the COBRA-EN calculations demonstrated that the optimized SBU design always has a larger MDNBR than that for the baseline SBU. At full power conditions, only the optimized design has a MDNBR greater than 1.3. When the power level is increased to 112%, the MDNBR drops below 1.3, even for the optimized case with modified grid loss coefficients in the blanket and seed pins. Grid loss coefficients of K=0.86 were initially used, but it should be possible to tailor the resistance of the grid-spacers to reduce the loss coefficients in the seed pin sub-channels to K_{seed}~0.6, while increasing the loss coefficients in the blanket pin sub-channels to ~$K_{blanket}$~2.0 (Todosow, et al, 2002). If this is done, and the assembly peaking factor is reduced from 1.5 to 1.4, then even at 118% of full power, the optimized SBU assembly design will have an MDNBR greater than 1.3, while the baseline case remains below. At every power level, with modified grid loss coefficients, and a reduced assembly power

peaking factor, the optimized SBU design has a larger safety margin than the baseline case.

It should be noted that as an assembly undergoes burnup, a greater portion of the assembly power is generated in the blanket due to the depletion of U-235 in the seed, and the buildup of U-233 in the blanket. The pin power peaking factor also drops, and this helps increase the MDNBR. If a fresh fuel assembly is inserted into a partially burned blanket, the pin peaking factor will drop as well. For example, the optimized SBU at beginning of cycle (BOC) with a fresh seed inserted in a blanket sub-assembly recycled from a previous 80-GWd/t SBU burn has a pin power peaking factor of ~ 1.64, which is significantly less than 1.85 initial value. Thus, the most severe situation that the SBU must be designed to handle is that with a fresh seed sub-assembly inserted into a fresh blanket sub-assembly.

A more detailed discussion of the thermal-hydraulics analyses is presented in Section B3.2.

Proliferation Issues

The characteristics of the baseline and optimized SBU designs that affect "inherent" proliferation resistance (i.e., the quantity and isotopics of the generated plutonium, and the effective enrichment of the uranium in the blanket) were also examined. The quantity and quality of the plutonium were very similar for both cases (cf. Figure B3.1.4), while the proliferation mass ratio of the blanket (PMR):

$$\text{PMR} = \frac{(\text{mass of U-233} + \text{mass of Pa-233} + 0.6\times\text{mass of U-235})}{(\text{mass of U} + \text{mass of Pa-233})} < 0.12 \qquad \text{(B3.1.1)}$$

was slightly better for the optimized SBU. The Pa-233 is included in the calculation of the PMR because it will eventually decay to U-233 with a relatively short half-life.

Summary of SBU Optimization Studies

Following a series of parametric studies a baseline and optimized SBU design was developed as described above. The performance of both designs was found to be very similar with respect to key criteria such as reactivity as a function of burnup to ensure the ability to achieve the desired 18-month operating cycle, and reduction in the quantity and quality of the plutonium produced relative to a standard PWR. The optimized design has lower power peaking which improves thermal-hydraulic performance, and adheres more closely to the proliferation limit for mixtures of U-233 and U-235 than does the baseline. This was achieved at the expense of a more complicated design for the seed with a spatial grading of the uranium and poison loadings.

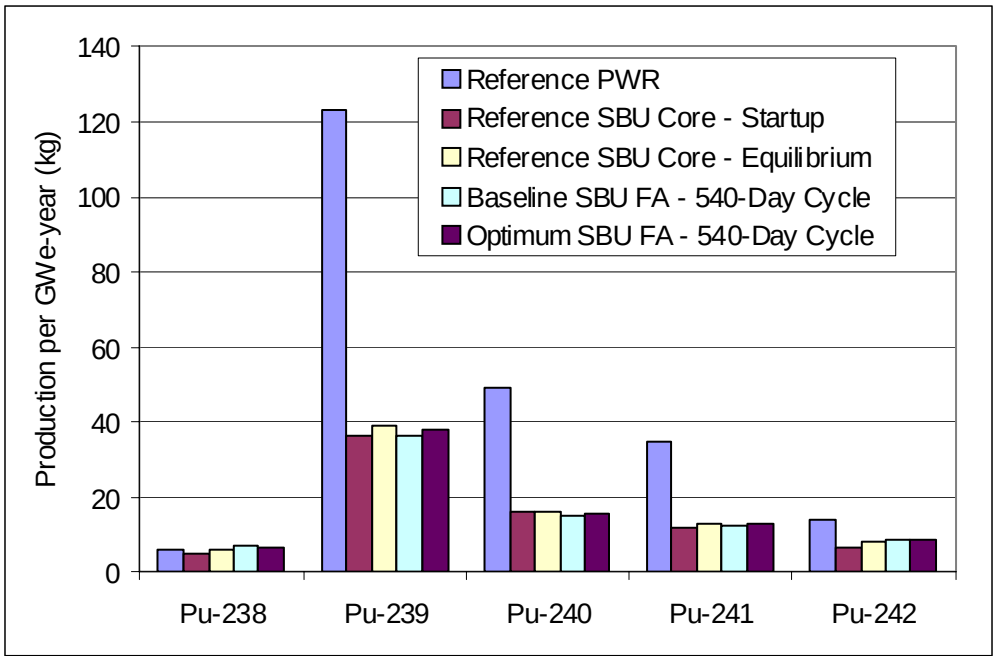

Figure B3.1.4 Plutonium Isotope Production per GWe-Year

B3.1.2 Core Neutronics Design (Task-7)

The core neutronics design analyses were performed by BGU for the baseline SBU design with the SILWER three-dimensional core simulator from the PSI ELCOS code system. The calculations included feedback effects from the moderator and fuel temperature. Based on the similar neutronic performance of the baseline and optimized SBU design (cf. Section B3.1.1) it is expected that the core-dependent results for the optimized SBU would be similar.

Six cycles were considered in the SILWER simulations. For simplicity, a single, enrichment and uniform burnable poison loading were used for all seed fuel batches. Only the seed fuel was shuffled between cycles based on studies that showed that the blanket performance was relatively insensitive to its location in the core.

A typical critical boron let-down curve is shown in Figure B3.1.5. The average cycle length for the 6-cycles was 480 days (18-months at a 90% capacity factor). It is interesting to note that the presence of the thorium results in a smaller burnup dependent reactivity shift in comparison with uranium-based fuels. This is due to the higher thermal absorption of thorium as compared to that of uranium, and the slower buildup of fissile U-233 compared to that of Pu-239. This results in a lower soluble boron concentration at the beginning of cycle.

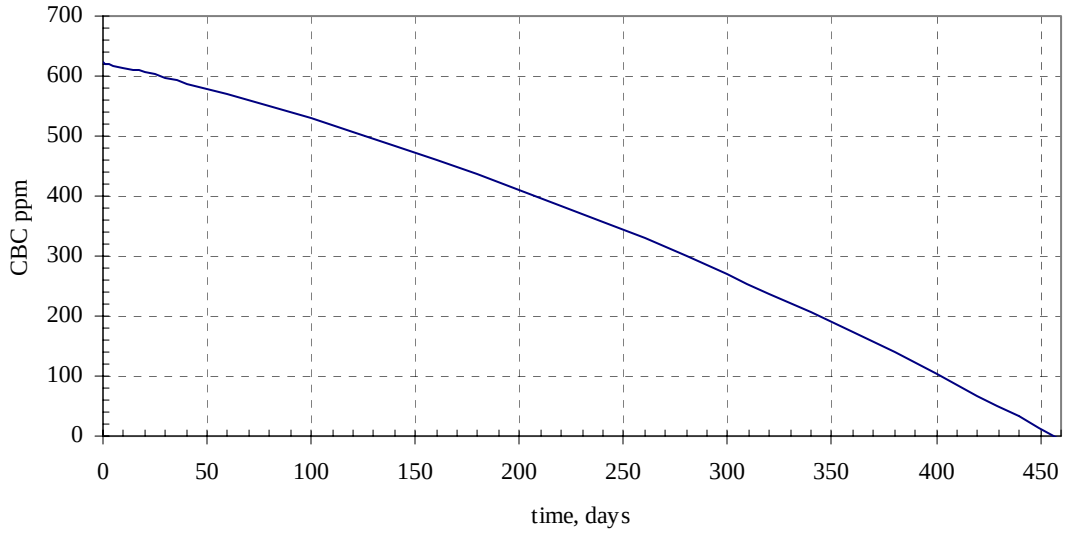

Figure B3.1.5 Critical Boron Concentration, Cycle 5

The burnup-dependent criticality curves for the seed and blanket are shown in Figures B3.1.6 and B3.1.7, respectively. The results for the seed show that the burnable poison loading burns out at ~90 GWd/T, while the average seed burnup during its first cycle is in the vicinity of 70 GWd/T. There is therefore a remaining penalty from the BP on discharge that could be reduced on optimization. It also provides additional flexibility for controlling SBU pin-power and core power peaking. The burnup dependent criticality curve for the blanket reflects the assumption that the seed sub-assembly is reloaded after 3 18-month fuel cycles while the blanket sub-assembly is reloaded as a single batch after 6 fuel cycles.

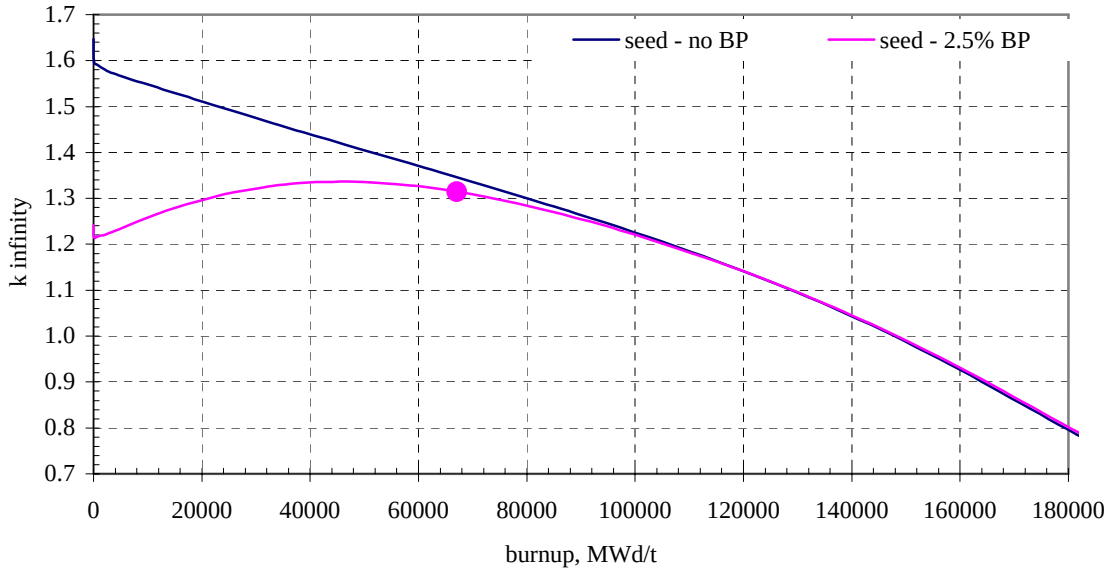

Figure B3.1.6 Seed Criticality as Function of Burnup

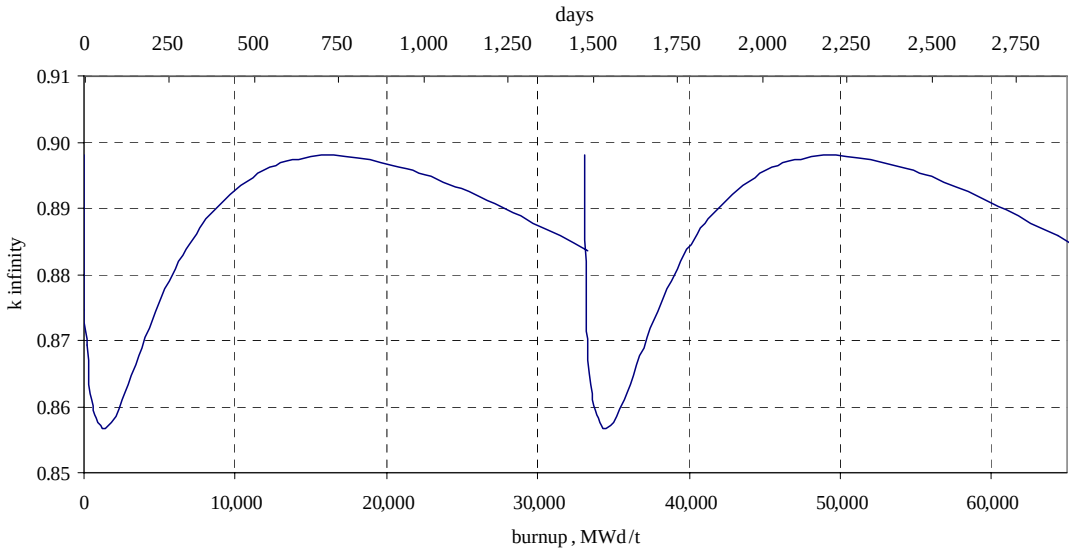

Figure B3.1.7 Blanket Criticality as Function of Burnup

The power sharing between the seed and the blanket is shown in Figure B3.1.8. The seed-blanket power share is typically ~60-40% at beginning of cycle (BOC) and 55-45% at end-of-cycle (EOC).

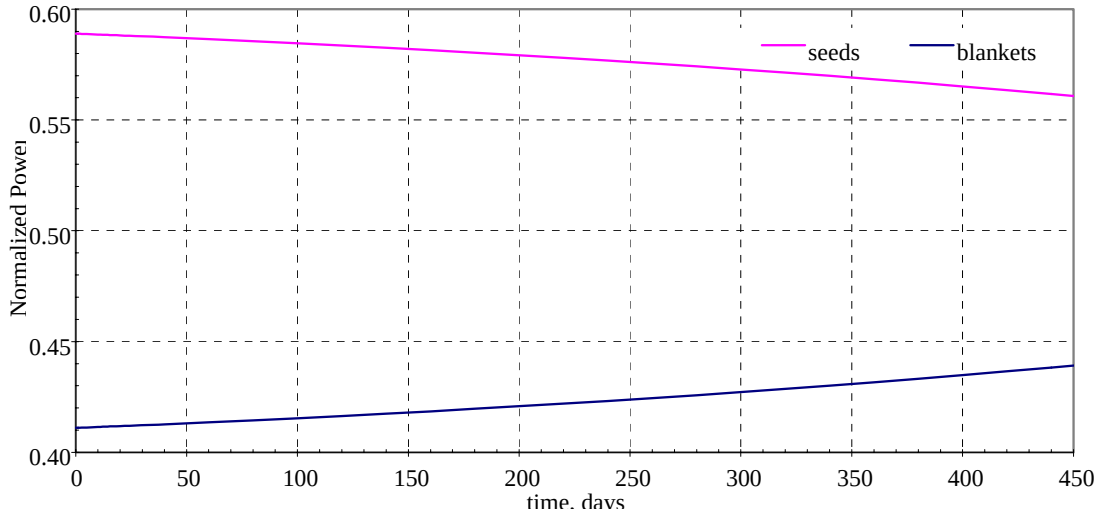

Figure B3.1.8 Seed and Blanket Power Shares (Cycle 6)

Typical axial and radial power distributions and fuel loading pattern are shown in Figures B3.1.9 and B3.1.10. Note that the axial power distribution does not vary significantly from cycle to cycle.

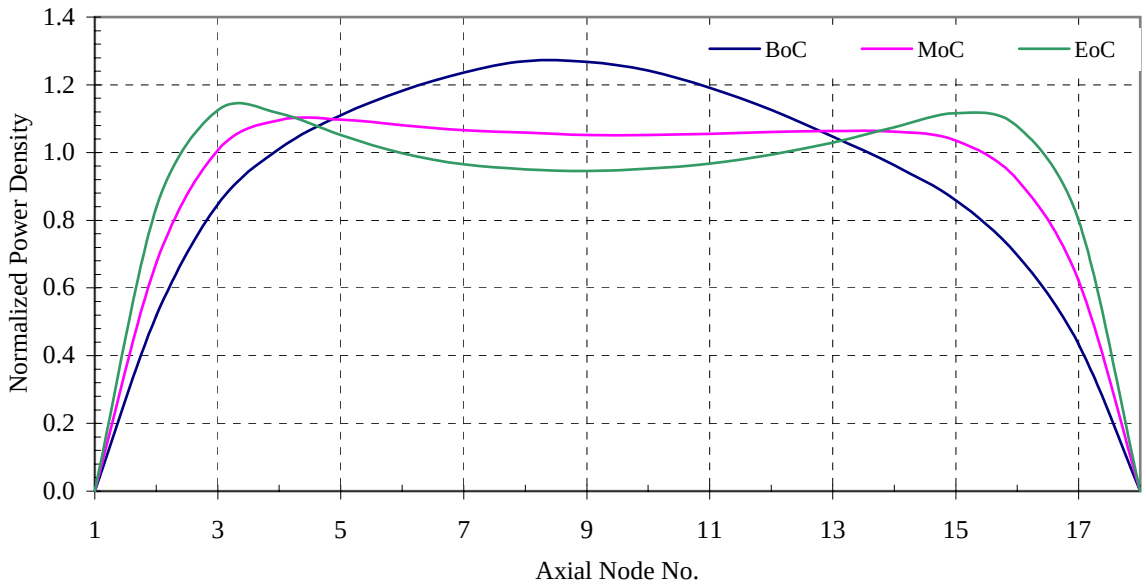

Figure B3.1.9 Core Average Axial Power Shape (identical for all cycles)

The radial power distribution tends to peak in fresh (and occasionally in once-burned) fuel, and decreases with cycle burnup. Also, a modified low-leakage fuel loading is used with once-burned fuel on the core periphery. Note that the terminology of fresh/once-burned/twice burned fuel refers the seed since the blankets remain in the core for six seed cycles.

1.001 0.680 0.617			Fresh Once Twice		
1.048 0.732 0.662	1.267 0.919 0.828				
1.127 0.855 0.781	1.329 1.040 0.946	1.182 0.971 0.893			
1.304 1.205 1.170	1.196 1.027 0.956	1.316 1.283 1.246	1.197 1.133 1.067		**BOC** **MOC** **EOC**
1.150 1.069 1.019	1.267 1.291 1.278	1.152 1.110 1.057	1.241 1.348 1.344	1.046 1.089 1.070	
1.165 1.247 1.273	1.067 1.063 1.043	1.150 1.271 1.300	1.111 1.184 1.174	0.981 1.151 1.222	0.655 0.733 0.774
0.912 0.934 0.947	0.979 1.091 1.159	0.829 0.880 0.906	0.883 1.039 1.127	0.736 0.843 0.894	0.496 0.563 0.604
0.707 0.736 0.764	0.693 0.734 0.768	0.656 0.711 0.754	0.535 0.600 0.647		

Figure B3.1.10 Radial Power Map (Cycle 6)

B3.2 Seed Blanket Unit (SBU) Thermal Analysis (Task-2)

The thermal-hydraulic performance of a seed blanket unit (SBU) was evaluated by using the COBRA-EN code (COBRA, 2001). One of the challenges to the thermal design of the SBU fuel assembly is to accommodate the relatively high radial power peaking (~2 versus ~1.2 in conventional PWR cores) because of the placement of high reactivity seed material in the central region of a SBU fuel assembly.

B3.2.1 SBU Assembly Model

The subchannel code COBRA-EN was developed in the 1980's at ENEL Spa, Milano, Italy. It has a number of enhancements as compared to COBRA-IIIC/MIT. The most significant change is an option to include the vapor phase continuity in the field equations, making it a four-equation model. An implicit solution based on the Newton-Raphson iteration for non-linear systems is applied to the four-equation model to solve for the local pressure and void fraction simultaneously. The code utilizes a full boiling curve (single-phase forced convection, subcooled nucleate boiling, saturated nucleate boiling, transition, and film boiling). It also has extended the list of available thermal-hydraulic correlations, including the EPRI correlations for CHF, two-phase friction multiplier, and void-quality relation.

The subchannel model of the SBU considers 1/8 of a 17x17 assembly. The basic data for the model, such as geometric dimensions, axial and radial power distributions, were derived from the reference RTF-18 design (Galperin, et al, 2001) in the initial evaluations. The geometry of the 1/8 SBU assembly and the numbering scheme for the fuel rods and coolant channels are shown in Figure B3.2.1. There are 45 rods and 45 coolant subchannels. The three types of rods are: seed (17), blanket (22), and guide tube (6) but only the 39 fuel rods are explicitly included in the subchannel model. The guide tubes are included only in the calculation of the channel wall friction. The gaps between rods define the boundaries of the coolant subchannels.

For the initial evaluations, a conservative assembly power factor of 1.5 (relative to the core average) was assumed for the 'hot' assembly. Also, the pin-wise power distribution was based on the results for the beginning of the first cycle. The effects of the cycle dependent power distribution are considered later in the 1/8-core analysis.

The regionally normalized relative rod power for the seed and blanket rods calculated by the BOXER code are shown in Figures B3.2.2 and B3.2.3 respectively. For rods in the seed (blanket) region the power factors in Figure B3.2.2 (Figure B3.2.3) are relative to the average seed (blanket) rod in the SBU assembly. The fraction of power generated in the seed and blanket region is 0.602 and 0.398 respectively. Note that as the cycle proceeds, the relative power in the seed decreases, while that in the blanket increases; therefore, the use of BOC values is conservative. The relative rod power normalized to the assembly-wide average rod power is calculated using the fractional power generation in the seed and blanket region and the result is shown in Figure B3.2.4. The hot rod has a relative pin power factor of ~2. The cycle-dependent relative axial power distributions

are shown in Figure B3.2.5. The axial power distribution for the first cycle was used in the present calculation and the peak axial power factor is ~1.6. The local power factor is the product of the 'hot' assembly power factor, the relative pin power factor, and the relative axial power factor. Given the conservatively assumed 'hot' assembly power factor of 1.5, the peak local power factor is ~4.8 for the hottest fuel pin. The main parameters of the COBRA-EN model are given in Table B3.2.1.

The hot assembly model was used for the evaluation of the following design parameters:

1) Effects of a hot assembly power factor of 1.5.
2) Effects of higher grid loss in the blanket region.
3) Effects of using different DNB correlations.

Two steady-state cases of the SBU model were analyzed by the COBRA-EN code. The nominal power case has a minimum critical heat flux ratio (MCHFR) of 1.28 while the case of overpower at 112% results in a MCHFR of 1.04. In both cases the MCHFR is associated with the hottest rod (seed rod #17) and the subchannel with the smallest flow area (channel #15). Since both the nominal and the 112% power cases have MDNBRs < 1.3, the target hot assembly factor would be ~1.2 (1.5x1.04/1.3) under the same assumptions.

It is noted from Figure B3.2.1 that channel 15 is surrounded by only two fuel rods (two seed rods) instead of the usual three (the third rod in this case is a guide tube). That explains the lower than maximum coolant exit temperature for channel 15 as compared to the other subchannels in the seed region.

As a means to divert more flow to the seed rod region, several calculations were done by using higher spacer grid loss coefficient in the blanket region than the seed region. The base case used a uniform loss coefficient of 0.86 for both the seed and blanket regions of an SBU assembly. The effect of increasing the loss coefficient in the blanket region is shown in Table B3.2.2 that lists the resulting MDNBR for different loss coefficients. Over the range of coefficients considered (0.86 to 1.5), only modest improvement in the MDNBR is noted.

The COBRA-EN code has seven built-in correlations for calculating the DNBR. Results from using these seven correlations to determine the MDNBR are summarized in Table B3.2.3. Among the correlations programmed in COBRA-EN the EPRI correlation is the most recent one. The MDNBR predicted by the W-3 correlation and the EPRI correlation appear to be very close and for the rest of the analysis the W-3 correlation is used for the evaluation of DNBRs.

B3.2.2 1/8-Core Analysis

The 1/8th assembly model discussed in the previous section was extended to a core-wide model. The core model considers one 1/8th symmetric octant of the 193-assembly core (see Figure B3.2.6). In a sub-channel analysis, the further away an SBU assembly is from the hot assembly the less influence it will have on the thermal-hydraulic response of the hot assembly. This allows for the lumping of assemblies some distance from the hot assembly. Figure B3.2.7 is a conceptual layout of the 1/8th core sub-channel model. The core is divided into one hot assembly region and eight lumped assembly regions. This represents a finer structure towards the center and coarser structure away from the center. The hot assembly is assumed to be located at the center of the core, and individual fuel rods in the seed and blanket modules are modeled for the 1/8th assembly. Adjacent to the 1/8th assembly are lumped regions. Each lumped region constitutes an increasing number of SBU assemblies as the distance from the center is increased. A lumped region is treated as an effective sub-channel that represents the total flow and total power of all the seed and blanket rods in the region. Inter-region communication is facilitated by crossflow between adjacent sub-channels. It is evident from Figure B3.2.7 that the outer regions have effective sub-channels that encompass more fuel assemblies than their counterparts in the interior regions. Based on the RTF18 –oxide reference design a set of conservative assembly power factors were used for the core-wide sub-channel analysis.

The geometry and numbering scheme for the 1/8th SBU core is shown in Figure B3.2.7. The 1/8th hot assembly is at the center of the 1/8th core sub-channel model. The 1/8th assembly includes 39 heated rods and 45 coolant subchannels (see Figure B3.2.1). In addition to the 17 seed and 22 blanket rods the hot assembly also includes 6 guide tube rods. The boundaries of the coolant subchannels are defined by the gaps between rods, or the centerline of the gap between adjacent assemblies. The rest of the 1/8th SBU core model is divided into 8 lumped assembly regions with increasingly coarser structures moving away from the center. The lumped assemblies include combined seed and blanket regions resulting in one rod and channel pair. Each lumped module represents the total flow and total power in the partial or combined assembly sub-channel.

The cycle dependent radial power map from the reference RTF-18 design (Galperin, 2001) was re-ranked in descending order, to ensure that the 1/8th assembly and adjacent lumped modules have the highest power factors as shown in Table 3.2.4 for cycle 1. The axial power distribution for the hot assembly at the beginning of the first cycle is shown in Figure B3.2.8, It is seen that both the seed and blanket regions have almost identical axial power shape. The axial power distribution for the hot seed region is conservatively applied to all rods in the analysis and it has a peak value of 1.555. The relative rod power distribution for the 1/8th assembly rods is shown in Figure B3.2.4. The local power factor for rods within the 1/8th assembly is a product of the radial power factor, the relative rod power and the relative axial power factor. The power factor for a lumped module is simply the product of the radial power factor and the relative axial power factor. The fractions of power generated in the seed and blanket region for cycle 1 are again taken as the conservative BOC values: 0.602 and 0.398, respectively. The peak local power factor for cycle 1 is 3.65 (1.189 x 1.973 x 1.555). The main parameters of the COBRA-EN are listed in Table B3.2.5.

In order to obtain an appropriate working SBU 1/8th core model, the core pressure drop was adjusted in COBRA-EN such that the total flow was equal to 1/8th of the total core flow rate. The Newton-Raphson iteration scheme was used to achieve convergence for both 1/8th core and 1/8th assembly models.

Two steady-state cases of the SBU model were analyzed by the COBRA-EN code: one 1/8th core case and one 1/8th assembly case for the first fuel cycle and assuming nominal power conditions. The first cycle is considered the most conservative case, and thus is the initial case to be analyzed. The 1/8th assembly case was done for comparison with the 1/8th core method assuming the same core pressure drop and correlation as the corresponding 1/8th core model. Based on the W-3 CHF correlation, the 1/8th core nominal power case has a minimum departure from nucleate boiling ratio (MDNBR) of 1.588, while the 1/8th assembly nominal power case has a MDNBR of 1.585. This shows that the effect of the surrounding assemblies on the hot channel is minimal. In fact, the 1/8th core model consistently has a higher MDNBR due to increased crossflow resulting from the addition of the lumped modules. These results are shown in Table B3.2.6.

Several sensitivity cases were done at 112% and 118% power, both at upset conditions of +2°C in inlet temperature and -5% in core flow. Results are summarized in Table B3.2.7. At 112% overpower the MDNBR is above 1.3 while at 118% overpower the MDNBR is slightly below 1.3.

The cycle dependence of MDNBR was assessed by a series of calculations using cycle specific core power distributions. The MDNBR for each of the six fuel cycles is shown in Table B3.2.8 and the first cycle power distribution is indeed the most limiting one.

Table B3.2.1 Summary of the COBRA-EN Model Parameters for the SBU Assembly

Model	Open subchannels with crossflow mixing
Modeled region (Figure 1)	1/8 SBU assembly, full axial length
Coolant channels	45
Channel types	6
Number of rods	45 (17 seed, 22 blanket, 6 guide tube)
Axial nodes	48, evenly spaced over 3.6576 m
Radial power distribution	Figure B3.2.4
Axial power distribution	Figure B3.2.5
Nominal reactor power	3400 MW
Number of fuel assemblies in core	193
System pressure	15.5 MPa
Core inlet temperature	289.1° C (562.25 K)
Core average mass flux	4112.7 kg/s-m^2
Spacer grids	7, evenly spaced
Form loss coefficient for grids	0.86
Turbulent mixing model	$w' = \beta\ s\ \overline{G}$, $\beta = 0.038$
Cross-flow resistance	$K_{ij} = 0.5$
Momentum turbulent factor	FTM = 0.0
Transverse momentum factor	S/L = 0.5
Single-phase friction factor	Default smooth tube friction factor
Two-phase friction	EPRI correlation
Subcooled boiling	EPRI model
Void fraction correlation	EPRI drift flux
Heat transfer models	Dittus-Boelter for single-phase, Thom correlation plus single-phase convection for subcooled and saturated nucleate boiling
Critical heat flux correlation	W-3
Inlet flow condition	Uniform mass flux
Pressure drop constraint	Uniform pressure drop in all flow channels

Table B3.2.2 Sensitivity of MDNBR to Spacer Grid Loss Coefficient

Spacer Grid Loss Coefficient For the Blanket Region	MDNBR (W-3)
0.86	1.280
1.1	1.303
1.3	1.320
1.5	1.335

Table B3.2.3 MDNBR Predicted by Various CHF Correlations

DNB Correlation	MDNBR	Axial Location (m)	Local Heat Flux (MW/m^2)	Rod # / Channel #
W-3	1.280	1.638	2.829	17 / 15
B&W-2	1.089	1.562	2.850	17 / 14
EPRI	1.241	2.095	2.476	17 / 15
MacBeth, 12 coefficients	1.107	1.867	2.693	17 / 14
MacBeth, 6 coefficients	1.142	1.943	2.624	17 / 14
Biasi	1.055	1.867	2.693	17 / 14
Modified Barnett	2.516	1.791	2.748	17 / 15

Table B3.2.4 Radial Power Map (Cycle 1)

Rod Number	Radial Power Factor
1/8th assembly	1.189
Rod 40 (1/4 assembly)	1.184
Rod 41 (1/4 assembly)	1.184
Rod 42 (1/2 assembly)	1.171
Rod 43 (1/2 assembly)	1.170
Rod 44 (1 assembly)	1.166
Rod 45 (1/2 assembly)	1.152
Rod 46 (7 assemblies)	1.114
Rod 47 (14 assemblies)	.905

Table B3.2.5 Summary of the COBRA-EN Model Parameters for the SBU Assembly

Parameter	Specification	
	1/8th assembly model	***1/8th core model***
Model	Open subchannels with crossflow mixing	
Modeled Region	1/8th SBU assembly, full axial length	1/8th SBU core, full axial length
Coolant Channels	45	52
Channel Types	6	11
Number of Heated Rods	39 (17 seed, 22 blanket)	47 (17 seed, 22 blanket, 8 lumped)
Axial Nodes	48, evenly spaced over 3.6576m	
Radial Power Distribution	Table B3.2.4	
Axial Power Distribution	Figure B3.2.8	
Nominal Reactor Power	3400 MW	
Number of Fuel Assemblies in Core	193	
System Pressure	15.5 MPa	
Uniform Pressure Drop (cycle 1)	.141 MPa	
Core Inlet Temperature	289.1° C (562.25 K)	
Total Core Flow Rate	18.63 Mg/sec	
Core Average Mass Flux	3933.3 kg/m^2/s	
Desired Flow Rate	-	2328.8 kg/s

Table B3.2.6 Cycle 1 Results

	1/8th assembly model	***1/8th core model***
MDNBR	1.585	1.588
Axial Location (m)	1.2757	1.2757
Local Heat Flux (MW/m^2)	2.231	2.231
Rod #/Channel #	17/19	17/19
Local Axial Mass Flux in Channel 19 ($kg/m^2/s$)	3661.78	3675.44
Minimum Axial Mass Flux in Channel 15 ($kg/m^2/s$)	3620.51 (2.286m)	3618.23 (2.286m)
Minimum Axial Mass Flux in Channel 19 ($kg/m^2/s$)	3644.77 (2.286m)	3641.66 (2.286m)
Average Mass Flux in Channel 15 ($kg/m^2/s$)	3684.06	3665.97
Average Mass Flux in Channel 19 ($kg/m^2/s$)	3693.90	3673.68

Table B3.2.7 Cycle 1 Sensitivity Cases

Model	**Conditions**	**MDNBR**
1/8 Core		
	100% Power	1.588
	112% Power (Temp: +2K, Flow:-5%)	1.349
	118% Power (Same Temp and Flow as 112% overpower)	1.241
1/8 Assembly		
	100% Power	1.585
	112% Power (Temp: +2K, Flow:-5%)	1.349
	118% Power (Same Temp and Flow as 112% overpower)	1.237

Table B3.2.8 Cycle Dependence of MDNBR

Cycle	1/8 Core		1/8 Assembly	
	MDNBR	Axial Location (m)	MDNBR	Axial Location (m)
1	1.588	1.257	1.585	1.257
2	1.607	1.257	1.598	1.257
3	1.696	1.257	1.688	1.257
4	1.681	1.638	1.674	1.638
5	1.655	1.257	1.647	1.257
6	1.759	1.257	1.753	1.257

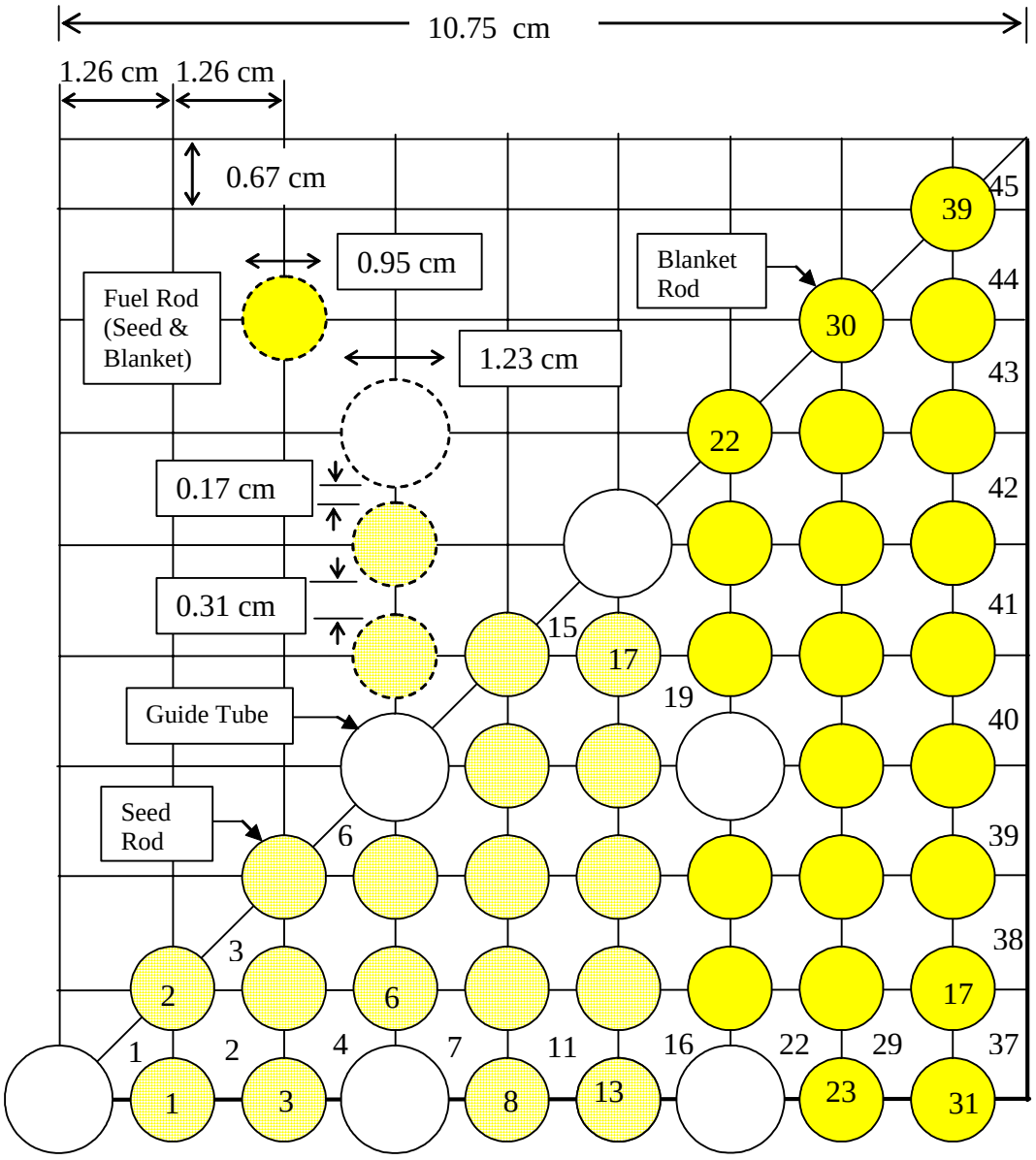

Figure B3.2.1 Subchannel Model of 1/8 SBU Assembly

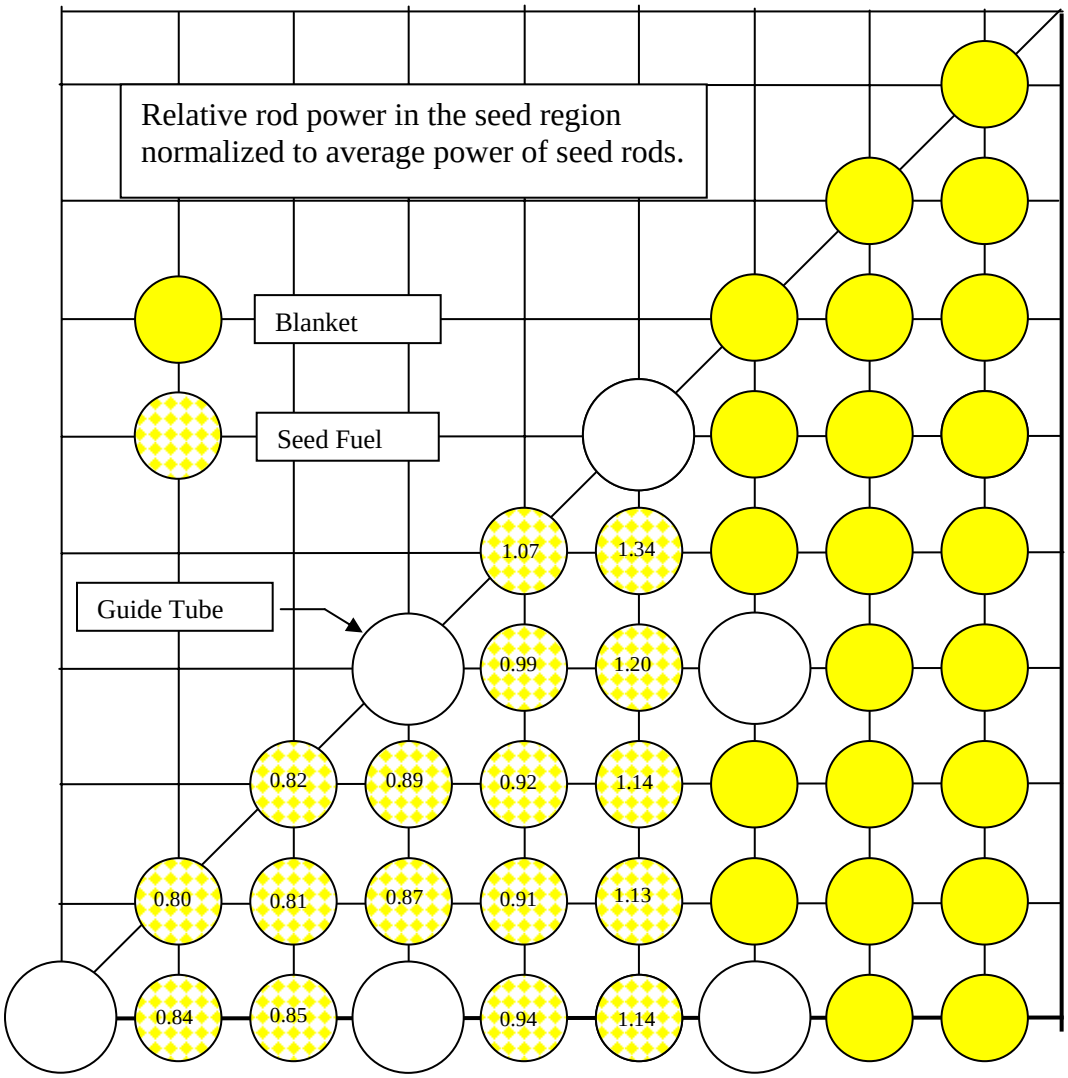

Figure B3.2.2 Relative Power in the Seed Region Normalized to the Average Seed Power

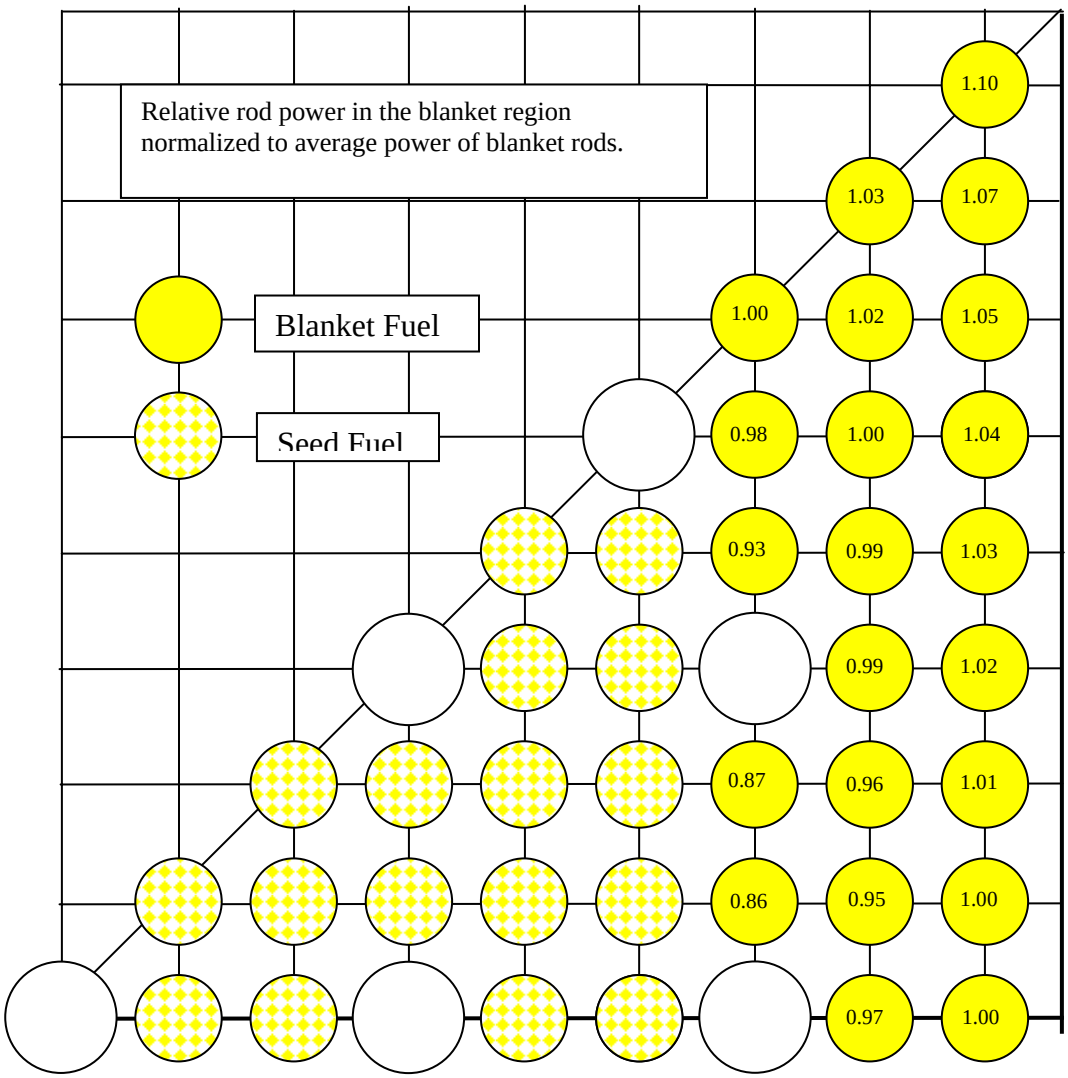

Figure B3.2.3 Relative Power in the Blanket Region Normalized to the Average Blanket Power

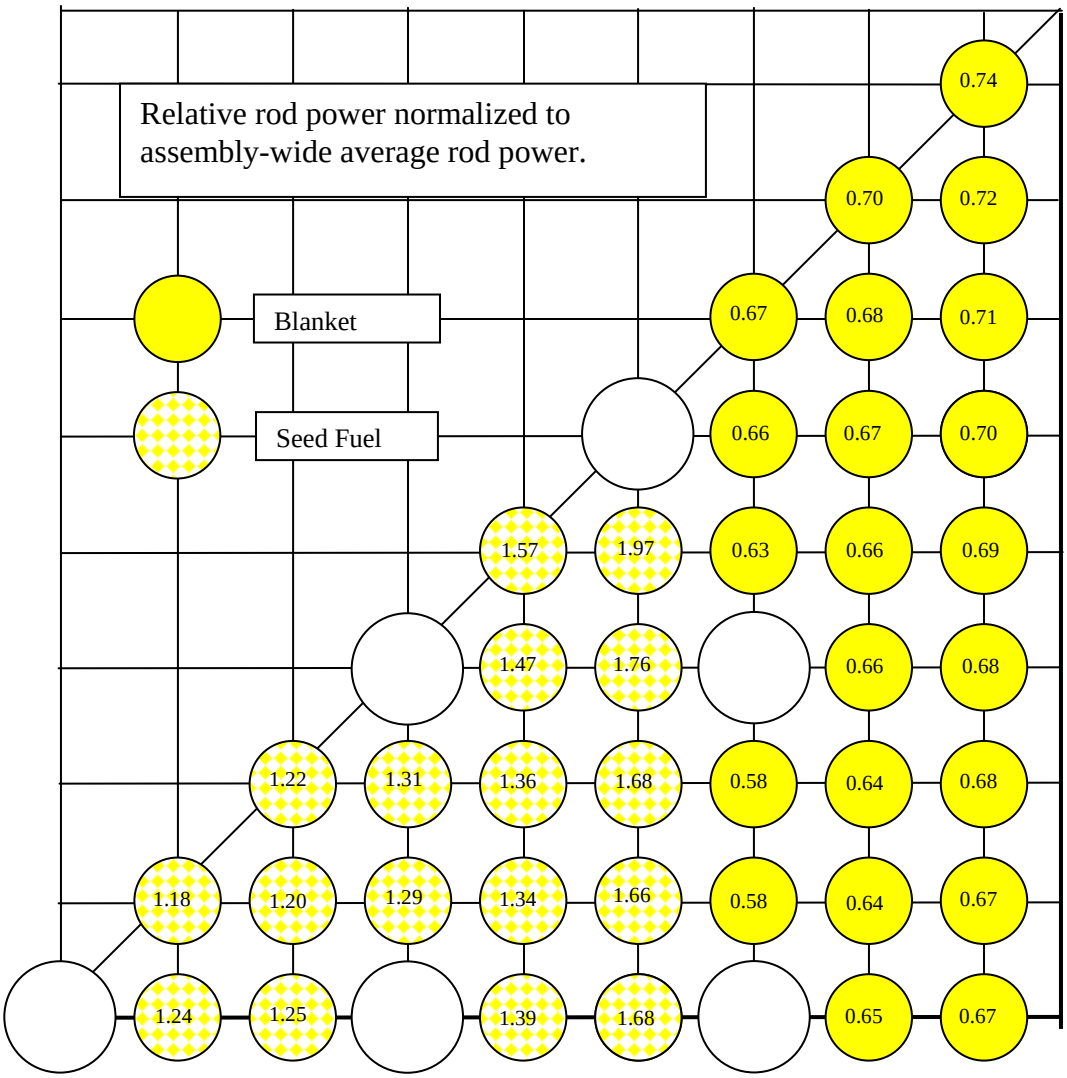

Figure B3.2.4 Relative Rod Power Distribution in an SBU Assembly

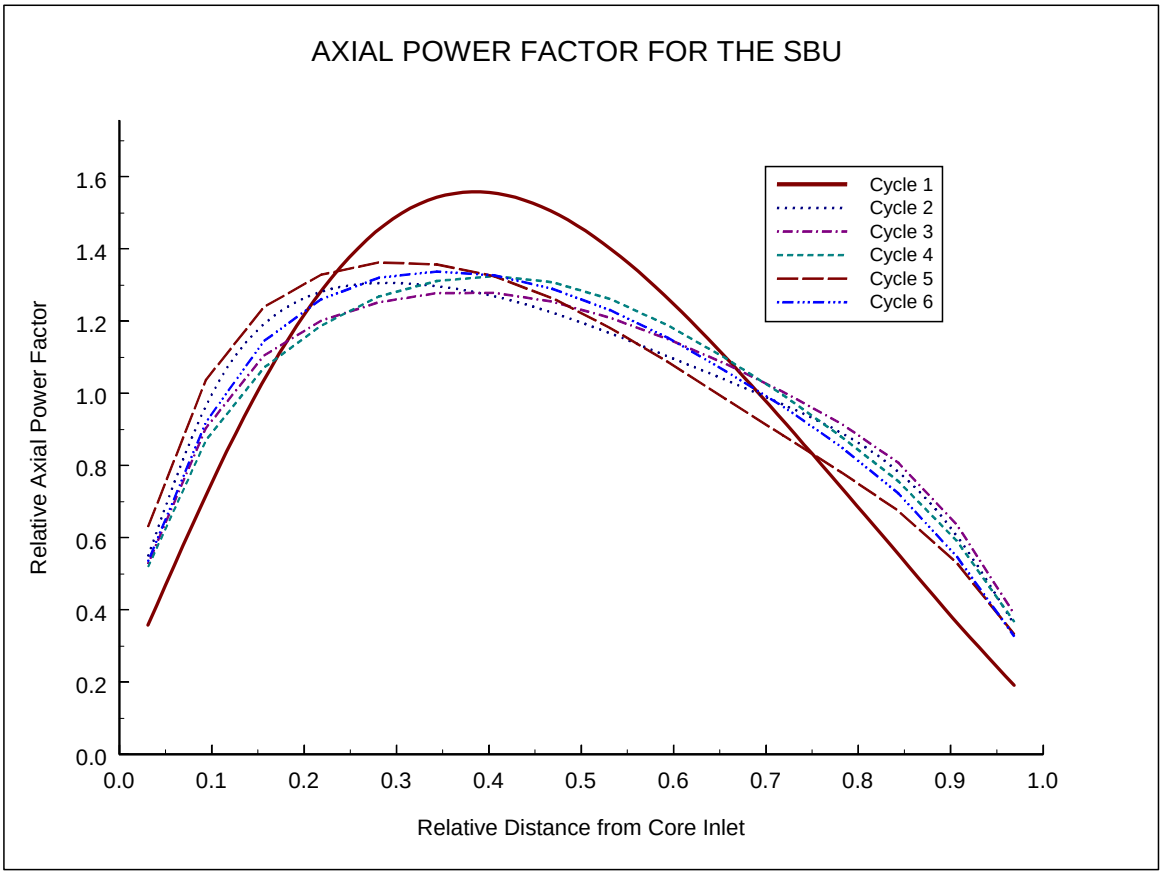

Figure B3.2.5 Axial Power Distribution for the SBU Hot Assembly (Seed Region)

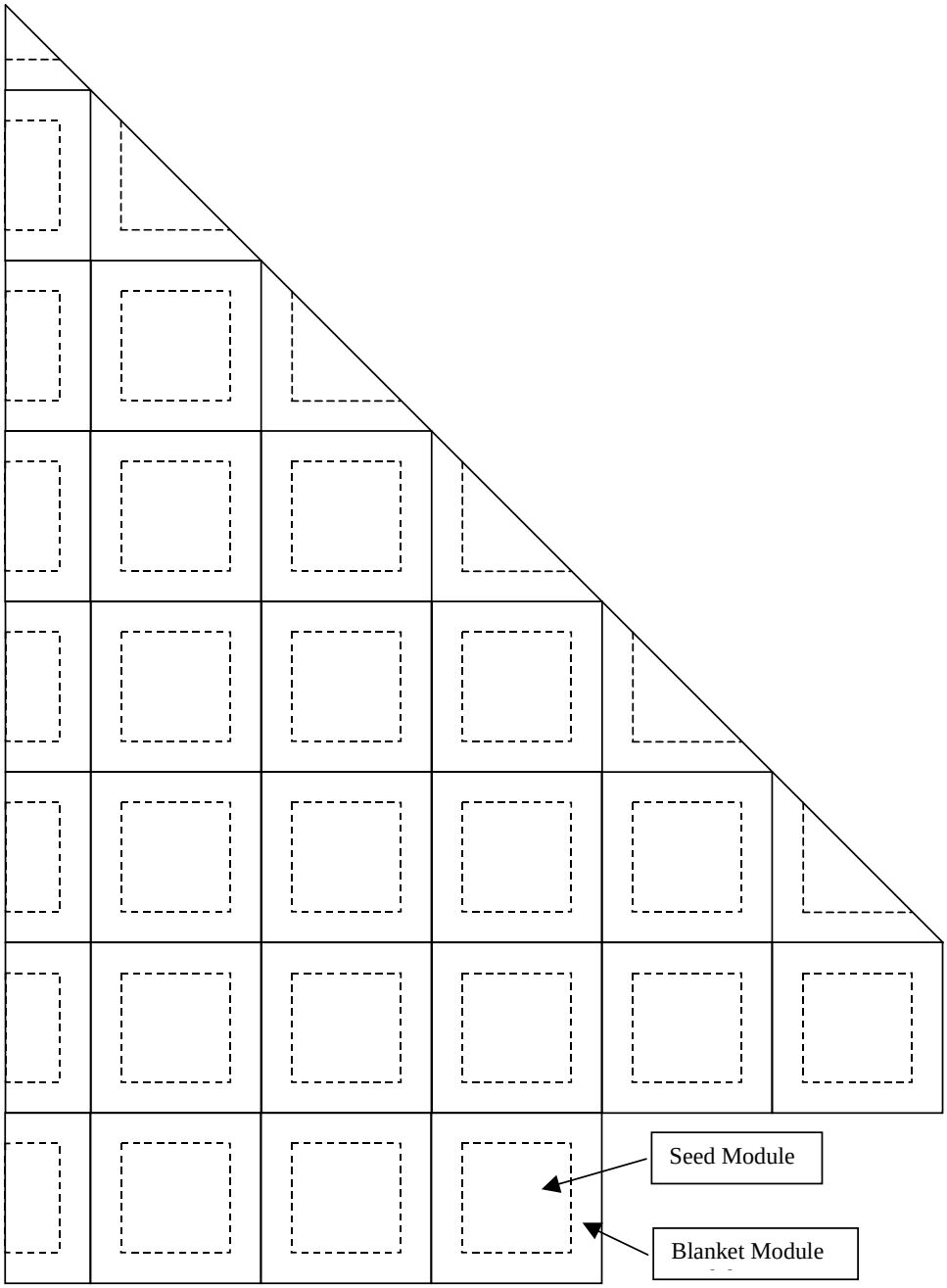

Figure B3.2.6 Configuration of 1/8th Core with SBU Assemblies

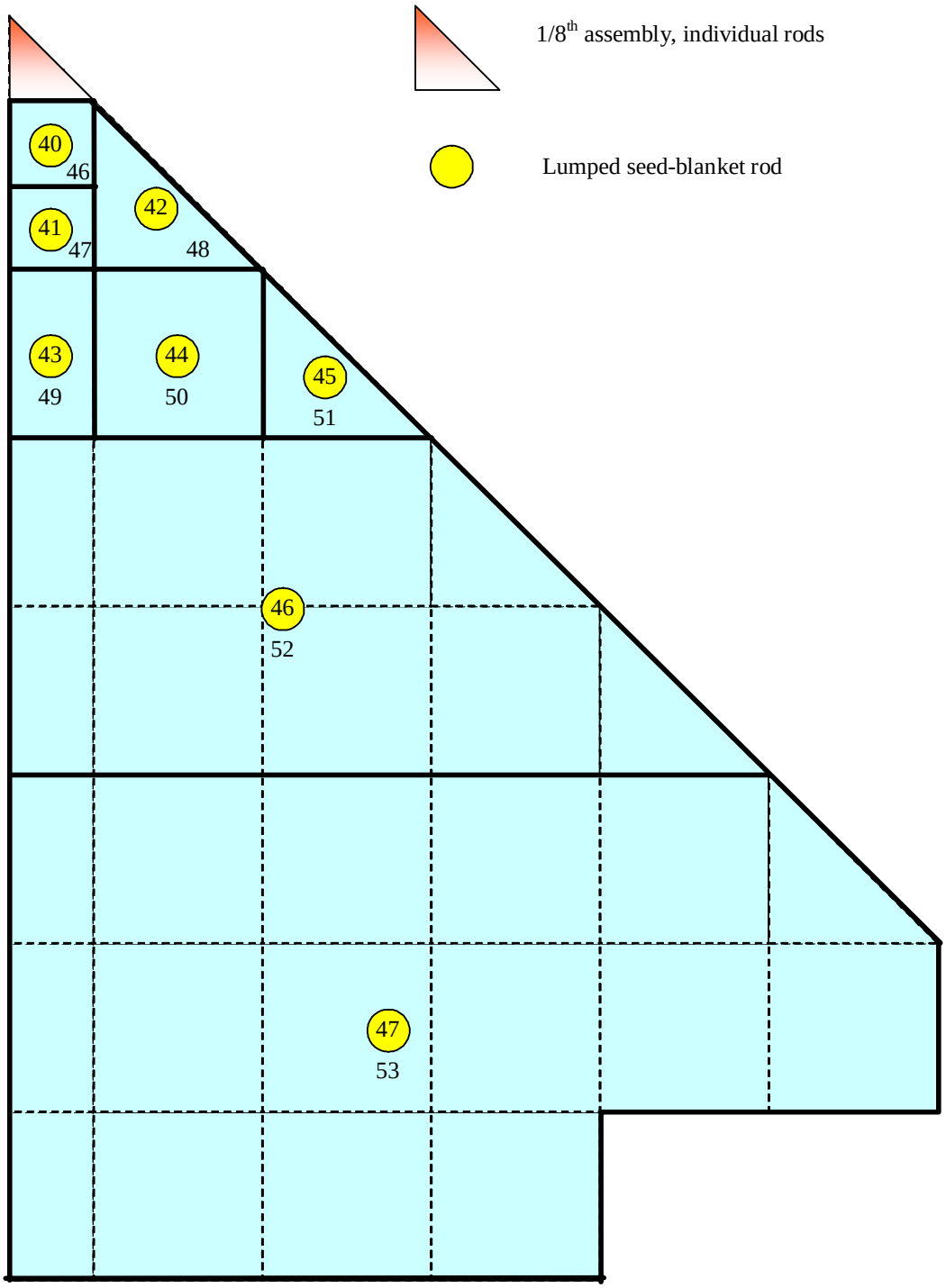

Figure B3.2.7 Conceptual Layout of Sub-channels in the 1/8th Core

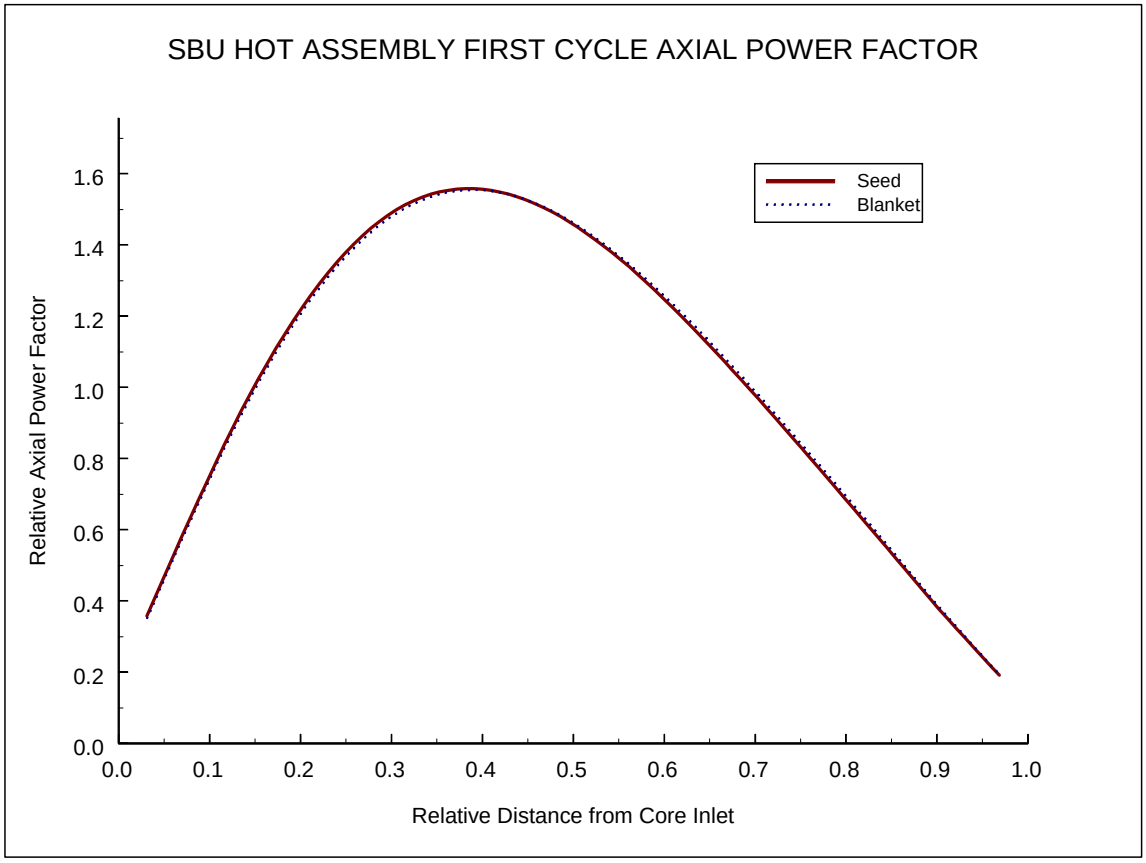

Figure B3.2.8 Hot Assembly Axial Power Shape (Cycle 1)

B3.3 Assembly and Fuel Mechanical Design (Task-3)

Several design options for the mechanical design of the SBU have been proposed by a consultant who has experience in the mechanical design of advanced fuel assemblies for PWRs. These SBU design options include:

- Option 1: Separate seed and blanket modules with an open lattice ("open" configuration).
- Option 2: Separate seed and blanket modules with an internal flow baffle between the modules ("canned" configuration).
- Option 3: This option permits use of the standard PWR assembly essentially unmodified.

This work was funded by Thorium Power, Inc. under a separate sub-contract.

In Options 1 and 2 where the seed and blanket are assumed to be distinct modules (as was initially envisioned), the additional clearances required for both the "open" and "canned" configurations are obtained by reducing the diameter of the peripheral seed fuel rods along the outer boundary of the module.

The impacts of Options 1 and 2 on the neutronic behavior of the SBU have been evaluated, and found to not negatively impact performance. In addition, concerns about the effect of long-term operation on the guide tubes led to the recommendation that they be fabricated of stainless steel instead of Zircaloy; the impact of this modification was also evaluated, and found to be ~0.012 Δk.

Option 3 takes advantage of experience in the industry with replacing failed/damaged fuel rods individually. In this approach the mechanical design of the SBU is essentially identical to that of a standard PWR assembly, obviating the need for detailed mechanical design and testing. The replacement of the seed rods is accomplished via a special machine whose design exists, and which has operated successfully. The SBU is moved to the spent fuel pool, and the machine removes and replaces the seed rods one-by-one [cf. Figures B3.3.1 and B3.3.2]. The estimated time required to remove the 108 spent seed rods and replace them with fresh rods is less than ~2.5 hours based on previous experience; therefore these operations should not adversely affect the refueling outage. In addition, design improvements to the refueling machine that could reduce this time further are possible. This approach has therefore been selected as the reference for the SBU option.

Despite these advantages, the fact that the seed sub-assembly (SSA) is not a single module may introduce some issues with respect to proliferation resistance; these are discussed in Section B3.5.

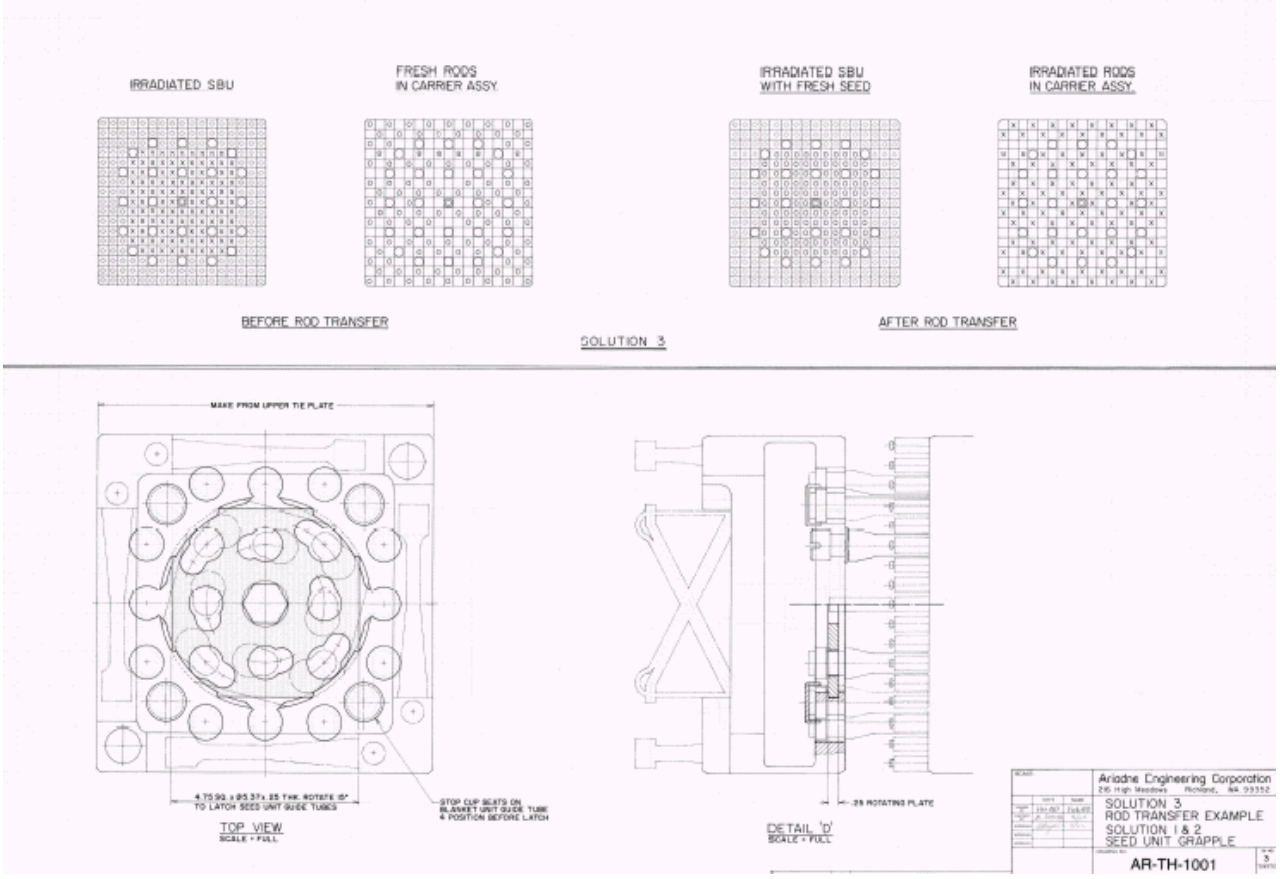

Figure B3.3.1 Seed Rod Replacement Scenario

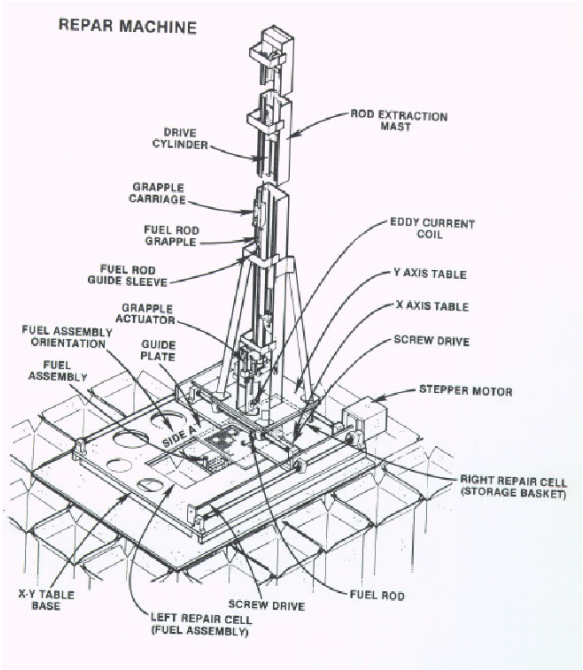

Figure B3.3.2 Re-Fueling Machine

B3.4 Fuel Cycle Cost (Task-5)

The approach followed to address the fuel cycle costs associated with the SBU design is identical to that described in Section B2.4. The assumptions that served as the basis for the estimates are summarized in Tables B3.4.1 and B3.4.2, and resultant fuel cycle cost for the 18-month seed/6-9 cycle blanket are given in Table B3.4.3. Note that under the given set of assumptions, the fuel cycle cost for the SBU concept is from ~7-10% lower than that for the reference PWR. Even accounting for the fact that the uncertainties for the SBU are inherently higher than for the standard PWR, it is likely that the concept is at least competitive.

Table B3.4.1 Component Unit Cost

Thorium	50 $/kg
Natural Uranium	50 $/kg
Conversion	6 $/kg
Enrichment	80 $/kgSWU
Fabrication (UO_2 – PWR)	250 $/kg
Fabrication (Seed)	500 $/kg
Fabrication (Blanket)	300 $/kg
Spent Fuel Storage	50000 $/Assembly
Spent Fuel Disposal	500 $/kg

Table B3.4.2 Lead and Lag Time to Irradiation, months

U_3O_8 (Natural Uranium)	12 (time to irradiation)
Thorium	6 (time to irradiation)
Conversion (UF_6)	6 (time to irradiation)
Enrichment	6 (time to irradiation)
Fabrication	3 (time to irradiation)
Spent Fuel Storage	0 (time after discharge)
Spent Fuel Disposal	90 (time after discharge)

Table B3.4.3 Fuel Cycle Cost, mills/kWe-hr

Component	Reference PWR	SBU		
		Seed	Blanket	
			U	Th
Purchase	1.63	1.17	0.20	0.05
Conversion	0.19	0.14	0.02	0
Enrichment	1.53	1.44	0.24	0
Fabrication	0.75	0.25	0.31	
Front End Cost	**4.10**	**3.01**	**0.82**	
Spent Fuel Storage	0.28	0.11	0.05	
Total	**4.38**	**3.98**		
Spent Fuel Disposal	0.72	0.26	0.29	
Total, (+ disposal)	**5.10**	**4.53**		

B3.5 Waste Characteristics and Non-Proliferation Performance (Task-6)

Enhanced proliferation resistance and improved waste characteristics have been among the key drivers for considering thorium-based fuels.

The proliferation characteristics of the reference 18-month, oxide seed SBU configuration are summarized in Table B3.5.1, and compared to those of a standard PWR. The data have been normalized to the production per GWe-year.

Table B3.5.1

Plutonium Content of Typical Discharge Fuel

	Typical Present-Day PWR		Typical SBU Seed + Blanket	
Plutonium isotope	kg/GWe-yr	Fraction of Pu (%)	kg/GWe-yr	Fraction of Pu (%)
238	6	3	5	7
239	124	55	38	47
240	47	21	17	20.5
241	34	15	12	15.5
242	14	6	8	10
Total	225	100	80	100.0

- For the 18-month cycle, the total annual production of Pu is reduced by a factor of ~3 relative to a standard PWR; the reduction in plutonium production is greater for 12-month cycles.

- The plutonium that is produced has a higher content of Pu-238, Pu-240, and Pu-242, which makes it impractical for use in a weapon due to the high heat production (Pu-238), and high spontaneous neutron yields (Pu-240, Pu-242), which contribute to a high probability of pre-ignition, and hence unreliable performance as fuel for an explosive. Indeed, the Pu-238 content is above the proposed 5% threshold to make plutonium non-proliferative (Rahn, 1984).

- Concerns about the proliferation potential of the bred U-233 are addressed by burning it *in situ*, and then placing the blanket fuel into storage. In addition, the U-233 that is produced is denatured by the other uranium isotopes from the initial fuel loading. This means that it can not be separated chemically, and isotopic separation would be required should extraction and use of the bred U-233 be attempted. The combined concentrations of U-233 and U-235 are always kept below the proliferation limit proposed by ORNL (Section 3.1.1).

Figure B3.5.1 shows the behavior of the radioactivity and decay heat per GWe-yr in the spent fuel, respectively, as a function of time following removal from the reactor. Note that both are generally lower than the corresponding values for the standard PWR, though not significantly, except for around 100,000 years. The increase is characteristic of thorium-based fuels and is due

to the decay products of U-233. In the near term, where the fission products dominate, the values are essentially the same as those for standard uranium fuel.

Because of the long residence time of the blankets (six 18-month cycles), and the small size of the SSA, the equivalent number of fuel rods removed per reload in the SBU design is reduced by ~30% compared to a standard PWR. The mechanical design and the individual, rod-by-rod reloading approach for the seed rods described in Section B3.3, may allow even further reductions in the actual volume that is sent to the repository, depending on the details of the design of the container since there will be a higher heat load from the Pu-238. The higher heat load is a benefit for proliferation resistance, but a potential drawback for storage. There is an additional downside to the rod-by-rod reloading scheme from a non-proliferation perspective since individual rods may have to be tracked and accounted for making materials control and accountability more complicated. Design of an appropriate "receipt container" to receive the discharged seed fuel rods during refueling may partially obviate, or eliminate, this concern.

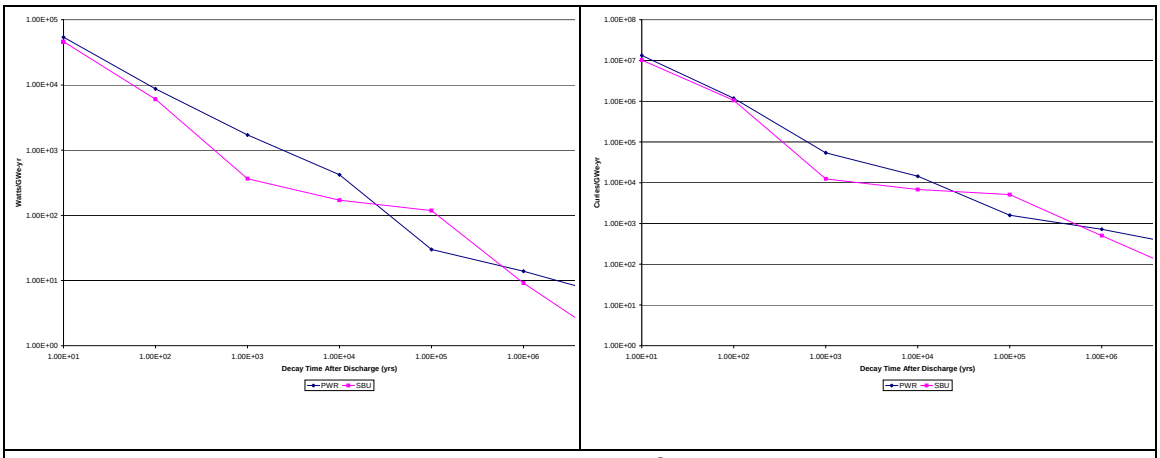

Figure B3.5.1 Decay Heat and Radioactivity of the SBU Spent Fuel per Electrical Energy Generation

B3.6 Safety Analyses (Task-8)

B3.6.1 Approach for Safety Analyses

The main objective of this task is to perform a limited set of bounding accident analyses to ensure that the heterogeneous configuration of the core created by the presence of SBU assemblies does not move the reactor out of the bounds of the existing safety envelope. The development of the analysis methodology and the selection of representative transients have benefited from the work performed in Russia and Israel on the Radkowsky Thorium Fuel (RTF) project, which is funded jointly by the U.S. DOE and Thorium Power, Inc. (formerly the Radkowsky Thorium Power Corporation (RTPC)). BNL manages the technical work on the RTF project for the U.S. DOE under the Initiatives for Proliferation Prevention (IPP) program and for Thorium Power, Inc. through a CRADA. The Russian Research Center – "Kurchatov Institute" (RRC-KI) has performed a similar task of safety analysis for using seed-blanket type assemblies in a VVER. There is significant synergy gained from the Russian work because the approach and concepts developed for the analysis of the VVERT (VVER with thorium-based SBUs), are in general applicable to the task of analyzing a typical Westinghouse PWR loaded with SBU assemblies. The following discussion outlines the methodology adopted for the transient analysis of a PWR SBU-core, and the selection of a limited set of transients to be analyzed.

Core Thermal-Hydraulics

The SBU assemblies are designed to replace conventional fuel assemblies in a typical Westinghouse PWR. The SBU neutronic calculations have been done for a 193-assembly core. For the accident and transient analysis an existing RELAP5 model of a PWR plant has been adapted to have a core reloaded with SBU assemblies. The core is typically represented in a RELAP5 model by collapsing the 193 fuel assemblies into a few lumped thermal-hydraulic channels. A hot channel is used to represent the most limiting fuel pin in the core. Average channels are used to represent the rest of the core, including unheated channels to allow for core bypass flow.

The determination of the power and flow to the hot channel requires a separate sub-channel analysis that models the core thermal-hydraulics down to the scale of individual fuel rods. The COBRA-EN code is used for the sub-channel analysis of the SBU core. As a result of core symmetry, only $1/8^{th}$ of the core needs to be analyzed, as shown in Figure B3.2.6. The main objective of the sub-channel analysis is to identify the limiting fuel pin and its associated flow sub-channel. The limiting fuel pin is the fuel rod with the minimum departure from nucleate boiling ratio (DNBR) and is usually found in the hottest assembly of the core. The limiting fuel pin and its associated flow channel are then treated as the hot channel in the RELAP5 model. In a sub-channel analysis, due to the presence of radial cross-flow, the main flow in the axial direction can be non-uniform, even in a steady-state situation. In the RELAP5 model multiple-junction components will be used to facilitate the lateral (radial) communication between adjacent vertical flow channels. For the hot channel in the RELAP5 model the initial flow will be adjusted such

that the coolant exit temperature is similar to that calculated by COBRA-EN for sub-channels surrounding the limiting pin under steady-state operating conditions. Since the power split between the seed and blanket module varies throughout the fuel cycle, it becomes necessary to model two hot channels, one for the hottest seed module and the other for the hottest blanket module.

Accident Analysis

Transient and accident analyses are performed to evaluate the safety of a nuclear reactor in the event of anticipated occurrences (transients) and postulated malfunctions or failures of equipment (accidents). Results of these safety analyses are used for the design specifications of components and systems for the protection of public health and safety (e.g. the design of the emergency core cooling systems - ECCS). They also form the technical bases for defining the safety limits (envelope) for the operation of the reactor and the limits on steady-state operation (operating limits). The steady-state limits are set by the limiting conditions for operation (LCO), and/or the limiting safety system settings (LSSS).

In a safety analysis the occurrence of an event, according to its frequency of occurrence, is categorized as a transient or accident. In the USNRC regulations the likely or anticipated events are referred to as anticipated operational occurrences (AOO) or simply as transients, and unlikely or unanticipated events are treated as accidents. Transients are further subdivided into incidents of moderate frequency (~1 to 10 per year), and infrequent incidents (~10^{-2} per year). The spectrum of accidents considered for the USNRC licensed power reactors generally has a frequency of occurrence in the range of ~10^{-2} to ~10^{-5} per year.

Under USNRC regulations, transients analyzed for a nuclear power plant need to meet two acceptance criteria:

(1) The pressure in the primary and main steam system shall not exceed values that can violate the primary coolant system boundary.

(2) No fuel damage shall be calculated. In the case of PWRs, this is satisfied by ensuring that the hot fuel rod does not experience departure from nucleate boiling (DNB).

For postulated accidents, some fuel damage is expected. A few fuel rods may experience DNB or cladding failure. In general the acceptance criterion for postulated accidents is required to meet the radiological limits stipulated in 10-CFR-100. However, for some specific accidents, criteria are defined in terms of peak clad temperature, fraction of metal-water reaction (e.g. see 10-CFR-50.46 for the LOCA), etc. Lower frequency accidents generally result in more severe radiological consequences. In comparing the performance of a core loaded with conventional fuel assemblies versus SBU assemblies, the intent of the present analysis is to determine the potential fuel damage in both cores for the same postulated accident, not to calculate anticipated radiological consequences.

Safety limits are prescribed for selected process variables related to the integrity of barriers to fission product release from the plant. Compliance with the safety limits assures that barriers will perform as assumed in the safety analysis. LCOs and LSSSs are chosen such that no plant transient violates safety limits and no postulated accident will have radiological consequences that do not meet the acceptance criteria for that postulated plant condition. LCOs and LSSSs then form the bases for the setpoints for the reactor protection system (RPS) and the engineered safety feature (ESF) systems.

USNRC Regulatory Guide 1.7 provides a comprehensive list of transients and accidents analyzed by plants applying for a construction permit (CP) or operating license (OL). These are similar to those considered by Gosatomnadzor, the Russian Nuclear Regulatory body, and RRC-KI in their evaluation for the VVER version of an SBU core. Based on the RRC-KI review, three accident scenarios have been identified for the RELAP5 analysis, including control rod ejection, LOCA, and station blackout. We propose to consider these accidents as initial "bounding cases" for the SBU-PWR.

- The control rod ejection accident is a fairly rapid reactivity insertion transient. It not only raises the reactor power but also skews the core power distribution with more severe local peaking. This accident initiator also has the potential of raising the system pressure. It is noted that the point kinetics model in a stand-alone RELAP5 analysis will not have the capability to delineate the power peaking in a rod drop accident.

- A rupture in the reactor coolant system (RCS) initiates a large break loss of coolant accident (LBLOCA) resulting in rapid system depressurization with loss of primary inventory. This low probability accident is considered to be one of the design basis accidents (DBA). LBLOCA is used as the basis for designing a number of safety systems for the core and the containment because of its potential for leading to substantial fuel failure.

- A station blackout is a coincidental loss of onsite and offsite AC power to the station. This initiator leads to a decrease in heat removal by the secondary system. The progression of this accident would challenge the responses of safety systems to provide emergency decay heat removal and to limit plant temperatures and pressures within the safety envelope.

In addition to the above postulated accidents a loss of flow transient also will be analyzed. The initial phase of this transient is more severe than the station blackout accident since the reactor trip is on low flow and that means there is a short period of time in which the reactor will be operating at full power with reduced flow.

The above discussion presents the methodology to be used to couple the detailed core thermal-hydraulic analysis to the system transient and accident analysis. It also introduces the acceptance criteria for the safety analysis, and the list of accidents to be analyzed by using RELAP5. Results of the core thermal-hydraulic analysis have been presented earlier in Section B3.2. The RELAP5 accident/transient analysis of the SBU-core is presented in Section B3.6.3.

B3.6.2 Reactivity Coefficients

Reactivity coefficients and control worths for the baseline and optimized designs were evaluated with the BOXER lattice code at beginning-of-life (BOL), and as a function of burnup to ensure that they remain acceptable. The results for the Moderator Temperature Coefficient (MTC), Doppler Coefficient, Soluble Boron Worth, and Control Rod Worth are shown in Table B3.6.1 at BOL, and in Table B3.6.2 for SBU average burnups of 40 and 80GWd/T. It should be noted that the coefficients and worths are similar to those for the original Reference SBU designs, which in turn were similar to those typical of a PWR, supporting the design constraint that the SBU design remain within the existing safety envelope. These results, coupled with those presented in Section B3.1.1 demonstrate that the key performance and safety characteristics of the "optimized" and "baseline" SBU designs are very similar, with reduced rod-wise power peaking, and improved DNBR.

Table B3.6.1 Reactivity Coefficients and Control Worths for Reference and "Optimized" SBU Designs at BOL

Coefficient	Ref. (16w/o)	Ref. (20w/o)	Optimized (20w/o)
MTC (Δρ/C)	-2.52E-04	-2.33E-04	-2.33E-04
Doppler (Δρ/C)	-2.30E-05	-2.15E-05	-2.14E-05
Soluble Boron (Δρ/ppm)	-7.39E-05	-6.65E-05	-6.59E-05
Control Rods (Δρ)	3.92E-01	3.58E-01	3.54E-01

Table 3.6.2 Reactivity Coefficients and Control Worths for "Optimized" SBU with Burnup

Coefficient	0 GWd/T	40GWd/T	80GWd/T
MTC (Δρ/C)	-2.33E-04	-3.66E-04	-5.01E-04
Doppler (Δρ/C)	-2.14E-05	-2.55E-05	-3.18E-05
Soluble Boron (Δρ/ppm)	-6.59E-05	-6.88E-05	-9.29E-05
Control Rods (Δρ)	3.54E-01	-3.92E-01	-4.96E-01

B3.6.3 SBU Accident Analysis

The accident analysis of the SBU core was done by using the DOE version of the RELAP5 code, namely RELAP5-3D ver. 2.2.4 (RELAP5-3D, 2003). The steady state and LBLOCA input decks from MIT for the conventional PWR design, described earlier in Section B2.6, were used as templates for the SBU model. Modifications to the MIT model were made to replace the standard PWR assemblies with the corresponding SBU assemblies. This effort enables a comparison between the accident analysis of the SBU design and the conventional PWR. Furthermore, in order to facilitate a comparison between the WASB and the SBU design the same three accident sequences for the WASB study are repeated for the SBU core. Since two different versions of the RELAP5 code are used in the accident analysis, MIT using MARS and BNL using RELAP5-3D, a comparison of two sets of results for the same accident can serve as a gauge for code dependence of the accident analysis.

RELAP5 Model of the SBU Core

The model for a typical 4-Loop PWR plant has been described in Section B2.6 and will not be repeated here. The following is a description of the RELAP5 model for a core filled with SBU fuel assemblies.

Similar to a typical 4-Loop PWR, the SBU core has 193 fuel assemblies. Each fuel assembly has 108 seed rods, 156 blanket rods, and 25 guide tubes. The geometry and composition of the seed and blanket rods are shown in Figure B3.6.1. The layout of an SBU fuel assembly is shown in FigureB3.6.2. The imaginary boundary between the seed rods in the central region and the blanket rods in the peripheral region is set in the middle of the gap between the two regions.

In the RELAP5 model the SBU fuel assemblies are grouped into three hydraulic channels with corresponding heat structures representing the fuel rods. A schematic diagram of the hydraulic channels representing the core is shown in Figure B3.6.3. The hottest fuel assembly is represented by two hydraulic channels, one each for the seed and blanket region respectively. The rest of the core, 192 fuel assemblies, is assigned to a third hydraulic channel representing the average fuel assembly. Cross flow junctions along the axial length of adjacent hydraulic channels are used to model the lateral mixing of coolant between the hot seed and the hot blanket channel. Similarly cross flow junctions are defined in the RELAP5 model between the hot blanket channel and the average fuel assembly channel. With this set up there is no direct cross flow connection between the hot seed channel and the average fuel channel. Any lateral mixing between the hot seed channel and the average fuel channel is via the hot blanket channel. A hydraulic channel parallel with the fuel channels represents the core bypass flow path.

The hot seed channel has 2 heat structures. One represents the hottest seed pin in the hottest fuel assembly. The other is an effective fuel pin representing the rest of the seed rods (107) in the hottest fuel assembly. The hot blanket channel receives energy directly from an effective blanket pin representing all blanket rods (156) in the hottest fuel assembly. The average fuel assembly channel has two heat structures, one each to represent the seed rods and the blanket rods respectively. These two heat structures are effective fuel pins for the 192 fuel assemblies with a total of 20,736 (192x108) seed rods and 29,952 (192x156) blanket rods.

Blanket region power factor = 0.398/(156/264) = 0.6735

Hot seed pin power factor (relative to average seed pin in hot assembly) = 1.341

Thus, the ratio of the power of the hot seed pin to the power of an average pin in the core is,

1.189 x 1.4716 x 1.341 = 2.346

It is noted that the pin by pin power distribution for the hot assembly has been shown earlier in Figures B3.2.2 through B3.2.4.

The first cycle axial power distributions in the seed and blanket regions of the hot assembly are almost identical, as shown in Table B3.6.3 and Figure B3.2.8. The active fuel is divided uniformly into 16 axial nodes. In the RELAP5 model all SBU assemblies assume the same axial power distribution with separate values from Table B3.6.3 for the seed and blanket regions respectively. The maximum axial power factor for the seed pins is 1.555. Thus, the maximum local power factor becomes 3.636 (2.346 x 1.555) for the SBU core.

Heat structures that represent the fuel pins assume a cylindrical geometry with three radial zones; fuel, gap, and clad. The fuel is characterized by uniform internal heat generation. By assumption, 2.6% of the reactor power goes to direct moderator heating (coolant in the core hydraulic channels). Thus internal heat generation in the fuel accounts for 97.4% of the reactor power. Fuel in the seed rods is assumed to be annular with a central void while the blanket rods have solid cylindrical fuel. For the SBU accident analysis the same gap conductance and core kinetics parameters as the typical PWR design have been used. For the three accident sequences analyzed for the SBU design the only core neutronics parameter of significance is the control rod worth. It is assumed that the scram characteristics of the SBU will be made similar to those of the standard PWR (for example by the use of slightly enriched boron if necessary). Thus the use of the same neutronics parameters as the PWR for the SBU accident analyses is justified.

RELAP5 Accident Analysis

The three accident sequences analyzed for a typical PWR using two different fuel designs, namely the UO_2 only fuel and the SBU fuel assemblies, are:

1) Large Break Loss of Coolant Accident (LBLOCA)
2) Complete Loss of Primary Flow (LOPF)
3) Loss of Off-site Power (LOSP)

Steady State Analysis

Results of a steady-state initialization for the typical PWR design are summarized in Table B3.6.4. The case was executed by RELAP5-3D version 2.2.4 running on a PC with an input deck from MIT (see Section B2.6 for a description of the steady-state model). As expected there is little difference in the steady-state results calculated by MARS and RELAP5-3D.

Steady-state results for the SBU core using RELAP5-3D are summarized in Table 3.6.5. Initial calculations using nominal flow area for the hot seed channel (i.e. as indicated in Figure B3.6.2) resulted in the water boiling near the exit of the hot seed channel. This was not the case predicted by COBRA-EN using the 1/8th assembly model and the 1/8th core model. The cross flow in RELAP5 is basically pressure driven and the increased channel pressure drop due to boiling tends to divert coolant away from the channel with steam voids. It is not clear there is a method to implement the more realistic COBRA mixing models in RELAP5 without doing some source code modifications. If the COBRA mixing models were implemented in RELAP5 then the exit coolant temperatures calculated by COBRA-EN and RELAP5 should agree. In lieu of modifying the RELAP5 cross flow model an alternate method was used to achieve similarity in channel exit temperature. It was done by adjusting the fractional flow area of the hot assembly that is assigned to the hot seed channel. According to the pin power distribution shown in Figure B3.2.4 the hot seed rod is rod 17 and is surrounded by sub-channels 14, 15, 19 and 20 (see Figure B3.2.1). The corresponding exit coolant temperatures for these sub-channels had been calculated by using the COBRA-EN 1/8th assembly model and the 1/8th core model presented in Section B3.2. The exit coolant temperature for the sub-channels surrounding the hot seed pin ranges from 600K to 607K. These temperatures are lower than the maximum exit temperature of 609K predicted for sub-channel 1 that is at the center of an assembly. It was found that by increasing the nominal hot seed flow area by about 15% in the RELAP5 model, the hot seed exit temperature becomes 612K, a few degrees higher than the maximum temperature predicted by COBRA-EN for the whole hot seed region. This increased flow area was assumed for the hot seed channel in the RELAP5 model and a corresponding reduction was taken in the hot blanket channel flow area. In summary, an effective flow area is used in the RELAP5 model of the SBU hot seed to emulate the enhanced heat removal from the hot seed channel due to cross-flow mixing.

Large Break Loss of Coolant Accident (LBLOCA)

This accident simulates a double-ended cold-leg break and is similar to the one analyzed for the WASB design in Section B2.6. For the standard PWR and the SBU core, the RELAP5-3D default critical flow model, the Ransom-Trapp model, was used to calculate the break flow. The LBLOCA analysis used the same containment back pressure model and the same conservative boundary conditions as noted in the WASB LBLOCA analysis.

The transient behavior of the clad temperatures for the hot rod of the standard PWR design (Figure B3.6.4) and the hot seed of the SBU design (Figure B3.6.5) are fairly similar. In both cases there is a sharp initial blowdown peak followed by a more gradual reflood peak where the coolant channels are again refilled with water from the ECCS system. The blowdown peak is seen to reach a slightly higher clad temperature than the reflood peak but in any case the peak clad temperature (PCT) is less than 1100K for both designs. It is observed that the axial location of the blowdown peak is in the 10th node for both the hot rod of the standard PWR design and the hot seed of the SBU design. A comparison of the clad temperature of the 10th node for both designs is shown in Figure B3.6.6. It is seen from the figure that the two peak temperatures (blowndown and reflood) are slightly higher for the SBU hot seed pin than that for the PWR hot rod.

In comparing the clad temperatures for the standard PWR design calculated by the MARS code and RELAP5-3D, it is observed that the former predicted reflood peaks more than 150K lower than the blowdown peaks while the latter predicted reflood peaks that are close in magnitude to the blowdown peaks. The trend of the blowdown peak and the reflood peak reaching similar magnitudes is consistent with the results calculated by RELAP5-3D for the SBU design and by MARS for the WASB design.

The LBLOCA analysis indicates the PCT for the SBU design is less than 100K higher than that for the standard PWR design and is more than 300K lower than the generally accepted PCT limit of 1477K. In comparing the SBU and the WASB design, the PCT for the SBU hot seed is roughly 200K lower than that for the WASB hot seed.

Complete Loss of Primary Flow (LOPF)

This accident simulates a complete loss of primary flow due to the tripping of all four reactor coolant pumps (RCP) at time zero. The reactor trips on low core flow (87% of nominal flow) some time later with a 1.0 second delay. The turbine is also assumed to trip immediately, which caused the turbine stop valve to close. The main interest of this transient is to observe the clad temperature behavior during the time period before the reactor trip when the reactor is still at power while the primary flow is decreasing. The significant part of this transient, similar to the one analyzed for the WASB design, is over once the reactor is tripped and thus the accident was only simulated up to ten seconds.

The loss of primary flow transient is expected to have similar trends for both the PWR and the SBU design since they use the same RELAP5 pump model. This is supported by results presented in Figure B3.6.7 for the reactor power, Figure B3.6.8 for the primary pressure, and Figure B3.6.9 for the peak clad temperature. There is no significant rise in clad temperature for both designs. The PCTs of various fuel pins modeled for the SBU core are shown in Figure B3.6.10. In all cases the maximum clad temperature rise is only in the order of 10K. In general both MARS and RELAP5-3D predicted similar peak clad temperatures for the standard PWR hot rod and the respective hot seed rod for the two designs.

Loss of Off-Site Power (LOSP)

This transient is similar to the loss of primary flow accident except the reactor is also tripped at time zero with loss of off-site power. The interest is to observe the temperature response of the fuel with reduced capacity to deliver feedwater to the steam generators. It is assumed in the RELAP5 simulation that 75 seconds after reactor trip only one emergency feedwater pump could be started to inject water into the four steam generators. The transient was run for 200 seconds for both the standard PWR and SBU design.

The reactor power for both designs is shown in Figure B3.6.11. The primary pressure of the standard PWR and the SBU design is shown in Figure B3.6.12. The initial spike in pressure is caused by pressure build up in the steam generators after the turbine is isolated by the closure of the turbine stop valve The PCTs of the PWR hot rod and the SBU hot seed are shown in Figure B3.6.13. Their response is similar and for the time period greater than 100 seconds the SBU

PCT is about 5K higher than that of the standard PWR. The PCTs of various fuel pins modeled for the SBU core are shown in Figure B3.6.14. In all cases the initial clad temperature rise is only in the order of 1K. Both MARS and RELAP5-3D predicted very gradual temperature change in the clad after 100 seconds. The system has reached quasi-steady state by then and the clad temperature is reflecting the slow decay of reactor power.

Summary and Conclusions

Based on the RELAP5-3D accident analysis of the SBU design and the standard PWR design under three different scenarios, the SBU design is found to have peak clad temperature responses very similar to the standard PWR with UO_2 only fuel. For the LBLOCA case the PCT for the hot seed pin of the SBU is about 100K higher than that for the hot rod of the standard PWR. For the LOPF and LOSP accidents the difference in PCT between the two designs is much lower, in the order of 10K or less. There are some differences in the details between the results obtained by RELAP5-3D and MARS for the same accident and the same plant design. Some of the differences are attributable to slight variations in the definition of the scenario.

There are several areas of the accident analysis that warrant additional investigation:

1. Tighter integration between the core subchannel analysis and the accident analysis using system codes.
2. Incorporate dynamic gap model in the accident analysis.
3. Analyze a broader spectrum of accident scenarios, such as those initiated by reactivity transients.

Table B3.6.3 Axial Power Distribution for the Hot SBU Assembly (Cycle 1)

Axial Node No.	Seed Rods	Blanket Rods
1	0.358	0.351
2	0.717	0.708
3	1.035	1.024
4	1.284	1.273
5	1.455	1.444
6	1.543	1.536
7	1.555	1.553
8	1.504	1.506
9	1.402	1.407
10	1.264	1.273
11	1.101	1.112
12	0.925	0.935
13	0.741	0.751
14	0.554	0.562
15	0.367	0.372
16	0.192	0.194

Table B3.6.4 Steady-State Values for the Typical 4-Loop PWR Design

Parameter	Value
Core Power (MWt)	3479.2
Pressurizer Pressure (Bar)	155.2
Cold Leg Temperature (K)	566.7
Hot Leg Temperature (K)	598.8
Total Loop Flow (kg/s)	18688
Effective Core Flow (kg/s)	17776
Bypass Flow Fraction (%)	4.74
Core Pressure Drop (Bar)	2.07
Pressurizer Level (%)	66.6
SG Secondary Pressure (Bar)	61.3

Table B3.6.5 Steady-State Values for the SBU Core Design

Parameters	Value
Core Power (MWt)	3479.2
Pressurizer Pressure (Bar)	155.1
Cold Leg Temperature (K)	564.8
Hot Leg Temperature (K)	597.7
Total Loop Flow (kg/s)	18420
Effective Core Flow (kg/s)	17595
Bypass Flow Fraction (%)	4.3
Core Pressure Drop (Bar)	1.76
Pressurizer Level (%)	63.7
SG Secondary Pressure (Bar)	59.6
Hot Seed (Channel 335) Inlet Flow (kg/s)	44.1
Hot Seed (Channel 335) Outlet Flow (kg/s)	42.8
Hot Blanket (Channel 435) Inlet Flow (kg/s)	47.1
Hot Blanket (Channel 435) Outlet Flow (kg/s)	47.3
Average Assembly (Channel 333) Inlet Flow (kg/s)	17503
Average Assembly (Channel 333) Outlet Flow (kg/s)	17504
Hot Seed Outlet Temperature (K)	613.1
Hot Blanket Outlet Temperature (K)	596.8
Average Assembly Outlet Temperature (K)	599.1

Seed Fuel Rod
Geometry and Composition Used for Seed Region (335) and Average Assembly (333)

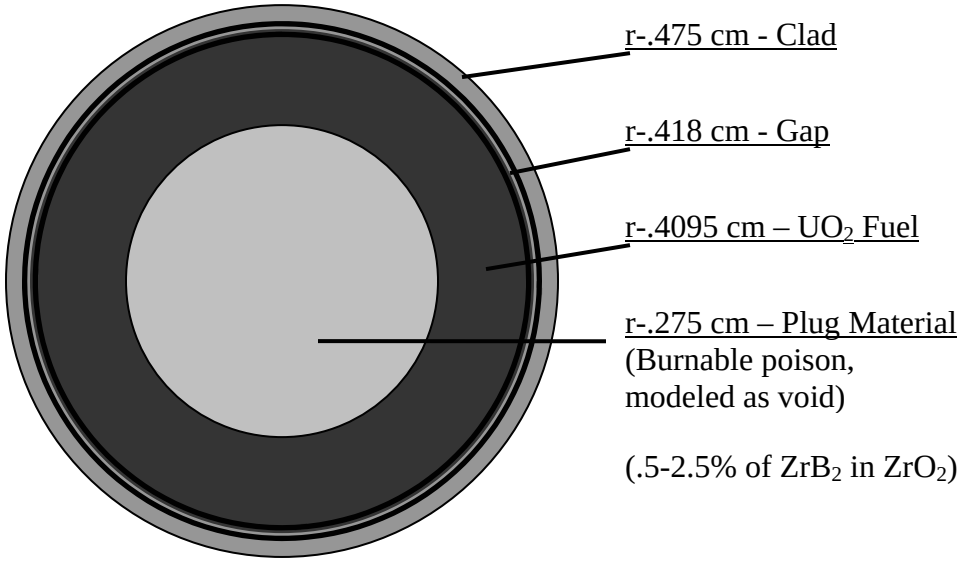

Blanket Fuel Rod
Geometry and Composition Used for Blanket Region (435) and Average Assembly (333)

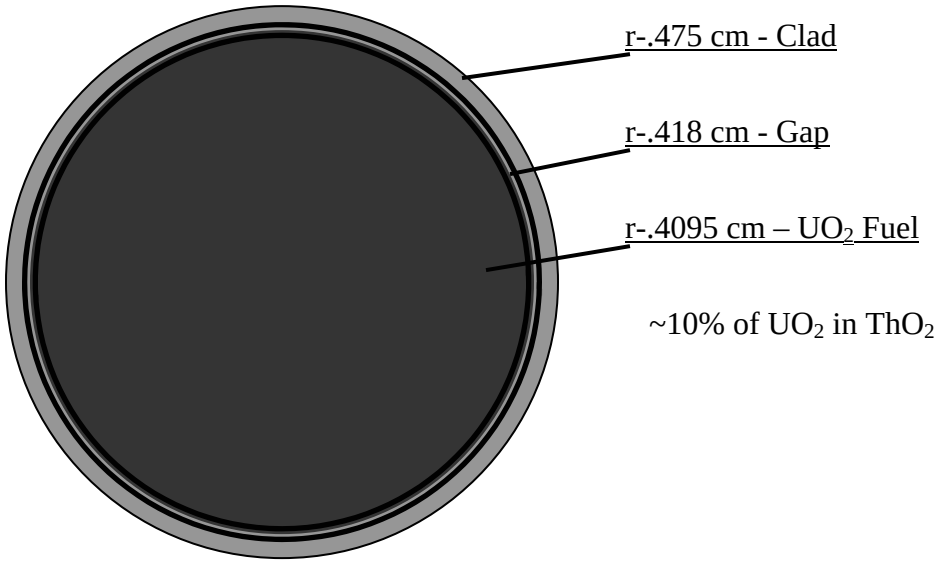

Figure B3.6.1 Geometry and composition of seed and blanket rods of the SBU

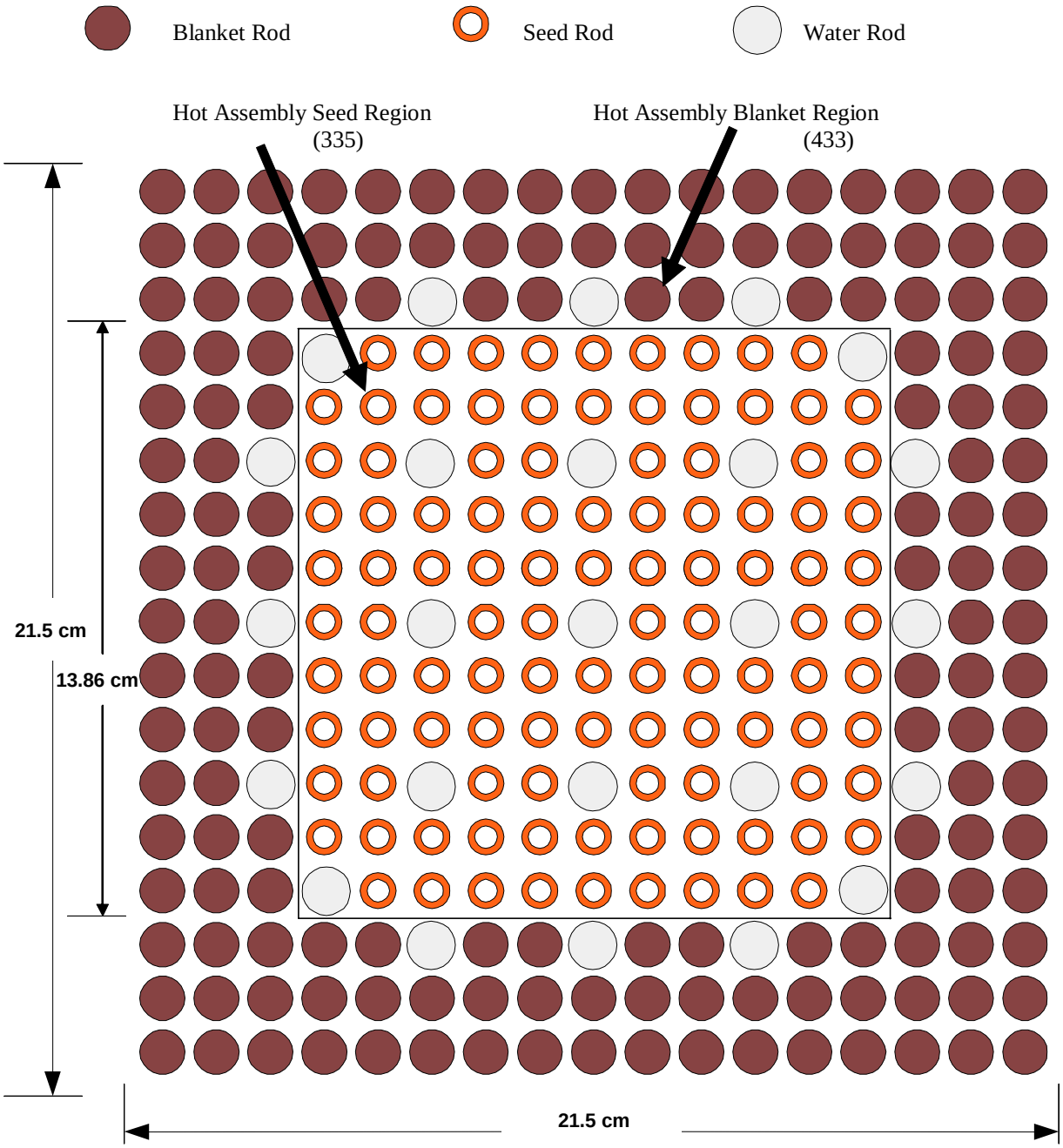

Figure B3.6.2 RELAP5 SBU Hot Assembly Layout

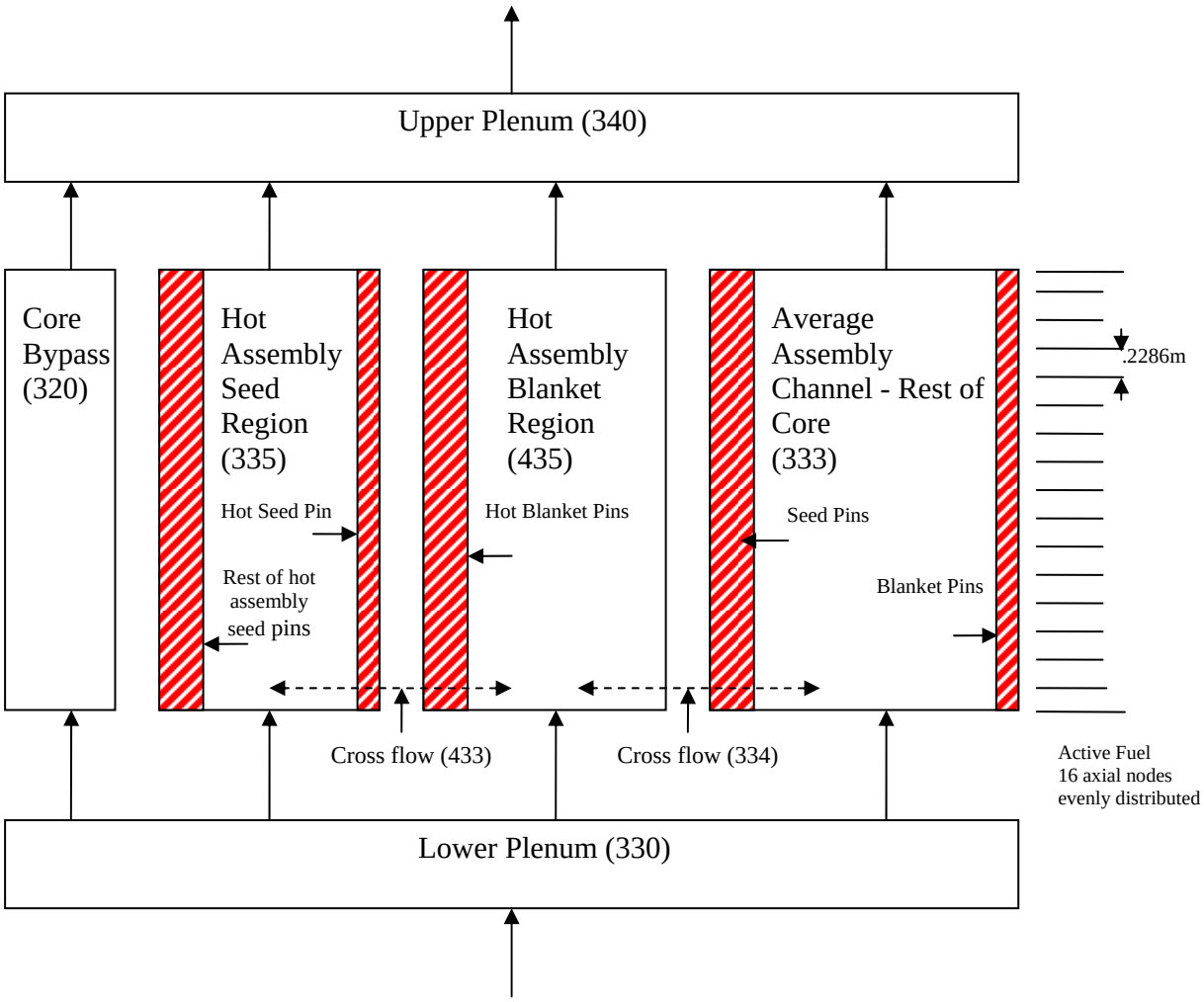

Hot Assembly Seed Region (335) represents 108 heated rods
Hot Assembly Blanket Region (435) represents 156 heated rods
Average Assembly Channel (333) represents 192 FA

Figure B3.6.3 RELAP5 SBU Core Nodalization

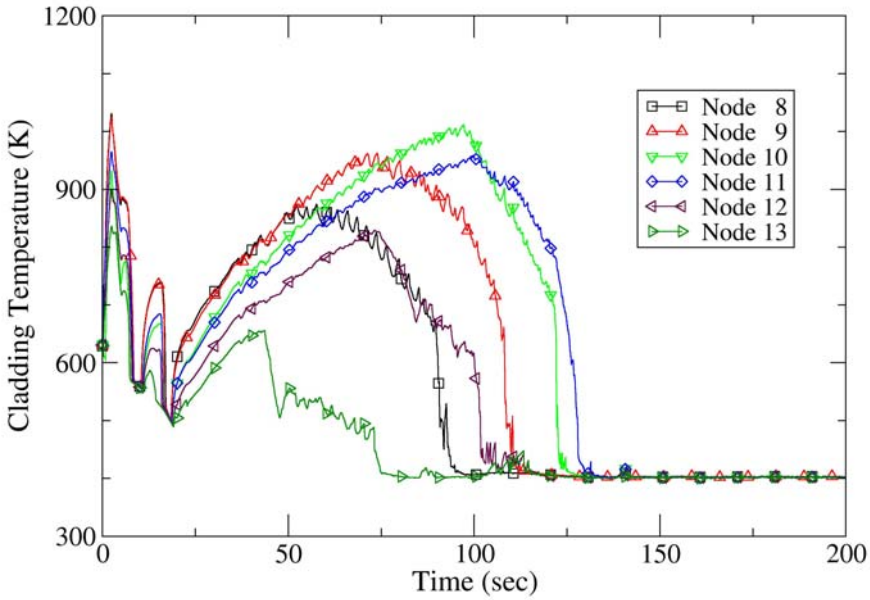

Figure B3.6.4 Hot Rod Cladding Temperature during LOCA for PWR Design

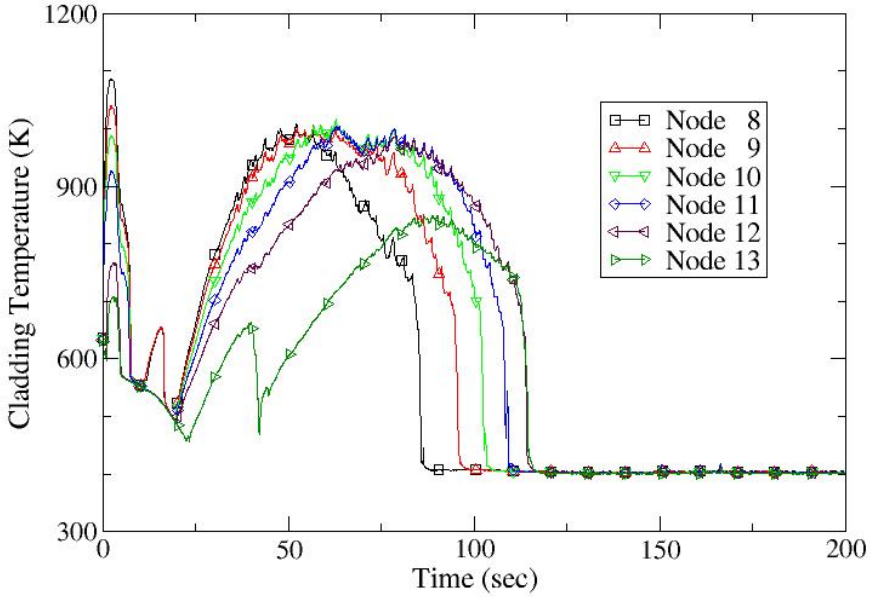

Figure B3.6.5 Hot Seed Cladding Temperature during LBLOCA for SBU Design

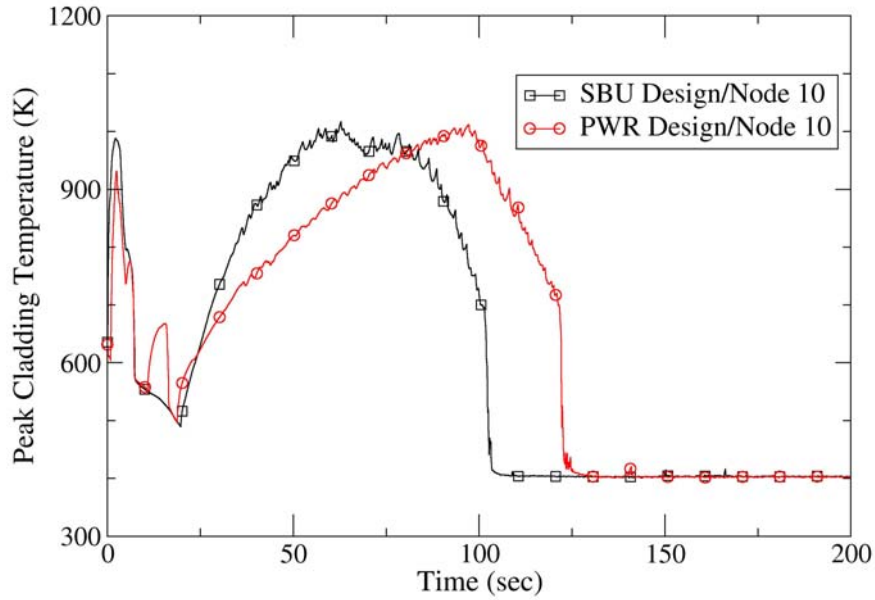

Figure B3.6.6 Comparison of LBLOCA PCTs between the PWR and SBU Designs

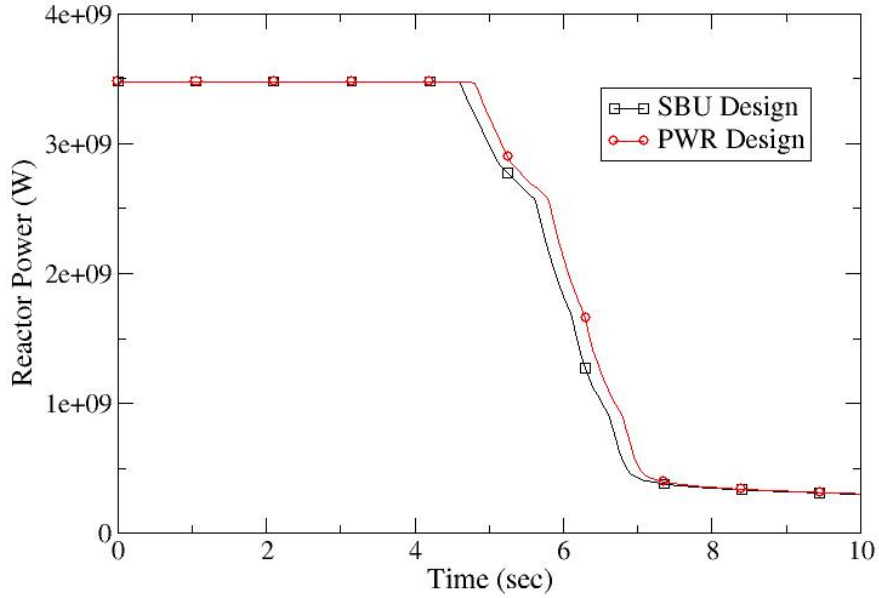

Figure B3.6.7 Reactor Power during LOPF Transient (PWR and SBU)

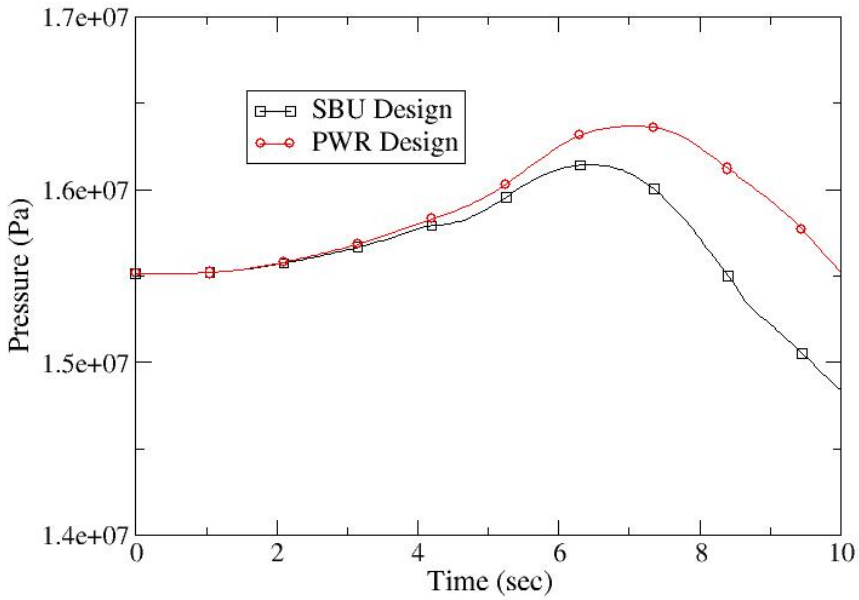

Figure B3.6.8 Primary (Pressurizer) Pressure during LOPF Transient (PWR and SBU)

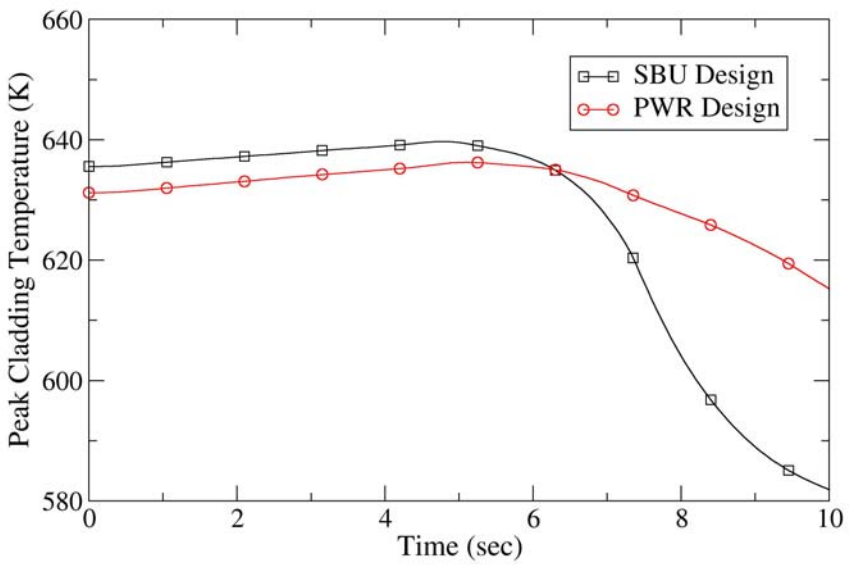

Figure B3.6.9 PCTs during LOPF Transient (PWR and SBU)

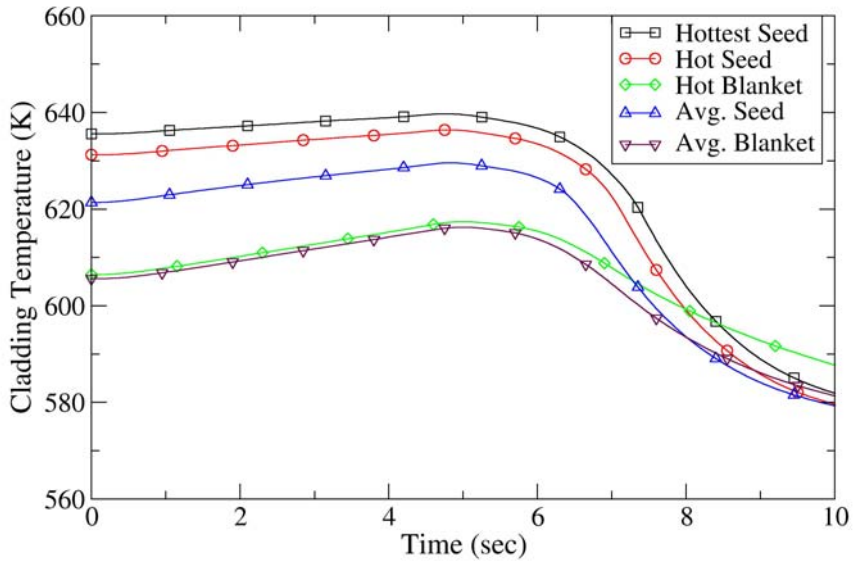

Figure B3.6.10 PCTs of Various Fuel Pins of the SBU Core during LOPF Transient

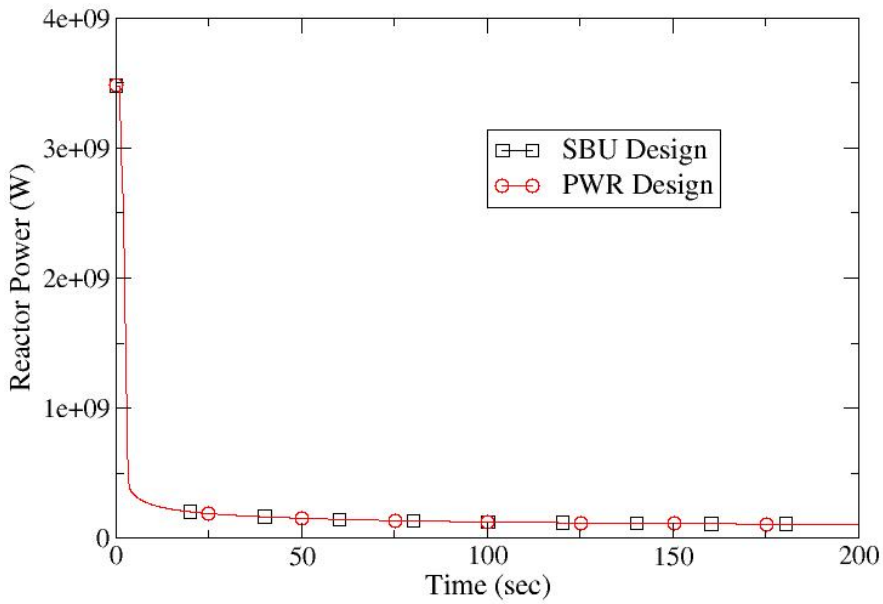

Figure B3.6.11 Reactor Power during LOSP Transient (PWR and SBU)

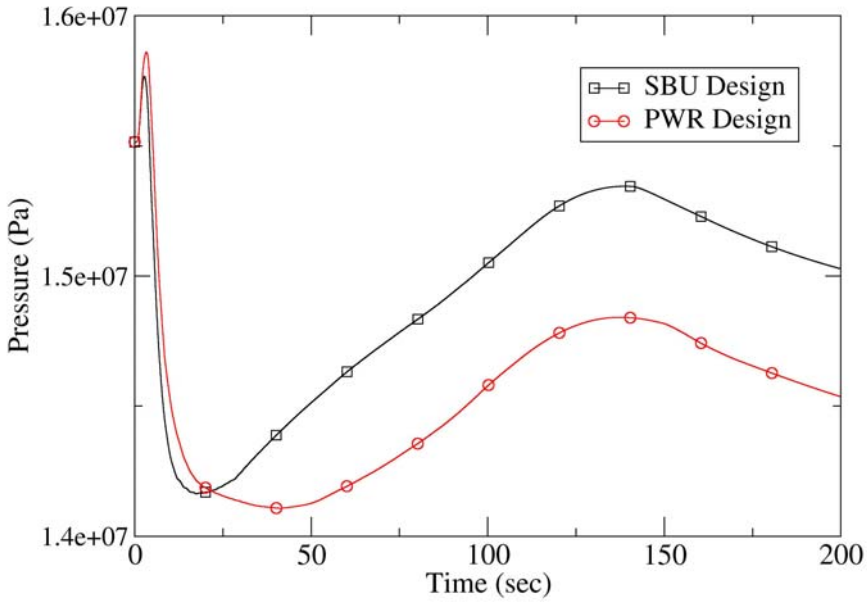

Figure B3.6.12 Primary (Pressurizer) Pressure during LOSP Transient (PWR and SBU)

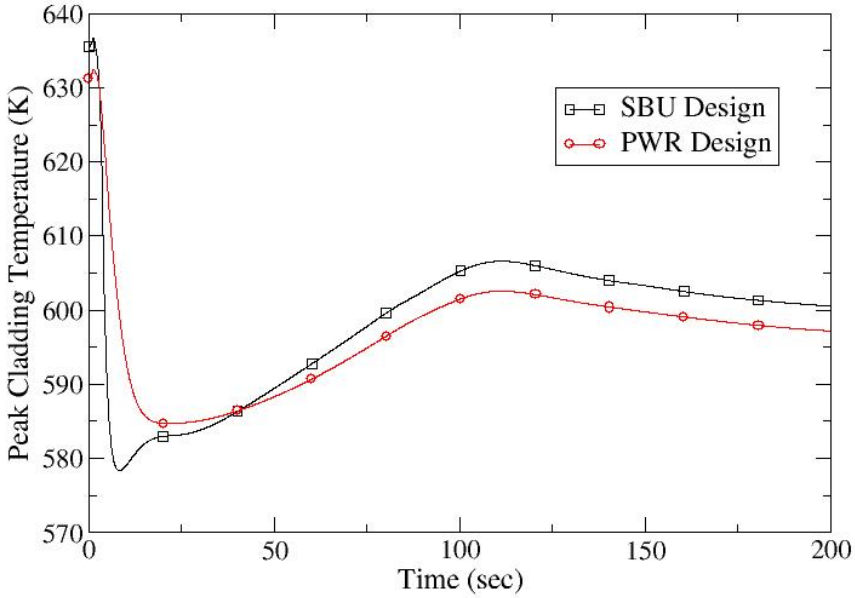

Figure B3.6.13 PCTs during LOSP Transient (PWR and SBU)

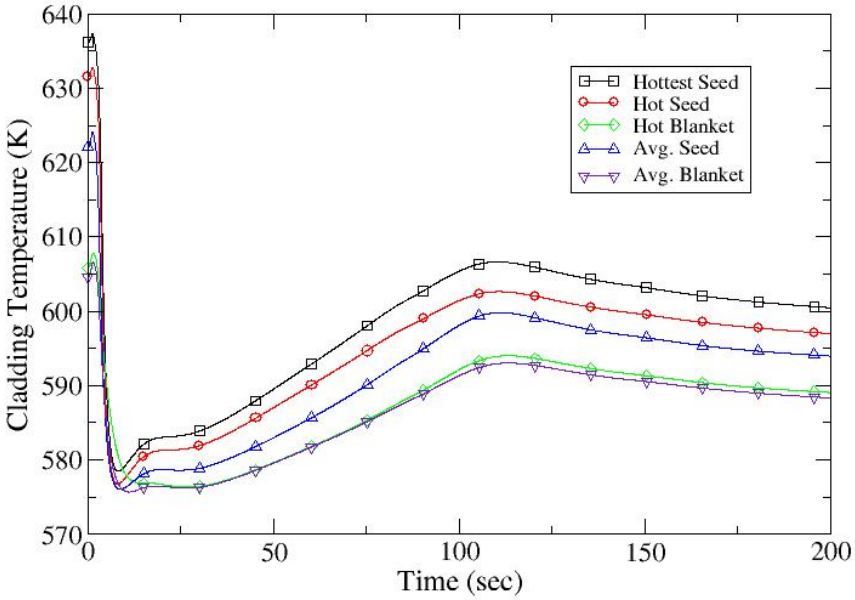

Figure B3.6.14 PCTs of Various Fuel Pins of the SBU Core during LOSP Transient

C. SUMMARY AND CONCLUSIONS

Based on the technical details presented in Sections B2 and B3, the WASB and SBU designs have similar performance and safety characteristics. These can be summarized as follows:

1. Scoping studies using commercial (or accepted state-of-the art) core design methods, benchmarked for use with thorium and seed-blanket cores, indicate that retrofittable seed-blanket cores can be successfully designed for use in large Westinghouse type PWRs. The scoping designs meet the targets of reduced plutonium production, competitive economics, and comparable Environmental, Safety and Health (ES&H) characteristics to those of existing PWRs (i.e., within the current "safety envelope"). The arrangement of the control assemblies may have to be altered to facilitate optimum performance of the core, and fuel rod length would probably have to be altered to allow for a larger gas plenum.

2. Both concepts use the same 17x17 rod array and guide/instrument tube locations found in typical Westinghouse PWRs. For the WASB design there are separate seed and blanket assemblies, while for the SBU the seed and blanket rods are all located within a single assembly. In both concepts the seed rods use annular uranium pellets (or duplex pellets with inert central materials) to allow for acceptable fuel temperature in the high power seed assemblies, and conventional rods for the blanket. Since the seed and blanket in the WASB concept are associated with distinct assemblies, there are no fuel handling issues. In the SBU concept the reference approach is to replace seed rods individually using a machine that has been developed to replace failed fuel rods.

3. After investigating a number of core designs, the MIT researchers recommend a design for the WASB concept consisting of 84 seed assemblies with annular fuel pellets containing 20 percent enriched U235 in UO_2, and 109 blanket assemblies with solid fuel pellets, 87 percent ThO_2 and 10 percent enriched U235 in the remaining UO_2. Cycle lengths of 18-months are achieved with typical three-batch fuel management for the seeds, which attain a discharge burn-up of about 145 MWd/kgU. The 109 blanket assemblies are loaded and discharged together, spending up to nine cycles in the core and achieving a discharge burn-up of about 90 MWd/kgHM. On average, about two thirds of the energy is generated in the seed, about one third in the blanket.

4. In the SBU design, the seed region was optimized to the central 11x11 portion of the assembly (108 rods), with the blanket rods occupying the remaining locations (156 rods). The resulting seed-to-blanket ratio is 0.69 is similar to that of the WASB design (0.77). Several SBU design options have been explored to optimize nuclear performance and minimize power peaking to achieve acceptable thermal-hydraulics characteristics. The seed rods are 20 w/o U235 in UO_2, and the blanket rods are 13-15 v/o of ~11 w/o U235 in UO_2, with the remainder ThO_2. The seed discharge burnup is comparable to that for the WASB design, while the blanket discharge burnup is ~80 MWd/kgHM corresponding to a core residence time of six cycles.

5. The annual rate of plutonium production for both concepts is only about 40 percent of that of a present-day conventional PWR with a discharge burnup of 50MWd/kgHM. Moreover, the total heat generated by the plutonium is much higher than that produced by the typical PWR grade plutonium due to the significantly higher content of Pu-238. There is also a significant increase in the spontaneous neutron generation rate making the plutonium less attractive/unsuitable for weapons development. Finally, the blanket uranium proliferation index (weighted fractions of U233 and U235) has been kept within the accepted limit of 12 percent, which, for uranium containing both the U233 and U235 fissile isotopes, corresponds to the well-known 20 percent limit applicable when U235 is the only fissile isotope present.

6. The WASB design discharges about 40 percent fewer assemblies per GWe-yr than a typical 18-month cycle PWR. The discharged mass of heavy metal for WASB is about half of that for a similar PWR. WASB spent fuel produces less radioactivity, and less decay heat than the conventional all-UO_2 fuel in the short term (up to about 5 years after discharge), and a comparable amount in the near term (up to about 10,000 years). After 10,000 years, there is a local peak due to the decay products of U233 in the blanket, but by that time both the radioactivity and the decay heat are at relatively low levels. The volume and mass reductions for the SBU design, and the behavior of the radioactivity and decay heat of the discharged fuel are very similar.

7. Operating characteristics of the WASB and SBU cores are generally similar to those of a standard PWR core. These include Doppler and moderator temperature coefficients, critical boron concentrations and kinetics parameters. Some control rod modifications are required to achieve adequate control rod worths and shutdown margin. Power peaking is higher than in a standard core, but this is compensated as explained in the next item.

8. Acceptable DNB margins under overpower conditions during Anticipated Operational Occurrences are attained by two design techniques for the WASB concept. First, the seed fuel rod diameter being smaller than the blanket fuel rod diameter diverts some flow from the low power blanket assemblies to the higher power seed assemblies. Second, the grid/spacer resistances are increased in the blanket assemblies to enhance this diversion. For the SBU design, acceptable performance is achievable by grading the poison enrichment in the seed, and tailoring the grid loss coefficients to force flow into the seed.

9. Using a version of RELAP5, called MARS, available at MIT, researchers have analyzed three accidents/transients, namely, large break loss of coolant accident (LBLOCA), complete loss of primary flow (LOPF) and loss of off-site power (LOSP), for both the WASB and the conventional PWR designs. For LBLOCA, the peak cladding temperature (at the hottest rod in the hottest seed assembly) for the WASB design is calculated to be about 250°C higher than that for the conventional PWR design. However, this higher peak cladding temperature for the WASB design is still about 200°C lower than the present regulatory limit of 1,204^{o}C. For the LOPF and LOSP transients, the results of the WASB and the typical PWR designs are very similar—no post-DNB type rapid cladding temperature rise was calculated. Although these results indicate adequate safety margin for the WASB design, one should analyze other accidents and transients before a more definitive conclusion is drawn.

10. Accident analysis for the SBU design were performed by using the system code RELAP5-3D. For the convenience of comparison, the analysis used the same basic plant model and accident sequences as those employed in the WASB accident analysis. The difference between the RELAP5 inputs for the SBU and the WASB designs is in the modeling of the seed and blanket regions of the core. The figure of merit used in identifying the limiting condition during the progression of a postulated accident is the peak clad temperature (PCT). Analysis of the large break loss of coolant accident (LBLOCA) indicates that the PCT for the SBU design (in the hot seed pin) is less than 100K higher than that for the standard PWR design (in the hottest pin) and is more than 300K lower than the generally accepted PCT limit of 1477K. The other two accidents analyzed for the SBU core are the complete loss of primary flow (LOPF) and loss of off-site power (LOSP). For these two accidents the PCT predicted for the SBU is higher than that for a conventional PWR, but only on the order of 10K or less. In predicting the behavior of conventional PWR during LOPF and LOSP accidents, the two versions of RELAP5, RELAP5-3D for the SBU analysis and MARS for the WASB analysis, produced similar results. The initial accident analysis shows adequate safety margin for the SBU design but a wider set of accidents and conditions should be considered to form a comprehensive set of design basis accidents (DBA).

11. Studies of fuel performance for the WASB design show that the high burn-up of seed fuel leads to significant fission gas release and consequently high internal pressure in the seed rods, but analyses suggest that this pressure can be reduced if a significantly longer plenum is used. The long irradiation period of blanket fuel leads to excessive oxide growth on their surface if Zircaloy is utilized as the cladding, but analyses indicate that this can be contained if improved material such as M5 is used for the blanket cladding material. These conclusions are also applicable to the SBU design based on similar residence times and burnups for the seed and blanket fuels.

12. The economics of both the WASB and SBU designs are competitive (±10%) with those of all-UO_2 PWR fuel. The primary uncertainties are in the cost of fuel fabrication (both seed and blanket, but mostly seed) and in the costs of storage and disposal for spent fuel. The WASB design requires about the same amount of uranium as standard fuel and about 30% more SWU for enrichment; about 35% fewer assemblies are fabricated, although the seed fuel with its annular pellets is of a more complex design. Most of the fuel cost (typically 85%) is attributable to the seed fuel. The fuel cost is therefore most sensitive to SWU cost and insensitive to thorium cost. The WASB and SBU designs would have an advantage if incentives were to be given for the improved non-proliferation and spent fuel characteristics of their discharged fuel.

13. Further work on this project could include:

    a. More detailed investigation of fuel mechanical behavior – fission gas release and cladding corrosion.
    b. Analysis of Anticipated Operational Occurrences (AOO) utilizing actual transient calculations rather that an equivalent steady state calculation at overpower.
    c. More detailed analyses of transients and accidents. This includes looking into various filler materials for the seed rod and their effects on LOCA analysis, and analyses of

other transients and accidents not investigated in the present research. The analyses should include the dynamic gap effect, and the buildup of oxide film on the cladding.

d. More detailed investigation of fabrication costs expected for both seed and blanket designs.
e. Further optimization of fuel and core design to reduce power peaking and enhance the cooling of the seed rods.
f. Design of spent fuel casks for seed fuel.

D. INTERNATIONAL COLLABORATION

This project has benefited from several international collaborations:

- BGU has been an integral part of the team developing the SBU-RTF concept. In particular, as noted earlier (Section B3.1), they performed the three-dimensional coupled neutronic-thermal hydraulic calculations that form the basis of the performance, cost and safety analyses. In addition, several of the sensitivity/optimization studies for the SBU were performed at BGU, as well as the fuel cycle cost.

- The work performed in Korea expanded the scope of the study to include reactors designed by Combustion Engineering, and employs a metallic seed in conjunction with the WASB approach.

- The work performed in Russia further expanded the scope of reactors considered to include the VVER-1000. The work performed by the Russian Research Center- Kurchatov Institute included design and safety analyses, and fuel fabrication, characterization, and irradiation performance (which are continuing at the IR-8 reactor), as well as thermal-hydraulic experiments. The IR-8 reactor provides a thermal and nuclear environment prototypic of modern commercial PWRs, and the irradiation program will provide valuable data on fuel performance.

Since the work in Korea and Russia was performed for significantly different reactor configurations (CE-System-80 and VVER-1000, respectively), and for different fuel cycle assumptions and costs, their results are not included in this report.

E. REFERENCES

Section A

P.E. Macdonald, "Advanced Proliferation Resistant, Lower Cost, Uranium-Thorium Dioxide Fuels for Light Water Reactors," U.S. Department of Energy Nuclear Energy Research Initiative, NERI 99-0153 (1999).

E. Shwageraus, P. Hejzlar, M.J. Driscoll, And M.S. Kazimi, "Optimization of Micro-Heterogeneous Uranium-Thorium Dioxide PWR Fuels for Economics and Enhanced Proliferation Resistance," MIT-NFC-TR-046, MIT, Nuclear Engineering Department, Cambridge, MA, July 2002.

M. Todosow, A. Galperin, S. Herring, M. Kazimi, T. Downar, A. Morozov, "Use of Thorium in Light-Water Reactors", Advances in Nuclear Fuel Management –III, October 2003.

Section B2: Whole Assembly Seed Blanket

Bayless, P. D. and Divine, J. M, (1982), "Experiment Data Report for LOFT Large Break Loss-of-Coolant Experiment L2-5," NUREG/CR-2826, EGG-2210, August 1982.

Busse, M. and Kazimi, M. S, (2000), "Thorium-Uranium Seed-Blanket Fuel Assembly Thermal Hydraulics," Trans. Am. Nucl. Soc., Vol. 82, June 2000.

Busse, M. and Kazimi, M. S, (2000), "Thermal and Economic Analysis of Thorium-Based Seed-Blanket Fuel Cycles for Nuclear Power Plants," MIT-NFC-TR-025, August 2000.

Cochran, R. G. and Tsoulfanidis, N., (1999), "The Nuclear Fuel Cycle: Analysis and Management," American Nuclear Society, 2nd Edition.

Cuta, J. M., et al, (1985), "VIPRE-01: A Thermal-Hydraulic Code for Reactor Cores, Volume-2, User's Manual (Revision 2)," EPRI-NP-2511-CCM, Electric Power Research Institute (EPRI), July 1985.

Driscoll, M. J., Downar, T. J., and Pilat, E. E., (1990), "The Linear Reactivity Model for Nuclear Fuel Management," ISBN 0-89448-035-9, American Nuclear Society.

Forsberg, C. W., Hopper, C. M., and Vantine, H. C., (1999), "What is Nonweapons-Usable U-233?" Trans. Am. Nucl. Soc., Vol. 81, p. 62, Long Beach, California, November 14-18, 1999.

Jonsson, A., Parrette, J. R., and Shapiro, N. L., (1991), "Application of Erbium in Modern Fuel Cycles," The 6th KAIF/KNS Annual Conference, Seoul.

Kloosterman, J. L., and Bende, E. E., (2000), "Plutonium Recycling in Pressurized Water Reactors: Influence of the Moderator-to-Fuel Ratio," *Nuclear Technology*, Vol. 130.

Lee, W. J., et al, (2002), "Development of Realistic Thermal-Hydraulic System Analysis Code," KAERI/RR-2235/2001, 2002.

Levy, S., (1999), *Two-Phase Flow in Complex Systems, Chapter 1,* John Wiley & Sons, Inc., 1999.

Long, Y., Kazimi, M. S., Ballinger, R. G., and Meyer, J. F, (2002), "Modeling the Performance of High Burnup Thoria and Urania PWR Fuel," MIT-NFC-TR-044, July 2002.

OECD/NEA, (1994), "The Economics of the Nuclear Fuel Cycle."

Pettus, W. G., (1987 & 1989), "Void Plug for Annular Fuel Pellet," Babcock and Wilcox Co., New Orleans, LA. US patent document 4,853,177/A/.int. Cl. G21C 3/16. 1 Aug 1989; 21 May 1987. VP. Patent and Trademark Office, Box 9, Washington, DC 20232.

Rohatgi, U. S., Yuelys-Miksis, C., and Saha, P., (1987), "Determination of Appendix K Conservatism for Westinghouse Pressurized Water Reactors using TRAC-PD2/MOD1," *Nuclear Technology,* Vol. 76, pp. 41-50, January 1987.

Todosow, M., et al, (2003), "Optimization of Heterogeneous Utilization of Thorium in PWRs to Enhance Proliferation Resistance and Reduce Waste," Second Annual Progress Report, BNL-NERI 2000-014, March 2003.

Willse, J. T., and Garner, G. L., (2000), "Recent Results from the Fuel Performance Improvement Program at Framatome Cogema Fuels," International Topical Meeting on LWR Fuel Performance, Park City, April 2000.

Xu, Z., Hejzlar, P., Driscoll, M. J., and Kazimi, M. S., (2002), "An Improved MCNP-ORIGEN Depletion Program (MCODE) and Its Verification for High-Burnup Applications," International Conference on the New Frontiers of Nuclear Technology: Reactor Physics, Safety and High-Performance Computing (PHYSOR 2002), Seoul, Korea, Oct. 7-10.

Section B3: Seed Blanket Unit

"COBRA-EN: Code System for Thermal-Hydraulic Transient Analysis of Light Water Reactor Fuel Assemblies and Cores," PSR-507, RSICC, ORNL, May 2001.

Forsberg, C. W., Hopper, C. M., and Vantine, H. C., (1999), "What is Nonweapons-Usable U-233?" Trans. Am. Nucl. Soc., Vol. 81, p. 62, Long Beach, California, November 14-18, 1999.

Galperin, A., et al., (2001), "RTF18 – Oxide Reference Design Report", Reactor Analysis Group, Ben-Gurion University of the Negev, June 2001.

Paratte, J.M., Grimm, P., and Hollard, J.M., (1995), "ELCOS: The PSI Code System for LWR Core Analysis, Part II: User's Manual for the Fuel Assembly Code BOXER," Paul Scherrer Institute, Bericht, Switzerland, July 1995.

Paratte, J.M., Foskolos, K., Grimm, P., Maeder, C., (1996), “The PSI Code System ELCOS for LWR Core Analysis”, Paul Scherrer Institute, Villigen PSI, February 1996.

RELAP5-3D Code Manual Volume 1: Code Structure, System Models and Solution Methods, INEEL-EXT-98-00834, Revision 2.2, October 2003.

Rahn, F.J., Adamantiades, A.G., Kenton, J.E., Braun, C., “A Guide to Nuclear Technology-A Resource for Decision Making,” J. Wiley and Sons 1984.

Todosow, M., Kazimi, M., et al., (2002), “Optimization of Heterogeneous Utilization of Thorium in PWRs To Enhance Proliferation Resistance and Reduce Waste,” Progress Report for Seventh Quarter, April, 2001 - June, 2002, August 21, 2002.

Westinghouse Nuclear Energy Systems, (1973), “Reference Safety Analysis Report Volume II,” RESAR 41, December 1973.